Journal of
Medicinal Chemistry

Article

Novel Human Aminopeptidase N Inhibitors: Discovery and Optimization of Subsite Binding Interactions

Jisook Lee, Natalie Vinh, Nyssa Drinkwater, Wei Yang, Komagal Kannan Sivaraman, Luke Steven Schembri, Michelle Gazdik, Peter Grin, Georgina Butler, Christopher M Overall, Susan A. Charman, Sheena McGowan, and Peter J. Scammells

J. Med. Chem., **Just Accepted Manuscript** • DOI: 10.1021/acs.jmedchem.9b00757 • Publication Date (Web): 28 Jun 2019

Just Accepted

is published by the American Chemical Society. 1155 Sixteenth Street N.W., Washington, DC 20036

Novel Human Aminopeptidase N Inhibitors: Discovery and Optimization of Subsite Binding Interactions

Jisook Lee[†], Natalie B. Vinh[†], Nyssa Drinkwater[‡], Wei Yang[‡], Komagal Kannan Sivaraman[‡], Luke S. Schembri[†], Michelle Gazdik[†], Peter M. Grin[▽⊥], Georgina S. Butler[▽⊥O], Christopher M. Overall[▽⊥O], Susan A. Charman[§], Sheena McGowan[‡], Peter J. Scammells*[†]*

[†] Medicinal Chemistry, Monash Institute of Pharmaceutical Sciences, Monash University, Parkville Campus, VIC 3052, Australia.

[‡] Infection and Immunity Program, Biomedicine Discovery Institute and Department of Microbiology, Monash University, Clayton Campus, VIC 3800, Australia.

[§] Centre for Drug Candidate Optimisation, Monash Institute of Pharmaceutical Sciences, Monash University, Parkville Campus, VIC 3052, Australia

[▽] Department of Biochemistry & Molecular Biology and [O] Department of Oral Biological & Medical Sciences, University of British Columbia, Vancouver, BC V6T 1Z3, Canada

[⊥] Centre for Blood Research, Life Sciences Institute, University of British Columbia, Vancouver, BC V6T 1Z3, Canada

ABSTRACT: Aminopeptidase N (APN/CD13) is a zinc-dependent M1 aminopeptidase that contributes to cancer progression by promoting angiogenesis, metastasis and tumor invasion. We have previously identified hydroxamic acid containing analogues that are potent inhibitors of the APN homologue from the malarial parasite, *Plasmodium falciparum* M1 aminopeptidase (*Pf*A-M1). Herein we describe the rationale which underpins the repurposing of *Pf*A-M1 inhibitors as novel APN inhibitors. A series of novel hydroxamic acid analogues were developed using a structure-based design approach and evaluated for their inhibition activities against APN. *N*-(2-(Hydroxyamino)-2-oxo-1-(3',4',5'-trifluoro-[1,1'-biphenyl]-4-yl)ethyl)-4-(methylsulfonamido)benzamide (**6ad**) proved to be an extremely potent inhibitor of APN activity *in vitro*, selective against other zinc dependent enzymes such as matrix metalloproteases, and possessed limited cytotoxicity against Ad293 cells and favorable physicochemical and metabolic stability properties. The combined results indicate that compound **6ad** may be a useful lead for the development of anti-cancer agents.

■ INTRODUCTION

Aminopeptidase N (APN/CD13; EC 3.4.11.2) is an ubiquitous transmembrane ectoenzyme that is widely present in different types of cells including renal, intestinal, fibroblast, endothelial and tumor cells.[1, 2] APN is described as a "moonlighting" enzyme due to its multi-functional roles: an enzyme to cleave peptide substrates, a receptor, and a signaling molecule.[3] The enzyme cleaves hydrophobic and basic amino acid residues from the N-terminus of polypeptides with broad substrate specificity.[4] For example, APN catalyses the metabolism of angiotensin III to generate angiotensin IV to regulate the renin-angiotensin system[5] and levels of neuropeptides such as enkephalins.[6, 7] APN also acts as a viral receptor for mammalian coronavirus, and is a signaling molecule in phagocytosis, angiogenesis, and cell adhesion.[8-13]

APN is a member of the zinc-dependent M1 aminopeptidase superfamily of enzymes (protease clan MA) that can be found in all kingdoms of life except viruses.[4] M1 aminopeptidases are characterized by a thermolysin fold and two consensus sequence motifs; a $HEXXHX_{18}E$ zinc binding motif and a GXMEN substrate-guiding motif.[4, 14-16] Wong *et al*. reported the X-ray crystal structure of human APN, as well as structure of APN bound to generic inhibitors bestatin and amastatin, and an endogeneous peptide substrate, Angiotensin IV.[4] Human APN consists of a short intracellular tail, a transmembrane anchor, a small serine/threonine-rich extracellular stalk and a large ectodomain, comprised of four domains (I – IV) characteristic of M1 aminopeptidase superfamily.[4, 14] The catalytic domain II contains the consensus motifs ^{352}GXMEN^{356} and $^{388}HEXXHX_{18}E^{411}$, the latter of which includes the catalytic triad His^{388}, His^{392} and Glu^{411} that coordinates the essential zinc ion.[4]

APN has been extensively studied due to its significant role in the regulation of metastasis and angiogenesis.[17] A significant body of evidence supports the rationale that APN is an effective therapeutic target for malignancies.[17-20] Dysregulated activity of APN has been found to develop into a wide spectrum of human malignancies.[21-27] Metastasis is a complex multistep process of cell migration, cell

invasion, and angiogenesis and it is the major cause of cancer related deaths worldwide.[28-31] Multiple studies have shown that APN activity is involved in extracellular matrix (ECM) degradation, an essential step for metastasis, which was later determined to increase tumour cell migration and invasion by stimulating MAPK/PI3K signalling cascade.[24, 32, 33] Thus, there is an on-going interest to develop potent APN inhibitors as effective anti-cancer drug candidates.

A variety of APN inhibitors have been developed as potential anti-cancer candidates.[18, 19, 34, 35] Among them, a natural peptidomimetic, bestatin, is the most widely studied competitive APN inhibitor. Originally isolated from *Streptomyces olivoreticuli* as an immunomodulating agent, bestatin was found to have anti-tumor activity[36, 37] as well as clinical efficacy against acute myeloid leukemia and lung cancer in clinical trials.[38-41] Another APN inhibitor Tosedostat (CHR2797) is an orally bioavailable prodrug that is converted to a pharmacologically active drug (CHR79888) inside cells.[42] Tosedostat demonstrated significant anti-leukemic activity in phase II clinical trials in elderly or relapsing patients with acute myeloid leukaemia.[43]

Previous work by our group generated a series of hydroxamic acid-containing compounds that were inhibitors of the *Plasmodium falciparum* M1 aminopeptidase, *Pf*A-M1.[44-46] We described *N*-(2-(hydroxyamino)-2-oxo-1-[3',4',5'-trifluoro(1,1'-biphenyl)-4-yl]ethyl)pivalamide (**1**) (Figure 1) as a potent inhibitor of *Pf*A-M1, exhibiting an inhibitory constant ($K_i^{(app)}$) in the nanomolar range.[44] Here we show that **1** is also active towards APN and is more potent than both bestatin and Tosedostat. We have repurposed compound **1** as a novel APN inhibitor and developed a new series of analogues with improved potency against APN through structure-based approaches.

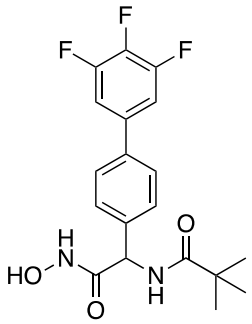

Figure 1. Structure of *N*-(2-(hydroxyamino)-2-oxo-1-[3',4',5'-trifluoro(1,1'-biphenyl)-4-yl]ethyl)pivalamide (**1**).

■ RESULTS AND DISCUSSION

Compound 1 can inhibit recombinant human APN. *Pf*A-M1 is a homologue of APN found in *Plasmodium falciparum* which is one of the parasites that causes malaria. Being part of the same M1 aminopeptidase family, *Pf*A-M1 shares a number of structural similarities with APN, particularly within the catalytic domain II. Overall, *Pf*A-M1 and APN share 19% sequence identity (35% similarity), however, in the highly conserved catalytic domain II, this sequence identity increases to 24 % (43% similarity). This conserved catalytic domain II adopts a thermolysin-like fold and in *Pf*A-M1, contains a $H^{496}EYFHX_{17}KE^{519}$ zinc-binding motif as well as a $G^{490}AMEN$ substrate-guiding motif.[16] The catalytic zinc in the active site is coordinated by a catalytic triad His^{496}, His^{500}, and Glu^{519} in the unbound state.[16] Therefore, we were interested to see how the potent *Pf*A-M1 inhibitor **1** would interact with human APN.

Our standard fluorescence-based aminopeptidase inhibition assay was used to measure the inhibitory activity of bestatin, Tosedostat and **1** against human APN. This assay used recombinant human APN and a commercially available fluorophore 7-amino-4-methylcoumarin as the competitive substrate to determine an inhibitory constant ($K_i^{(app)}$). We compared the inhibitory activity of bestatin, Tosedostat and **1** against human APN as well as *Pf*A-M1 (Table 1). Bestatin showed a moderate loss in potency toward APN compared to *Pf*A-M1, whereas Tosedostat exhibited a 6-fold improved potency toward APN when compared to *Pf*A-M1. Interestingly, compound **1** was significantly more potent than Tosedostat and bestatin, displaying a 10 to 20-fold increase in APN inhibition activity.

Table 1: $K_i^{(app)}$ comparison of bestatin, Tosedostat, and compound **1** against human APN and *Pf*A-M1.

Compound	$K_i^{(app)}$(APN) ± SEM (nM)	$K_i^{(app)}$(*Pf*A-M1) ± SEM (nM)
Bestatin	2370 ± 350	1530 ± 58
Tosedostat	1180 ± 8	6150 ± 275
1	118 ± 3	331 ± 12

In order to understand the mechanism by which **1** was able to inhibit both APN and *Pf*A-M1, we investigated the interactions the compound made with the active site of the enzymes. To do this, we used the X-ray crystal structure of *Pf*A-M1 bound to compound **1** (PDB ID 4ZX4)[44] as a scaffold to dock **1** into the active site of APN (PDB 4FYQ).[4] The catalytic domains of the two proteins share 24 % sequence identity and have an RMSD of only 1.244 Å (over 257 Cα atoms in domain II). The co-crystal structure of **1** bound to *Pf*A-M1 revealed extensive water-mediated interactions of the 3,4,5-trifluorophenyl ring with backbone residues located at the S1 substrate binding pocket, as well as key hydrophobic interactions with the biaryl system of **1** (Figure 2A).[44] Our docking analysis of **1** bound to APN showed a similar pose to that observed when bound to *Pf*A-M1 (Figure 2B). Each of the poses obtained from docking **1** were similar and showed the 3,4,5-trifluorophenyl ring in the same position, located deep within the S1 pocket of APN and minor rotations of the position of the *N*-pivaloyl group were observed. In general, there were significantly less interactions observed between **1** and the active site residues of APN than that of *Pf*A-M1 (Figure 2B).

To evaluate any potential dynamics of **1** bound within the active site of APN as well as any effect from water-mediated interactions, we performed molecular dynamics (MD) simulations of **1** docked into APN. Molecular modelling for metallo-proteins presents significant challenges and traditional force-fields are often not appropriate for simulation.[47] In the case of APN, the presence of zinc in the active site means that this problem cannot be computationally ignored. Recently, our team produced the necessary parameters to use the zinc Amber force-field (ZAFF) to simulate the active site of *Pf*A-M1.[48, 49] We used this system to simulate our docking of APN bound to **1**. MD simulations (n=3) were performed for the duration of 50 ns, which should be sufficient to observe the movements of small molecules. The results were surprising and showed that in two of the three MD runs, **1** experienced significant movement within the active site (Figure S2). Investigation into the motion of **1** indicated that the 3,4,5-trifluorophenyl ring engaged in interactions with a single water molecule and largely maintained face-face stacking interactions with relatively rigid Phe[472] at the S1 pocket of APN (Figure

2C). In addition, the pivaloyl group was facing the aromatic sidechain of Tyr^{477} residue. We hypothesised therefore that compounds that are capable of improved interactions in the S1′ subsite, as well as extend further to engage residues beyond the S1' pocket of APN may contribute to improved inhibitory activity toward APN. To this end, we turned our attention to residues Tyr^{477}, Arg^{381}, and Arg^{442} that are located within the S1′ and beyond the S1′ pocket of APN, and that may allow the formation of hydrophobic interactions as well as polar interactions with inhibitor compound(s).

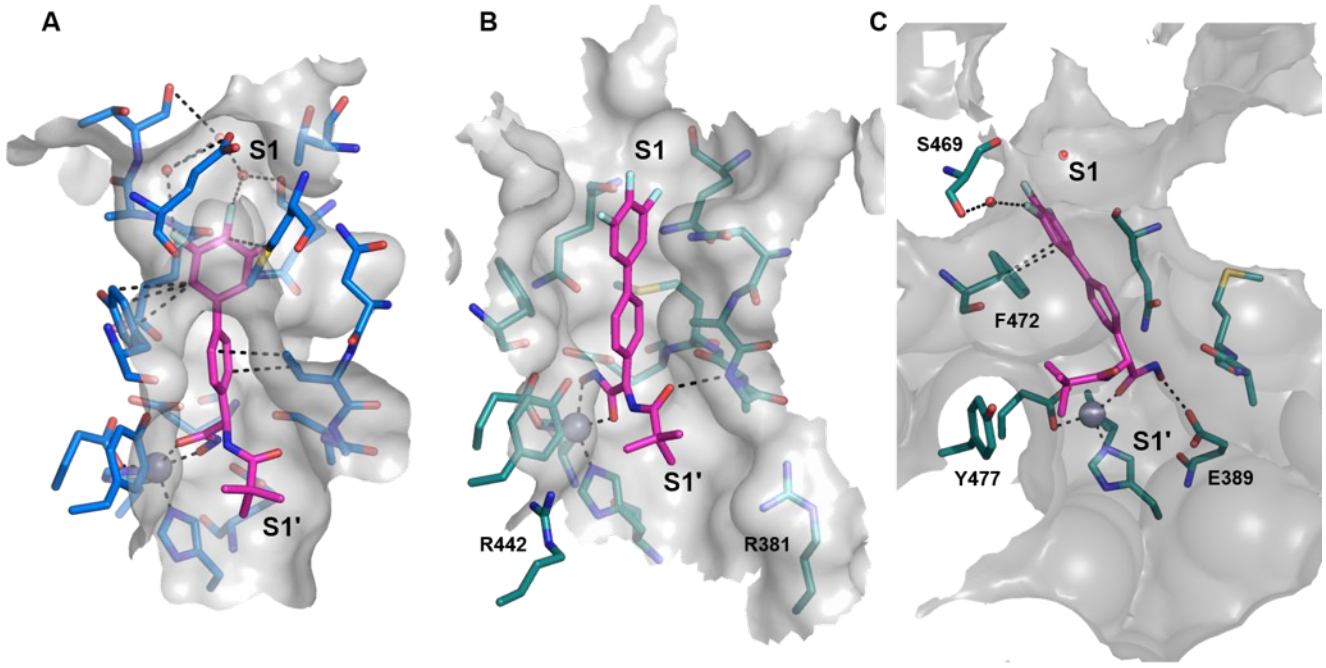

Figure 2. (A) X-ray crystal structure of **1** bound to *Pf*A-M1 (PDB ID 4ZX4). (B) A predicted binding pose of **1** bound to APN obtained from docking (PDB ID 4FYQ). (C) MD simulation of **1** docked to APN showed that the trifluorophenyl group formed stable interactions in the S1 pocket. The ligand is shown in magenta and residues of *Pf*A-M1 and APN are coloured in blue and dark green, respectively. Interactions between the ligand and proteins are depicted as black dashed lines. The zinc is represented by the grey sphere.

Substitution of the *N*-pivaloyl group to optimize binding at the S1′ subsite of APN. The molecular modelling revealed the potential to achieve an enhanced binding interactions at, and beyond, the S1′ pocket of APN by replacing the *N*-pivaloyl group of **1** with aromatic groups which target the Tyr^{477} residue. We designed and produced a series of hydroxamic acid analogues that contained elongated alkyl and aryl linkers to reach deeper into the pocket (Figure 3). Various hydrogen bonding groups were also incorporated to capture additional interactions with Arg^{381} or Arg^{442} residues and improve inhibition activities of the designed compounds. In addition, we were interested to investigate the effect of various heteroaromatic groups, such as indole and indoline. Analogues with benzyl linkers that contain an additional methylene group were also designed to increase flexibility and allow the phenyl group to penetrate more deeply beyond the S1′ pocket.

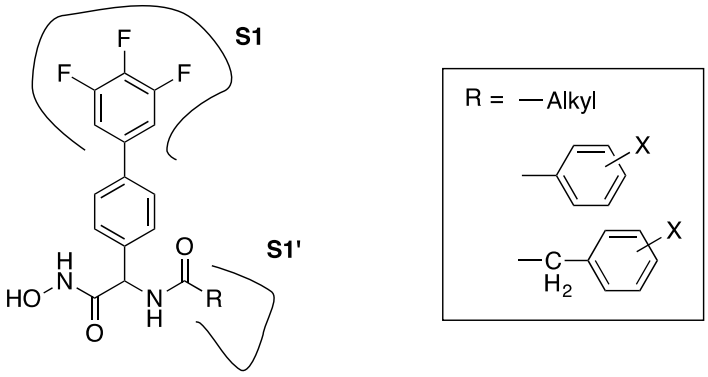

Figure 3. Structures of targeted hydroxamic acid analogues.

Chemistry. The synthesis of the key intermediate, the phenyl glycine derivative **4** (Scheme 1), was adapted from Mistry *et al*.[46] Installation of the 3,4,5-trifluorophenyl ring was successfully achieved using a Suzuki coupling reaction between 4′-bromoacetophenone and (3,4,5-trifluorophenyl)boronic acid under reported conditions producing acetophenone **2** in excellent yield (99%).[44] Oxidation of **2** with selenium dioxide in anhydrous pyridine[50] afforded the corresponding *α*-keto acid **3** in quantitative yield. The product produced from the reductive amination of **3** underwent an acid-catalysed esterification and subsequent debenzylation to successfully afford key precursor **4** in 47% yield over three steps.

The key intermediate (**4**) was then used to incorporate a range of functionalities in place of the *N*-pivaloyl group present in **1**, which was predominately achieved with traditional peptide coupling reagents such as HCTU or EDCI. The first synthetic attempt to obtain benzamide analogues **5r** and **5s** involved in the synthesis of their respective acid chlorides *in situ*, then subsequent acylation with intermediate **4**. However, benzonitriles **5n** and **5o** were produced instead by dehydration of the carboxamide group. Ring-opening reactions of cyclic acid anhydrides were also performed to synthesise alkyl carboxylate analogues. Cyclic anhydrides such as succinic anhydride and Meldrum's acid have been commonly used in literature to form amide bonds through ring-opening reactions.[51-59] The butyric acid analogue (**5e**) was synthesised from intermediate **4** via nucleophilic attack on the carbonyl π system present in succinic anhydride. Subsequent PyBOP amide coupling of **5e** converted the acid moiety to the corresponding carboxamide **5f**. However, reaction with Meldrum's acid under identical reaction conditions resulted in decarboxylation, generating the acetamide analogue (**5a**) instead of the expected propionic analogue.

Scheme 1. Synthesis of hydroxamic acid inhibitors[a]

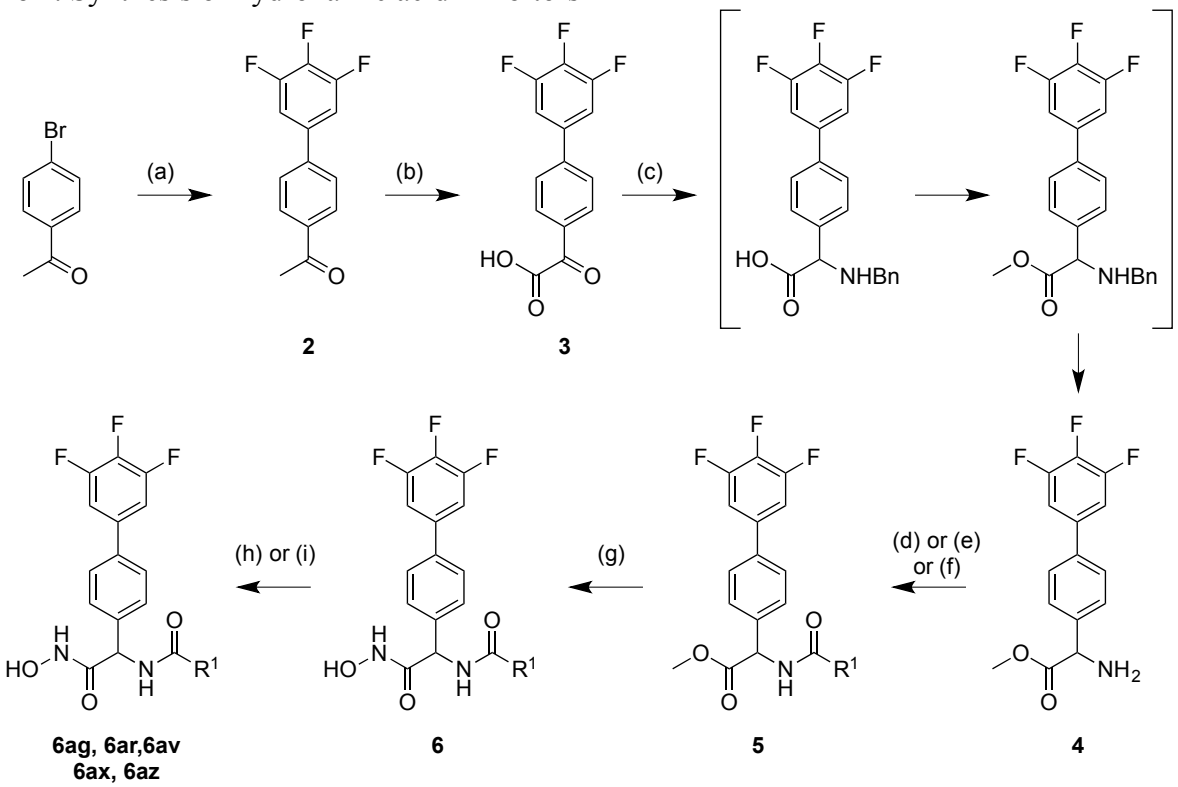

a	$-CH_3$	**r**	$-C_6H_4C(O)NH_2$ (*m*)	**aj**	-indol-5-yl
b	$-CH_2C(O)O^tBu$	**s**	$-C_6H_4C(O)NH_2$ (*p*)	**ak**	-indazol-5-yl
c	$-CH_2C(O)OH$ (**6c** from **5b**)	**t**	$-C_6H_4C(O)NHMe$ (*p*)	**al**	-benzotriazol-5-yl
d	$-CH_2C(O)NHOH$ (**6d** from **5b**)	**u**	$-C_6H_4C(O)NMe_2$ (*p*)	**am**	-benzimidazol-5-yl
e	$-CH_2CH_2C(O)OH$	**v**	$-C_6H_4C(O)NHEt$ (*p*)	**an**	-(2-oxoindolin-5-yl)
f	$-CH_2CH_2C(O)NH_2$	**w**	$-C_6H_4C(O)NH^iPr$ (*p*)		
		x	$-C_6H_4C(O)NHCH_2CH_2OH$ (*p*)	**ao**	$-CH_2C_6H_5$
g	$-C_6H_5$	**y**	$-C_6H_4SO_2NH_2$ (*p*)	**ap**	$-CH_2C_6H_4F$ (*m*)
h	$-C_6H_4F$ (*m*)	**z**	$-C_6H_4NHBoc$ (*m*)	**aq**	$-CH_2C_6H_4F$ (*p*)
i	$-C_6H_4F$ (*p*)	**aa**	$-C_6H_4NHBoc$ (*p*)	**ar**	$-CH_2C_6H_4OMe$ (*p*)
j	$-C_6H_4OMe$ (*m*)	**ab**	$-C_6H_4NH_2$ (*m*) (**6ab** from **5z**)	**as**	$-CH_2C_6H_4OH$ (*p*) (**6as** from **6ar**)
k	$-C_6H_4OMe$ (*p*)	**ac**	$-C_6H_4NH_2$ (*p*) (**6ac** from **5aa**)	**at**	$-CH_2C_6H_4C(O)NH_2$ (*p*)
l	$-C_6H_4OH$ (*m*) (**6l** from **6j**)	**ad**	$-C_6H_4NHSO_2Me$ (*p*)	**au**	$-CH_2C_6H_3$ (3,4-OMe)
m	$-C_6H_4OH$ (*p*) (**6m** from **6k**)	**ae**	$-C_6H_4NHSO_2NH_2$ (*p*)	**av**	$-CH_2C_6H_3$ (3,4-OH) (**6av** from **6au**)
n	$-C_6H_4CN$ (*m*)	**af**	$-C_6H_3$(3,4-OMe)	**aw**	$-CH_2C_6H_3$ (3-F,4-OMe)
o	$-C_6H_4CN$ (*p*)	**ag**	$-C_6H_3$ (3,4-OH) (**6ag** from **6af**)	**ax**	$-CH_2C_6H_3$ (3-F,4-OH) (**6ax** from **6aw**)
p	$-C_6H_4C(NHOH)NH_2$ (*m*) (**6p** from **5n**)	**ah**	$-C_6H_3$(3-F, 4-OH)	**ay**	$-CH_2C_6H_3$ (4-F,3-OMe)
q	$-C_6H_4C(NHOH)NH_2$ (*p*) (**6q** from **5o**)	**ai**	$-C_6H_3$(4-F, 3-OH)	**az**	$-CH_2C_6H_3$ (4-F,3-OH) (**6az** from **6ay**)

[a]Reagents and conditions: (a) 3,4,5-trifluorophenylboronic acid, $Pd(PPh_3)_2Cl_2$, 1 M Na_2CO_3, THF, reflux, 2 h; (b) SeO_2, anhyd. pyridine, reflux, 24 h; (c) (i) benzylamine, $Na(OAc)_3BH$, DCE, rt, 24 h; (ii) conc. H_2SO_4, MeOH, reflux, 24 h; (iii) H_2, 10% Pd/C, cat. HCl MeOH, rt, 24 h; (d) (i) carbamoylbenzoic acid, $(COCl)_2$, DMF, DCM, rt, 1 h; (ii) **4**, DIPEA, DCM, rt, 30 min; (e) carboxylic acid, HCTU, DIPEA, DMF, DCM, rt, 24 h; (f) carboxylic acid, EDCI, DMAP, DCM, rt, 24 h; (g) $NH_2OH.HCl$, 5 M KOH in anhyd. MeOH, rt; (h) 20 % TFA in DCM, rt; (i)1 M BBr_3 in DCM, -78 ºC to rt, 2-24 h.

The methyl ester in **5** was converted to the corresponding hydroxamic acids (**6**) using hydroxylamine hydrochloride and methanolic potassium hydroxide. In some cases, minor conversion to the carboxylic acid through base-mediated hydrolysis was detected. Occasionally, complete conversion to the desired product was not successful due to unexpected side reactions. For instance, LC-MS analysis of the *tert*-butyl propanoate analogue (**5b**) indicated only partial conversion. Interestingly, when more of the reagents were added to the reaction mixture, condensation of both methyl and *tert*-butyl esters occurred, generating the desired mono-hydroxamic acid **6b** and dihydroxamic acid analogue **6d**. For the benzonitrile compounds **5n** and **5o**, nucleophilic attack of hydroxylamine on the electrophilic nitrile carbon resulted in the formation of amidoxime compounds **6p** and **6q**, respectively.[60, 61] The APN inhibitory activity of these unintended analogues was still evaluated due to their potential ability to form hydrogen bonds or ionic interactions at the S1′ pocket. Compounds with acidic functionality (**5c**, and phenolic analogues) showed poor solubility in methanol when deprotonated by potassium hydroxide, which consequently resulted in a longer reaction times and poor reaction yields.

Further deprotection reactions were required in order to produce carboxylic acid **6c**, anilines **6ab** and **6ac** and phenols **6ag**, **6as**, **6av**, **6ax** and **6az**. The *tert*-butyl propanoate analogue (**5b**) and Boc-protected aniline analogues (**5z**, **5aa**) were hydrolysed under mild acidic conditions to give propionic acid **6c** and anilines **6ab** and **6ac**, respectively. *O*-Demethylation was carried out in the presence of boron tribromide to form the corresponding phenols / catechols **6ag**, **6as**, **6av**, **6ax** and **6az**.

In addition to the analogues with an amide linker, a benzylamine analogue (**9**) was also synthesised (Scheme 2). Further physicochemical studies on the parent compound (**1**) indicate it has an aqueous solubility ranging between 12 – 25 μM and a LogD of 3.0.[44] This study demonstrated that there was room to improve its physicochemical properties for optimal pharmacokinetic profiles. Incorporating bulkier groups inevitably increases the hydrophobicity of molecules, consequently decreasing aqueous solubility. However, the introduction of a secondary amine would allow the molecule to be formulated as a salt to overcome solubility issues. As described previously, reductive amination of intermediate **4**

with 4-fluoro-3-methoxybenzylaldehyde yielded **7**, which was converted to the corresponding hydroxamic acid (**8**). The methoxy group in **8** was readily deprotected using boron-tribromide, then reacted with hydrochloric acid to obtain the 4-fluoro-3-hydroxybenzylamine analogue (**9**) as a hydrochloride salt.

Scheme 2. Synthesis of benzylamine analogue **9**[a]

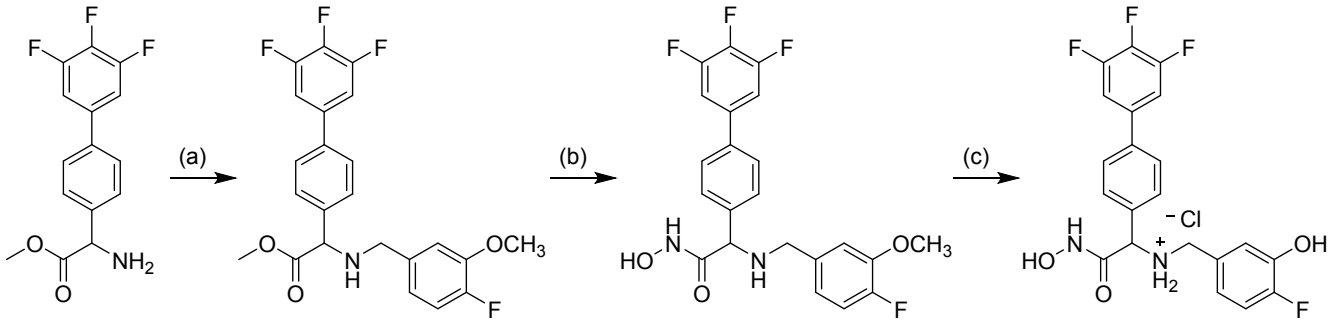

4 **7** **8** **9**

[a]Reagents and conditions: (a) benzaldehyde, $Na(OAc)_3BH$, anhyd. DCE, rt, 24 h; (b) $NH_2OH.HCl$, 5 M KOH in anhyd. MeOH, rt; (c) (i) 1 M BBr_3 in DCM, -78 ºC to rt, 2-24 h; (ii) 1 M HCl, MeOH, rt, 24 h;

A substituted aromatic group is important for potency toward human APN. The inhibitory activity ($K_i^{(app)}$) of the synthesised hydroxamic acids were measured against recombinant human APN (Table 2). Initial experimental triplicates were performed for all compounds to determine compounds of higher priority with $K_i^{(app)}$ value of ≤ 100 nM, which were assessed further in biological triplicate. In general, the aliphatic carboxamides (**6a-f**) were less potent than the lead compound (**1**), but more potent than bestatin and Tosedostat (Table 2). This suggests that the appended carboxylic acid and carboxamide moieties (in the case of **6a**, **6e** and **6f**) were unable to make the intended polar interactions with the S1′ subsite of APN, potentially due to the short linker length. The unsubstituted benzamide **6g** showed over 4-fold loss in inhibitory activity compared to **1**. However, introduction of hydrogen bond donating groups to the phenyl ring led to a recovery in potency. For example, hydroxyl, amidoxime and

carboxamide mono-substituted benzamides **6m-s** were all more potent than compound **1**. On the other hand, hydrogen bond acceptors such as fluorine (**6h** and **6i**) and methoxy (**6j** and **6k**) were not well tolerated. We also examined eight functionalized carboxamides (**6t-x**), sulfonamides (**6y** and **6ad**) and sulfamide (*para*-(sulfamoylamino)benzoic acid) (**6ae**) analogues which have the capacity to increase ligand binding interactions in the S1′ pocket via hydrogen bonding interactions. The benzamide derivatives **6t-x** exhibited a decrease in activity ranging from 2 to 8-fold compared to carboxamide **6s**. A trend of decreasing activity was observed from the benzamide derivatives as the size of hydrophobic group increases from methyl, dimethyl, ethyl and isopropyl, indicating that a loss in polar contacts may result in reduced binding to APN. Additionally, the inhibitory activity of the methyl (**6t**) and dimethyl (**6u**) analogues were essentially identical, suggesting the hydrogen bond donating capability of benzamide does not play a significant role in potency. 4-Methylsulfonamide **6ad** ($K_i^{(app)}$ = 4.5 nM) and sulfamide **6ae** ($K_i^{(app)}$ = 8.2 nM) were the most potent inhibitors of the series and showed a greater than 10-fold improvement in potency compared to **1**, potentially due to its multiple hydrogen bond forming capacity for strong binding interactions with APN.

Among the di-substituted benzamides (**6af-ai**), the fluorohydroxyl analogues (**6ah** and **6ai**) showed improved activity relative to **1**. When compared with the corresponding mono-substituted benzamide derivatives, di-substituted analogues showed stronger inhibition activity. For example, 3-fluorobenzamide **6h** and 4-hydroxybenzamide **6m** displayed activities of 919 nM and 366 nM respectively, whereas the potency of the 3-fluoro-4-hydroxyl analogue (**6ah**) significantly increased to 29 nM, suggesting both fluoro and hydroxyl are making important interactions with APN. A similar result was observed for the 4-fluoro-3-hydroxy analogue (**6ai**), which exhibited significantly greater potency ($K_i^{(app)}$ = 40 nM) than the corresponding mono-substituted analogues; 4-fluorobenzamide **6i** ($K_i^{(app)}$ = 704 nM) and 3-hydroxybenzamide **6l** ($K_i^{(app)}$ = 102 nM). Similarly, the 3,4-dimethoxy analogue (**6af**) exhibited an increased potency compared to 3- and 4-methoxy analogues, **6j** and **6k**, respectively.

The activities of compounds where benzamide was replaced with various heterocyclic amides (**6aj-an**) was also investigated. The indole analogue (**6aj**) was equipotent with the parent compound (**1**). A significant increase in the potency was observed from indazole **6ak** ($K_i^{(app)}$ = 19.2 nM) and benzotriazole **6al** ($K_i^{(app)}$ = 23.4 nM).

In general, replacement of benzamide to acetamide to introduce sp^2 characteristics for increased flexibility resulted into a significant loss in potency (**6ao-ay**). The 3-fluoro-4-hydroxyl analog **6ax** was the only compound in this series that proved to be more potent than **1** with inhibition activity of 43.1 nM. Inconsistent relationships were observed between the benzamide and matching acetamide analogues. For instance, the potency observed for the benzyl analogue (**6ao**) reduced drastically compared to the phenyl analogue (**6g**). This trend was also observed for the 4-methoxy (**6k** and **6ar**), 4-hydroxy (**6m** and **6as**), 4-fluoro-3-hydroxy (**6ai** and **6az**), and 4-benzamide (**6s** and **6at**) pairs. In contrast, an increase in potency was observed for the fluoro analogues (**6h, 6i, 6ap, 6aq**), and 3,4-dimethoxy (**6af** and **6au**), while 3-fluoro-4-hydroxyl compounds **6ah** and **6ax** were the most potent compounds in each series. The 4-fluoro-3-hydroxybenzylamine analogue (**9**) was the weakest inhibitor of this series; full inhibition was not achieved at a concentration of 1 mM, suggesting that carbonyl oxygen of the amide-linker is crucial for potent activity, potentially by providing appropriate rigidity and also hydrogen bonding interaction with nearby residues.

SAR investigations around the S1′ pocket of APN through modifications of the *N*-pivaloyl group of compound **1** indicated that substituted aryls were essential for inhibitory activity, where hydrogen bond donors were more favored than hydrogen bond acceptors. A substantial decrease in activity observed from acetamide and secondary amine analogues revealed that rigidity and the carbonyl oxygen of the benzamide were vital. In addition, studies on functionalized carboxamides and sulfonamides showed that there was a decreasing trend in activity as the size of the hydrophobic group increases while incorporating polar groups led to a significant rise in activity. This suggested that hydrogen bonding interactions played a major role to enhance activity against APN.

Table 2. Summary of inhibitory activity of hydroxamic acid analogues against APN.

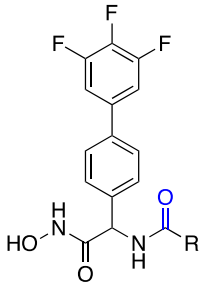

6a-6az

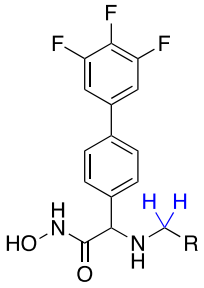

9

Compound	R	$K_i^{(app)}$ ± SEM (nM)
Bestatin	-	2370 ± 350
Tosedostat	-	1180 ± 77
1	-$C(CH_3)_3$	118 ± 3
6a	-CH_3	560 ± 50
6c	-CH_2COOH	188 ± 9
6d	-$CH_2C(O)NHOH$	348 ± 33
6e	-CH_2CH_2COOH	172 ± 9
6f	-$CH_2CH_2C(O)NH_2$	497 ± 35
6g	-C_6H_5	522 ± 37
6h	-C_6H_4F (*m*)	919 ± 160
6i	-C_6H_4F (*p*)	704 ± 68
6j	-C_6H_4OMe (*m*)	462 ± 6
6k	-C_6H_4OMe (*p*)	745 ± 53
6l	-C_6H_4OH (*m*)	366 ± 31
6m	-C_6H_4OH (*p*)	102 ± 5
6p	-$C_6H_4C(NHOH)NH_2$ (*m*)*	37.3 ± 2.9
6q	-$C_6H_4C(NHOH)NH_2$ (*p*)*	49.1 ± 3.7
6r	-$C_6H_4C(O)NH_2$ (*m*)	71.2 ± 6.5
6s	-$C_6H_4C(O)NH_2$ (*p*)*	82.1 ± 9.8
6t	-$C_6H_4C(O)NHMe$ (*p*)	185 ± 22
6u	-$C_6H_4C(O)NMe_2$ (*p*)	182 ± 5
6v	-$C_6H_4C(O)NEt$ (*p*)	277 ± 22
6w	-$C_6H_4C(O)NH^iPr$ (*p*)	631 ± 70
6x	-$C_6H_4C(O)NHCH_2CH_2OH$ (*p*)	163 ± 26
6y	-$C_6H_4SO_2NH_2$ (*p*)	240 ± 7
6ab	-$C_6H_4NH_2$ (*m*)	131 ± 10
6ac	-$C_6H_4NH_2$ (*p*)	205 ± 17
6ad	-$C_6H_4NHSO_2Me$ (*p*)*	4.50 ± 0.80
6ae	-$C_6H_4CNHSO_2NH_2$ (*p*)*	8.20 ± 0.90
6af	-C_6H_3 (3,4-OMe)	175 ± 16
6ag	C_6H_3 (3,4-OH)	430 ± 42
6ah	-C_6H_3 (3-F,4-OH)*	29.1 ± 3.6

6ai	-C_6H_3 (4-F,3-OH)*	40.0 ± 2.2
6aj	-indol-5-yl	111 ± 3
6ak	-indazol-5yl*	19.2 ± 2.5
6al	-benzotriazol-5-yl*	23.4 ± 2.3
6am	-benzimidazol-5-yl*	170 ± 17
6an	-(2-oxoindolin-5-yl)	156 ± 9
6ao	-$CH_2C_6H_5$	4420 ± 720
6ap	-$CH_2C_6H_4F$ (*m*)	442 ± 36
6aq	-$CH_2C_6H_4F$ (*p*)	158 ± 5
6ar	-$CH_2C_6H_4OMe$ (*p*)	978 ± 120
6as	-$CH_2C_6H_4OH$ (*p*)	235 ± 24
6at	-$CH_2C_6H_4C(O)NH_2$ (*p*)	604 ± 66
6au	-$CH_2C_6H_3$ (3,4-OMe)	119 ± 12
6av	-$CH_2C_6H_3$ (3,4-OH)	137 ± 6
6ax	-$CH_2C_6H_3$ (3-F,4-OH)	43.1 ± 5.0
6az	-$CH_2C_6H_3$ (4-F,3-OH)	138 ± 5
9	-$CH_2C_6H_3$ (4-F,3-OH)[a]	>1 mM

* Biological triplicates were performed for inhibitors with $K_i^{(app)}$ less than 100 nM from initial triage screenings. [a] The compound is secondary amine derivative.

The core biaryl system engages in hydrophobic interactions with flexible loop at the S1 pocket of APN. To understand why **6ad** and **6ae** displayed such an improvement in potency, we undertook molecular docking followed by MD simulations to generate a model of APN bound to both inhibitors. A rigid-docking into the APN crystal structure (PDB ID 4FYQ) of compounds **6ad** and **6ae** was performed based on the docked pose of compound **1** into APN using Surflex Docking software available from Sybyl 2.1. The common fragments of the biphenyl core structure and the hydroxamic group were set as constraints. Similar to the molecular docking of compound **1**, the most preferred structures of **6ad** and **6ae** bound to APN were selected based on the total docking score (Table S6). MD simulations showed that the ligands occupy different conformations in a time-dependent manner (Supp Movie 1 and 2). Compound **6ad** participated in water-mediated hydrogen bonding interactions with the fluorine atoms and the nearby residues at the S1 subsite of APN, both of which were

also observed in the co-crystal structure of compound **1** bound to *Pf*A-M1.[44] One compelling result from the MD simulation was a flexible loop located at domain IV acting as an effective 'cap' to close the active site of APN (Figure 4). The flexible loop and the Phe^{896} residue are believed to have important roles in conformational changes of APN.[4] The flexible loop consists of 8 amino acid residues (^{891}YGGGSFSF^{898}) and has been shown to undergo a dramatic change in conformation upon complex formation with a peptide substrate.[4] The binding mode of bestatin, which binds APN differently to other M1 aminopeptidases (non-canonical binding pose), is also thought to be related to the flexible loop, in particular Phe^{896}. As opposed to other M1-bestatin complexes in which the loop is shorter and different in sequence and therefore does not impede bestatin from binding with canonical geometry, the Phe^{896} of APN was positioned away from binding pocket to accommodate the bulky phenyl group of bestatin at the S1 pocket.[4] In our simulations, we saw that the biphenyl ring system of **6ad** maintained face to face stacking interactions with Phe^{896} to keep the inhibitor locked in the active site of APN, however, it was clear that this interaction varied within the biphenyl system between different poses. Generally, the sidechain of Phe^{896} interacted with the top trifluorophenyl (Figure 4B and C), but interactions with the central aromatic ring of compound **6ad** were also observed (Figure 4A).

Interestingly, stable hydrophobic stacking interactions between the flexible loop and compound **6ae** were not observed (Figure 4). Without the flexible loop stabilising the biaryl core moiety and restricting the movement of the molecule the flat biphenyl system of **6ae** gained freedom to move within S1 pocket.

Although prominent stacking interactions that were observed with **6ad** were missing from **6ae**; the phenylalanine rich region provided a favorable environment for the hydrophobic biaryl group to maintain its overall position within the pocket.

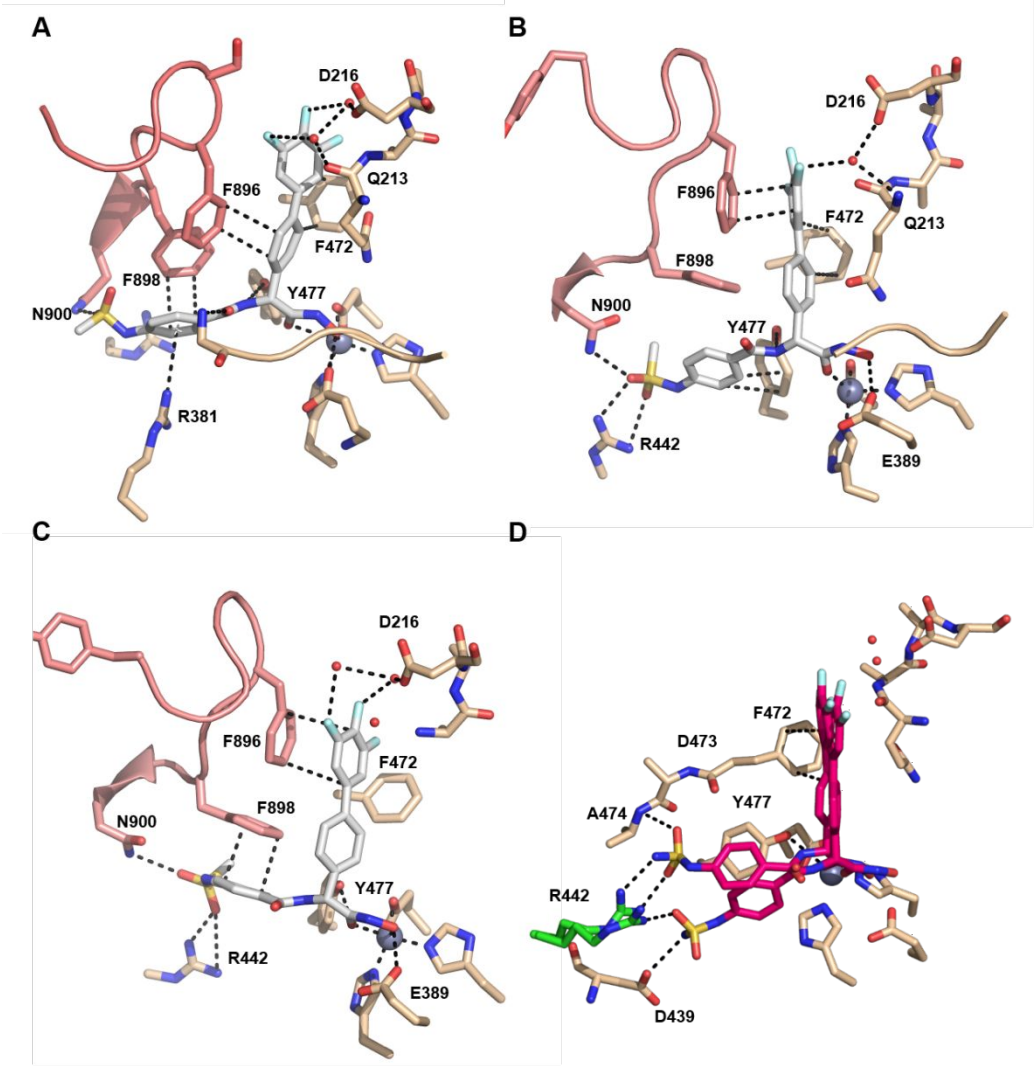

Figure 4. Three conformations of compound **6ad** (A, B and C) observed during MD simulation. The carbon atoms of the flexible loop is coloured in light pink, and other residues in the binding site are coloured in wheat. Interactions between compound **6ad** (carbon atoms in white) and APN are shown in black dashed lines. (D) Overlay of two predicted binding poses of compound **6ae**. Residues around compound **6ae** (carbon atoms in magenta) are coloured in wheat (PDB ID 4FYQ). Overlaid Arg^{442} residues are shown in green. Interactions between the compound and APN are depicted in black dashed lines.

Sulfonamide moiety provides multiple hydrogen bonding interactions at the S1′ pocket of APN. Based on our MD simulations, the large arylsulfonamide derivatives of both **6ad** and **6ae** were able to reach the S1′ pocket of APN. The bottom aromatic group of **6ad** was flexible enough to interact with the sidechain of Phe[898] or Tyr[477] (Figure 4A, B, and C). Due to the high flexibility of the sulfonamide moiety, these interactions were occasionally lost and replaced with a cation–π interaction between the Arg[381] sidechain and the electron-rich aromatic ring of arylsulfonamide. The results also revealed that the sulfonyl oxygen atoms can engage in dual hydrogen bonds with Asn[900] and Arg[442] (Table S3), where the arginine residue stayed in a relatively rigid manner throughout simulations.

Compound **6ae** behaved similarly to **6ad**, exhibiting multiple binding positions. The aromatic ring located in the S1′ pocket of APN displayed extensive interactions with the side chain of Arg[442] and Asn[900]. As described above, the flexible loop was not accessible to the molecule, but the bottom aromatic was located closer to Tyr[477], forming hydrophobic edge-face stacking interactions (Figure 4D). The backbone amide of Ala[474] could also participate in a hydrogen bond interaction with a sulfonyl oxygen atom of **6ae** (Table S4). In the case where the sulfamide was pointing deeper into the S1′ subsite of APN, the amino group is located in close proximity to Asp[439].

In order to rationalise our SAR analysis, we also investigated the interactions between one of the weaker inhibitors, **6ag** ($K_i^{(app)}$ = 430 nM) which contains 3,4-hydroxyl group (Figure 5). In contrast to compounds **6ad** and **6ae** which showed extensive hydrophobic interactions with the flexible loop, the biphenyl system of compound **6ag** made no interactions with the key phenylalanine residues of the flexible loop. Throughout most of the simulation, the trifluorophenyl moiety participated in a water-mediated hydrogen bonding network with Ser[469] and hydrophobic interactions between Phe[472]. However, the flexible loop was located too far away from the biphenyl system to capture essential non-polar interactions, which may explain the significant decrease in the potency. Hydrogen bonding interactions between the catechol group and the sidechain of Glu[418] residue were also observed. However these interactions appear not able to compensate the missing stacking interactions between the S1′ aromatic

group and Tyr[477] or the Phe[898] residues, which may contribute to the reduced inhibition activity of **6ag** against APN.

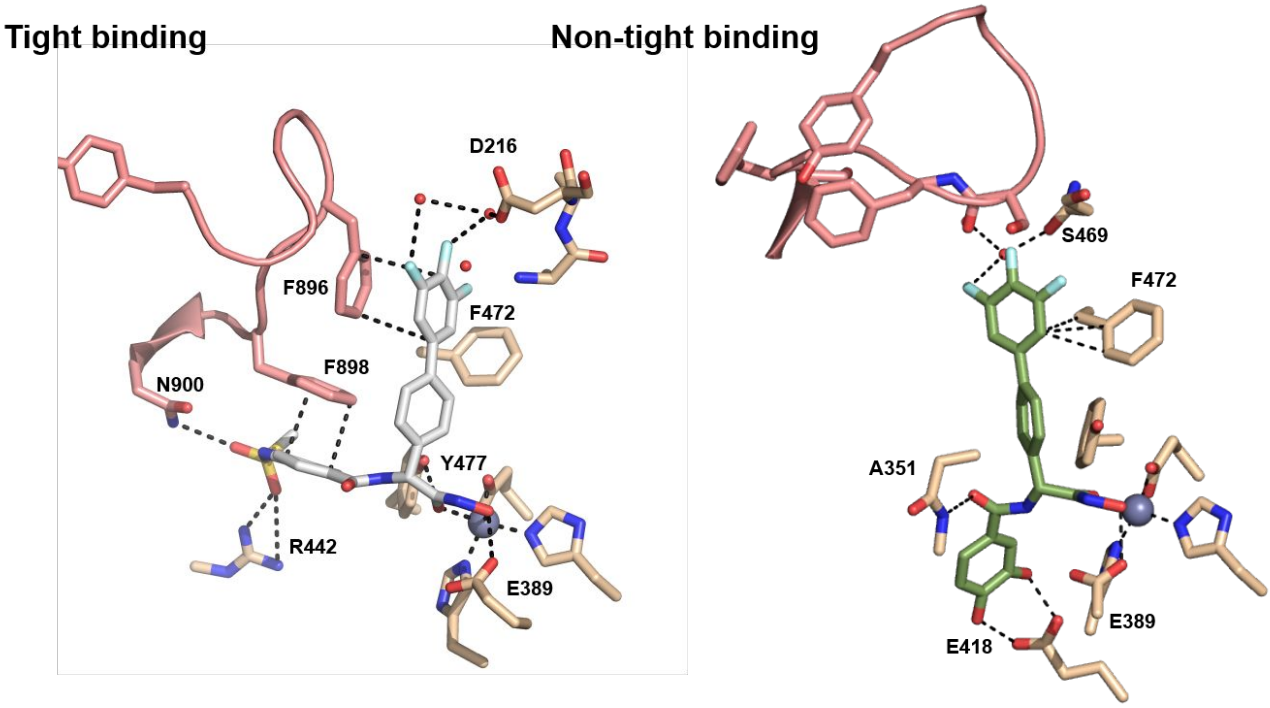

Figure 5. Comparison of the binding interactions occurred with tight binding inhibitor **6ad** (left) and the weaker inhibitor **6ag** (right) (4FYQ). The carbon atoms of the flexible loop is coloured in light pink, and other residues in the binding site are coloured in wheat. Compound **6ad** and **6ag** are coloured in white and green, respectively. Interactions between the ligands and APN are shown in black dashed lines.

Role of Glu[389] residue as the zinc-hydroxamic acid complex stabiliser. Another intriguing phenomenon was observed from the formation of the zinc-hydroxamic acid complex. In the M1 aminopeptidases, inhibitors often bind with a pentahedral coordination to the zinc, which mimic the transition state of the activated enzyme.[4, 62] In the simulations we performed, the hydroxyl group of hydroxamic acid readily lost contact with the zinc, with bond distance ranging from 2.2–3.4 Å while the carbonyl oxygen possessed a very stable coordination with a bond distance of 1.9–2.0 Å, resulting in tetrahedral coordination. Given the challenges associated with metallo-protein simulations, this observation is possibly biased by the ZAFF parameters used. To accurately simulate the change in ligand

interaction with the zinc ion, a quantum mechanics / molecular mechanics (QM/MM) simulation would be needed. However, we did observe was that the loss of pentahedral coordination of **6ad** and **6ae** to the zinc ion resulted in the formation of a hydrogen bond with Glu^{389} (Figure 6). This interaction was extremely stable and maintained a bond distance of 2.4 – 2.9 Å throughout our simulations (Table S3 & S4). Further computational and experimental investigation is required to determine whether this interaction plays a role in the catalytic mechanism by stabilizing the zinc-ligand complex.

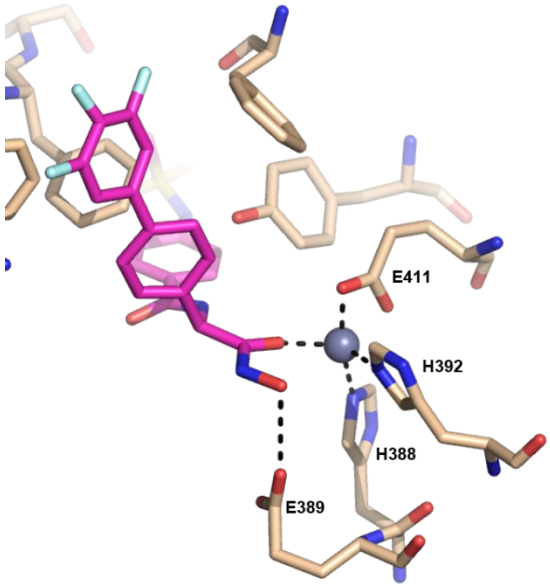

Figure 6. Hydroxamic acid – zinc complex in the active site of APN. APN residues are coloured in wheat and the ligand is shown in magenta. Interactions between the ligand and the catalytic triad and Glu^{389} are illustrated in black dashed lines (PDB ID 4FYQ).

Compound 6ad and 6ae show selectivity for APN over matrix metalloproteinases (MMPs). As the hydroxamic acid moiety is a strong zinc chelator there is a possibility that our potent APN inhibitors may interact with other zinc-dependent enzymes. To assess the selectivity and potential off-targets effects of **6ad** and **6ae**, we performed quenched fluorescence assays with MMP2, 7, 8, 9, and 13 (Supp

Figure S1). The activity of the parent compound (**1**), Tosedostat and the broad spectrum MMP inhibitor, Marimastat, were also evaluated as comparison and controls (Supp Table 1). MMP2 and 9 were effectively inhibited by Marimastat (IC_{50} 0.43 and 3.1 nM, respectively) and weakly by Tosedostat (IC_{50}: 0.19 and 1.5 μM, respectively), whereas **6ad** and **6ae** weakly inhibited MMP2 (1.3 μM and 2.1 μM respectively) and only inhibited MMP9 at relatively high concentrations (IC_{50} >100 μM). Similar observations were made for collagenases MMP8 and MMP13 as well as matrilysin MMP7, which were all inhibited with low nM IC_{50} by Marimastat, high nM IC_{50} by Tosedostat, and μM – mM IC_{50} by the novel inhibitors, with **1** demonstrating the lowest extent of inhibition (Supp Figure S1). Collectively, these findings show that the novel APN inhibitors demonstrate low off-target inhibitory effects on MMPs.

Cellular toxicity, physicochemical and pharmacokinetic properties of 6ad and 6ae. Evaluation of cellular toxicity, physicochemical and stability properties provide important early stage data to determine whether or not a compound has the necessary features to be pursued further as a drug candidate. In our cellular toxicity study, we used Ad293 cell line, which was used to measure cell toxicity in other reported literature, is derived from the Human Embryonic Kidney 293 (HEK293) cell line but transfected with a special gene for improved cell adherence to make handling cells easier during cell cultures and assays.[63] The compounds show limited cytotoxicity against Ad293 cells with CC_{50} values of 41 ± 2 μM for **6ad** and 149 ± 13 μM for **6ae**. *In vitro* physicochemical properties and metabolic/plasma stabilities of two potent APN inhibitors **6ad** and **6ae** were measured (Table 4). The kinetic solubility of each compound was determined by nephelometry. Both compounds showed moderate solubility under pH conditions representative of the stomach (pH 2) and upper fasted state small intestine (pH 6.5) suggesting that solubility could be a factor that limits oral absorption. The

partition coefficients at pH 7.4 ($LogD_{pH\ 7.4}$) were estimated using a chromatographic method and found to be 2.8 and 2.6, respectively. The metabolic stabilities were assessed by incubating compounds in mouse and human hepatic microsomes at 37 ºC and a protein concentration of 0.4 mg/mL. The compounds showed minimal degradation and very long half-lives of longer than 4 h in both mouse and human microsomes, resulting in low *in vitro* intrinsic clearance values (CL_{int} < 7 µL/min/mg protein). *In vitro* plasma stability studies were performed by incubating compounds in human and mouse plasma at 37 °C for up to 4 h. Both compounds displayed minimal loss indicating that they are not readily susceptible to the action of hydrolytic enzymes present in the plasma.

Table 4. Physicochemical and metabolic properties of **6ad** and **6ae**.

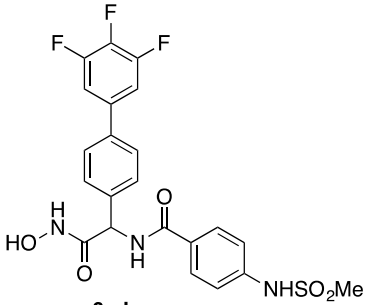

6ad

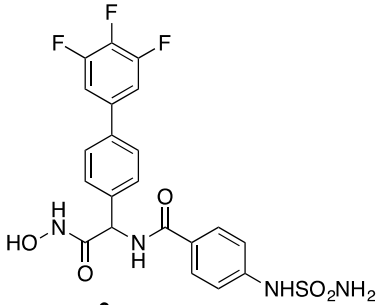

6ae

Compound	Kinetic Solubility		Liver Microsome Stability		Plasma Stability	
	$Sol_{pH\ 2.0}$	$Sol_{pH\ 6.5}$	Mouse $t_{1/2}$ (min)	Human $t_{1/2}$ (min)	Mouse $t_{1/2}$ (min)	Human $t_{1/2}$ (min)
6ad	12.5-25	12.5-25	>250	>250	>1020	>1020
6ae	6.3-12.5	12.5-25	>250	>250	>1020	>1020

■ CONCLUSIONS

Rapid metastasis of cancer cells through complex mechanisms of ECM degradation, angiogenesis, cell invasion and cell adhesion is a major burden in effective cancer therapy. Therefore, continuous development of novel anti-cancer agents targeting metastasis is urgently required. Being involved in mechanisms of angiogenesis and metastasis, APN has been broadly studied as a therapeutic target for cancer. Here we have reported the design, synthesis and biological evaluations of novel APN inhibitors that were derived from a potent inhibitor of parasitic homologue *Pf*A-M1. Through comprehensive structure-based design, we were able to generate a small library of novel hydroxamic acid analogues targeting APN and discover a potent compound **6ad** that showed 527-fold improved inhibition activity than a known APN inhibitor bestatin. Molecular docking and MD simulations highlighted the significance of the flexible loop in domain VI in providing hydrophobic interactions at the S1 pocket. The results also revealed the combination of stacking and dual-hydrogen bonding interactions was crucial to optimize the binding at the S1′ subunit of APN. In addition, cross-activity studies showed that **6ad** and **6ae** possessed low off-target activity on MMPs. The evaluation of the cellular activities of **6ad** and **6ae** against Ad293 cell line also indicated that they displayed limited cytotoxicity. Moreover, **6ad** and **6ae** had favorable metabolic and plasma stability in both human and mouse models. However, the solubility of these compounds is sub-optimal and should be addressed by further medicinal chemistry approaches.

■ EXPERIMENTAL SECTION

Chemistry. Chemicals and solvents were purchased from standard suppliers and used without further purification unless otherwise indicated. ^{1}H NMR, ^{19}F NMR and ^{13}C NMR spectra were recorded on a Bruker Avance Nanobay III 400 MHz Ultrashield Plus spectrometer at 400.13, 376.46 and 100.61 MHz, respectively. NMR experiments were obtained at the temperature of 298 K. Data acquisition and processing was managed using Topspin software package version 3. Chemical shifts (δ) are recorded in parts per million with reference to the chemical shift of the deuterated solvent. Coupling constants (*J*) and carbon-fluorine coupling constants (J_{CF}) are recorded in hertz and multiplicities are described as singlet (s), doublet (d), triplet (t), multiplet (m), doublet of doublets (dd), doublet of triplets (dt), doublet of doublets of doublets (ddd), and broad (br). Overlapped non-equivalent ^{13}C peaks were identified by HSQC and HMBC NMR.

Analytical thin-layer chromatography (TLC) was performed on Merck silica gel 60F^{254} aluminium-backed plates and were visualised by fluorescence quenching under UV lamp at 254 nm or by Fe(III)Cl_3 staining for hydroxamic acid compounds. Flash chromatography was performed with silica gel 60 (particle size 0.040–0.063 μm).

Analytical HPLC was performed using an Agilent 1260 Infinity Analytical HPLC with a Zorbax Eclipse Plus C18 Rapid Resolution 4.6 × 100 mm, 3.5 μm column. Buffer A: 0.1 % TFA in H_2O and buffer B: 0.1 % TFA in MeCN were used. Samples were run at a gradient of 5% buffer B/ buffer A (0−9 min) to 100% buffer B (9−10min) at a flow rate of 1 mL/min. Unless otherwise indicated, all compounds were > 95% by HPLC (254 nm and 214 nm) prior to biological evaluation.

Preparative HPLC was performed using an Agilent 1260 Infinity instrument coupled with a binary preparative pump and an Agilent 1260 FC-PS fraction collector using Agilent OpenLAB CDS software (revision C.01.04) and an Altima C8 22 × 250 mm, 5 μM column and a 1260 Infinity diode array detector

VL. The following buffers were used: buffer A: 0.1% TFA in H_2O and buffer B: 0.1% TFA in MeCN. The sample was run at a gradient of 30% to 100% buffer B over 10 min at a flow rate of 20 mL/min.

LC-MS was performed using system A or B. System A: Agilent 6100 Series Single Quadrupole instrument coupled to an Agilent 1200 series HPLC instrument fitted with a Luna 120 C8(2) 5 µ 50 × 4.6 mm column. Samples were run at a flow rate of 0.5 mL/min for 12 min: 5% buffer B/ buffer A (0−4 min), 100% buffer B (4−7 min) and 5% buffer B/ buffer A (7−12 min). Mass spectra were obtained in positive and negative ion modes with a scan range of 100-1000 *m/z*. UV detection was carried out at 254 nm. System B: Agilent 6120 series Single Quadrupole instrument coupled to an Agilent 1260 series HPLC instrument fitted with a Poroshell 120 EC-C18 50 × 3.0 mm, 2.7 µm column. The following buffers were used: buffer A, 0.1% formic acid in H_2O; buffer B, 0.1% formic acid in MeCN. Samples were run at a flow rate of 0.5 mL/min for 5 min: 5% buffer B/ buffer A (0−1 min), 100% buffer B (1−2.5 min) and held at this composition until 3.8 min, 5% buffer B/ buffer A (3.8−4 min) and held until 5 min at this composition. Mass spectra were obtained in positive and negative ion modes with a scan range of 100-1000 *m/z*. UV detection was carried out at 214 and 254 nm.

HRMS was carried out using an Agilent 6224 TOF LC-MS mass spectrometer coupled to an Agilent 1290 Infinity. All data were acquired and referenced via dual-spray electrospray ionization (ESI) source. Acquisition was performed using Agilent Mass Hunter Data Acquisition software version B.05.00 Build 5.0.5042.2 and analysis was conducted using Mass Hunter Qualitative Analysis version B.05.00 Build 5.0.519.13.

Instant JChem was used for data management; Instant JChem 16.9.12.0, ChemAxon (http://www.chemaxon.com).

General Procedure A: Amide coupling using HCTU and DIPEA. The carboxylic acid (1.1 eq.) and HCTU (1.2 eq.) were dissolved in anhydrous DMF (2 mL/mmol) and stirred for 30 min in a N_2 flushed microwave vial. DIPEA (2.1eq.) was added dropwise followed by compound **4** (1.0 eq.) in

anhydrous DCM (2 mL/mmol). The reaction mixture was stirred at rt for 1 d. If the reaction did not reach completion after 1 d, then a further 1.2 eq. HCTU and 2.1 eq. DIPEA was added. After completion, the reaction mixture was diluted with sat. $NaHCO_3$ (10 mL) and extracted with DCM (3 × 15 mL). The combined organic layers were washed with water (2 × 10 mL) and brine (15 mL). The organic layer was dried over anhydrous Na_2SO_4, filtered and concentrated *in vacuo*. The crude was purified by column chromatography using either DCM:MeOH or PE:EtOAc as the eluent.

General Procedure B: Amide coupling using EDCI and DMAP. Compound **4** (1.0 eq.), carboxylic acid (1.2 eq.), EDCI (1.2 eq.) and DMAP (1.3 eq.) were dissolved in DCM (8 mL/mmol) or DMF (8 mL/mmol) and stirred at rt overnight. If the reaction did not reach completion, then a further 1.2 eq. EDCI and 1.3 eq. DMAP was added. The reaction mixture was diluted with sat. $NaHCO_3$ (10 mL) and extracted with DCM (3 × 10 mL). The combined organic layers were washed with a 1 M HCl solution (15 mL), dried over anhydrous Na_2SO_4, filtered and concentrated *in vacuo*. The crude residue was purified by column chromatography using PE:EtOAc as the eluent.

General Procedure C: Direct aminolysis of methyl ester to the hydroxamic acid. To a solution of the methyl ester (1.0 eq.) in anhydrous MeOH (3 mL/mmol) was added NH_2OH•HCl (4-10 eq.), followed by KOH (5M in MeOH, 5-10 eq.). The reaction mixture was stirred at rt and was monitored by LCMS and TLC using an $Fe(III)Cl_3$ stain. Once the reaction was complete, the suspension was dry-loaded onto silica and purified by column chromatography.

General Procedure D: *O*-Demethylation using BBr_3. To a solution of the methyl ether substrate (1.0 eq.) in DCM (2 mL/mmol) was added BBr_3 (1 M in DCM, 5.0 eq. for mono *O*-demethylation, 10.0 eq. for double *O*-demethylation) at -78 ºC. The reaction mixture was stirred at rt for 2 h to 1 d. The reaction was quenched by the addition of a 1 M HCl and stirred vigorously for 10 min. The resulting precipitate was filtered and purified by preparative HPLC.

1-(3',4',5'-Trifluoro-[1,1'-biphenyl]-4-yl)ethan-1-one (2). To a nitrogen flushed 500 mL round bottom flask was added 4'-bromoacetophenone (5.00 g, 25.1 mmol), 3,4,5-trifluorophenylboronic acid (5.74 g,

32.7 mmol), anhydrous THF (180 mL) and a 1 M Na_2CO_3 solution (60 mL). $PdCl_2(PPh_3)_2$ (529 mg, 0.754 mmol) was added and the mixture was heated at reflux for 2 h. The reaction mixture was concentrated under reduced pressure and extracted with Et_2O (3 × 50 mL). The combined organic layers were dried over anhydrous Na_2SO_4, filtered and concentrated *in vacuo*. The crude product was purified by column chromatography (PE:EtOAc 100:0 to 50:50) to afford compound **2** as a yellow-brown solid (6.29 g, 100%); ^{1}H NMR (d_6-DMSO) δ 8.03 (d, J = 8.6 Hz, 2H), 7.89 (d, J = 8.5 Hz, 2H), 7.80 (dd, J = 9.6, 6.8 Hz, 2H), 2.62 (s, 3H); ^{19}F NMR (d_6-DMSO) δ -134.6 (d, J = 21.7 Hz), -162.1 (dd, J = 21.7/21.7 Hz); ^{13}C NMR (d_6-DMSO) δ 197.5, 150.6 (ddd, J_{CF} = 247.0/9.8/4.2 Hz), 141.1–141.0 (m), 138.79 (dt, J_{CF} = 250.5/15.6 Hz), 136.5, 135.6 (dt, J_{CF} = 12.8/6.4 Hz), 128.8, 127.1, 112.2–111.3 (m), 26.8; *m/z* MS $C_{14}H_{10}F_3O$ $[MH]^+$ calcd 251.1, found 251.0.

2-Oxo-2-(3',4',5'-trifluoro-[1,1'-biphenyl]-4-yl)acetic acid (3). Compound **2** (6.29 g, 25.1 mmol) and SeO_2 (4.18 g, 37.7 mmol) were dissolved in anhydrous pyridine (200 mL). The reaction mixture was sonicated and then heated at 110 ºC overnight under nitrogen. Once the reaction was complete, the mixture was filtered through Celite™ and the filtrate was concentrated *in vacuo*. A 1 M HCl solution (20 mL) was added and the compound was extracted with EtOAc (3 × 50 mL). The combined organic layers were dried over anhydrous Na_2SO_4, filtered and concentrated under reduced pressure to afford compound **3** as a brown solid (7.04 g, 100%); ^{1}H NMR (d_6-DMSO) δ 8.05–7.93 (m, 4H), 7.84 (dd, J = 9.5/6.7 Hz, 2H); ^{19}F NMR (d_6-DMSO) δ -134.4 (d, J = 21.7 Hz), -161.3 (dd, J = 21.7/21.7 Hz); ^{13}C NMR (d_6-DMSO) δ 188.0, 165.8, 150.7 (ddd, J_{CF} = 247.2/9.8/4.1 Hz), 142.9–142.8 (m), 139.1 (dt, J_{CF} = 248.4/14.2 Hz), 135.8–134.5 (m), 131.6, 130.2, 127.7, 116.5–105.3 (m); *m/z* MS $C_{14}H_6F_3O_3$ $[M-H]^-$ calcd 279.0, found 279.0.

Methyl 2-amino-2-(3',4',5'-trifluoro-[1,1'-biphenyl]-4-yl)acetate (4). Compound **3** (7.04 g, 25.1 mmol) and benzylamine (4.12 mL, 37.7 mmol) were dissolved in anhydrous DCE (200 mL) and stirred for 30 min. $Na(OAc)_3BH$ (7.99 g, 56.6 mmol) was added and the mixture was stirred at rt overnight. Once the reaction was complete, water (30 mL) was added and the mixture was stirred vigorously for 5

min. DCE was removed *in vacuo* and the solid was filtered and washed with ethanol to give 9.33 g of 2-(benzylamino)-2-(3',4',5'-trifluoro-[1,1'-biphenyl]-4-yl)acetic acid as a yellow solid. The crude solid was dissolved in MeOH (250 mL) and conc. H_2SO_4 (5.36 mL, 101 mmol) was added dropwise. The reaction mixture was refluxed for 16 h and then concentrated under reduced pressure. Sat. $NaHCO_3$ was added and the mixture was extracted with DCM (3 × 150 mL). The combined organic layers were dried over anhydrous Na_2SO_4, filtered and concentrated under reduced pressure to afford 7.86 g of methyl 2-(benzylamino)-2-(3',4',5'-trifluoro-[1,1'-biphenyl]-4-yl)acetate. The crude ester was subsequently dissolved in MeOH (200 mL) and 32% HCl (5 mL) was added. The flask was evacuated and flushed with nitrogen three times before the addition of 10% Pd/C (1.60 g). The reaction mixture was stirred vigorously under a hydrogen atmosphere at rt overnight. Upon completion, the reaction mixture was filtered through Celite™ and washed with MeOH (50 mL). The filtrate was concentrated *in vacuo* followed by dilution with sat. $NaHCO_3$ and extraction with EtOAc (3 × 100 mL). The organic layer was dried over anhydrous Na_2SO_4, filtered and concentrated under reduced pressure. The crude product was purified by column chromatography (PE:EtOAc 50:50 to 0:100) to afford compound **4** as a sticky yellow solid (3.51 g, 47% over 3 steps). ^{1}H NMR ($CDCl_3$) δ 7.47 (m, 4H), 7.20–7.10 (m, 2H), 4.67 (s, 1H), 3.72 (s, 3H), 2.30 (s, 2H); ^{19}F NMR ($CDCl_3$) δ -134.0 (d, J = 20.5 Hz), -162.4 (dd, J = 20.6/20.6 Hz); ^{13}C NMR ($CDCl_3$) δ 174.3, 151.5 (ddd, J_{CF} = 249.6/10.0/4.3 Hz), 140.5, 140.9–137.9 (m), 138.1–137.9 (m), 136.8 (td, J_{CF} = 7.8/4.7 Hz), 127.7, 127.3, 111.3–110.9 (m), 58.4, 52.6; *m/z* MS $C_{15}H_{13}F_3NO_2$ $[MH]^+$ calcd 296.1, found 296.1.

Methyl 2-acetamido-2-(3',4',5'-trifluoro-[1,1'-biphenyl]-4-yl)acetate (5a). To a mixture of compound **4** (300 mg, 1.01 mmol) in anhydrous toluene (4 mL) was added Meldrum's acid (161 mg, 1.12 mmol). The reaction mixture was refluxed for 3 h. After cooling to rt, the resulting precipitate was filtered and washed with Et_2O to afford compound **5a** as a white solid (172 mg, 50%). ^{1}H NMR (d_6-DMSO) δ 8.80 (d, J = 7.3 Hz, 1H), 7.89–7.64 (m, 4H), 7.48 (d, J = 8.3 Hz, 2H), 5.48 (d, J = 7.3 Hz, 1H), 3.63 (s, 3H), 1.91 (s, 3H); ^{19}F NMR (d_6-DMSO) δ -134.8 (d, J = 21.8 Hz), -163.3 (dd, J = 21.7/21.7 Hz);

^{13}C NMR (d_6-DMSO) δ 171.0, 169.3, 150.6 (ddd, J_{CF} = 246.6/9.7/4.2 Hz), 138.4 (dt, J_{CF} = 249.5/15.7 Hz), 136.9–136.8 (m), 136.7, 136.3 (td, J_{CF} = 8.1/4.5 Hz), 128.4, 127.2, 117.8–108.1 (m), 55.8, 52.3, 22.2; *m/z* MS $C_{17}H_{15}F_3NO_3$ $[MH]^+$ calcd 338.1, found 338.1.

***tert*-Butyl 3-((2-methoxy-2-oxo-1-(3',4',5'-trifluoro-[1,1'-biphenyl]-4-yl)ethyl)amino)-3-oxopropanoate (5b).** 3-(*tert*-Butoxy)-3-oxopropanoic acid (198 mg, 1.24 mmol) was coupled to compound **4** (330 mg, 1.12 mmol) according to General Procedure A. The crude product was purified by column chromatography (PE:EtOAc 0:100 to 50:50) to afford compound **5b** (185 mg, 38%) as an orange oil. ^{1}H NMR (d_6-DMSO) δ 9.00 (d, *J* = 7.3 Hz, 1H), 7.80–7.67 (m, 4H), 7.50 (d, *J* = 8.3 Hz, 2H), 5.52 (d, *J* = 7.3 Hz, 1H), 3.65 (s, 3H), 3.31–3.21 (m, 2H), 1.39 (s, 9H); ^{19}F NMR (d_6-DMSO) δ -134.9 (d, *J* = 21.7 Hz), -163.3 (dd, *J* = 21.7/21.7 Hz); ^{13}C NMR (d_6-DMSO) δ 170.6, 166.9, 165.5, 150.6 (ddd, J_{CF} = 246.6/9.8/4.2 Hz), 138.4 (dt, J_{CF} = 249.7/15.6 Hz), 136.9–136.8 (m), 136.6, 136.3 (m), 128.3, 127.2, 111.7–111.0 (m), 80.6, 55.8, 52.4, 43.2, 27.7; *m/z* MS $C_{22}H_{21}F_3NO_5$ $[M-H]^-$ calcd 436.1, found 436.1.

4-((2-Methoxy-2-oxo-1-(3',4',5'-trifluoro-[1,1'-biphenyl]-4-yl)ethyl)amino)-4-oxobutanoic acid (5e). To a mixture of compound **4** (428 mg, 1.45 mmol) in anhydrous toluene (10 mL) was added succinic anhydride (160 mg, 1.60 mmol). The reaction mixture was refluxed for 3 h. After cooling to rt, the resulting precipitate was filtered and washed with Et_2O to afford compound **5e** as a white solid (267 mg, 49%). ^{1}H NMR (d_6-DMSO) δ 12.11 (s, 1H), 8.83 (d, *J* = 7.3 Hz, 1H), 7.80–7.65 (m, 4H), 7.49 (d, *J* = 8.3 Hz, 2H), 5.49 (d, *J* = 7.3 Hz, 1H), 3.63 (s, 3H), 2.46–2.39 (m, 4H); ^{19}F NMR (d_6-DMSO) δ -134.82 (d, *J* = 21.8 Hz), -163.24 (dd, *J* = 21.8/21.8 Hz); ^{13}C NMR (d_6-DMSO) δ 173.7, 171.2, 171.0, 150.6 (ddd, J_{CF} = 246.4/9.6/4.0 Hz), 138.4 (m), 137.0 (m), 136.8, 136.3 (m), 128.4, 127.1, 111.5–111.2 (m), 55.8, 52.3, 29.6, 28.9; *m/z* MS $C_{19}H_{17}F_3NO_5$ $[MH]^+$ calcd 396.1, found 396.1.

Methyl 2-(4-amino-4-oxobutanamido)-2-(3',4',5'-trifluoro-[1,1'-biphenyl]-4-yl)acetate (5f). Compound **5e** (272 mg, 0.688 mmol) and PyBOP (531 mg, 1.02 mmol) in DMF (10 mL) were stirred for 10 min. DIPEA (0.2 mL, 1.02 mmol) and ammonium carbonate (332 mg, 3.45 mmol) were added to

the reaction mixture which was stirred at rt overnight. After completion, the mixture was diluted with water (10 mL) and extracted with DCM (3 × 15 mL). The combined organic layers were washed with sat. $NaHCO_3$ (2 × 30 mL) and brine (30 mL). The organic layer was dried over anhydrous Na_2SO_4, filtered and concentrated *in vacuo*. The crude product was purified by column chromatography (PE:EtOAc 50:50 to 0:100) to afford compound **5f** as a white solid (84 mg, 31%). ^{1}H NMR (d_6-DMSO) δ 8.81 (d, J = 7.3 Hz, 1H), 7.87–7.60 (m, 4H), 7.49 (d, J = 8.3 Hz, 2H), 7.29 (br. s, 1H), 6.75 (br. s, 1H), 5.49 (d, J = 7.3 Hz, 1H), 3.63 (s, 3H), 2.47–2.25 (m, 4H); ^{19}F NMR (d_6-DMSO) δ -134.8 (d, J = 21.8 Hz), -163.3 (dd, J = 21.8/21.8 Hz); ^{13}C NMR (d_6-DMSO) δ 173.4, 171.7, 171.0, 150.6 (ddd, J_{CF} = 246.5/9.7/4.2 Hz), 138.4 (dt, J_{CF} = 249.6/15.7 Hz), 136.8 (2C),136.34 (td, J_{CF} = 8.2/4.2 Hz), 128.4, 127.2, 111.6–110.9 (m), 55.8, 52.3, 30.2, 30.1; *m/z* MS $C_{19}H_{18}F_3N_2O_4$ $[MH]^+$ calcd 395.1, found 395.1.

Methyl 2-benzamido-2-(3',4',5'-trifluoro-[1,1'-biphenyl]-4-yl)acetate (5g). Benzoic acid (99.3 mg, 0.813 mmol) was coupled to compound **4** (200 mg, 0.678 mmol) according to General Procedure B. The crude product was purified by column chromatography (PE:EtOAc 100:0 to 50:50) to afford compound **5g** as a bright yellow foam (244 mg, 90%). ^{1}H NMR (d_6-DMSO) δ 9.26 (d, J = 7.3 Hz, 1H), 8.00–7.91 (m, 2H), 7.79–7.66 (m, 4H), 7.61 (d, J = 8.3 Hz, 2H), 7.58–7.53 (m, 1H), 7.51–7.45 (m, 2H), 5.79 (d, J = 7.3 Hz, 1H), 3.69 (s, 3H); ^{19}F NMR (d_6-DMSO) δ -134.8 (d, J = 21.7 Hz), -163.4 (dd, J = 21.6/21.6 Hz); ^{13}C NMR (d_6-DMSO) δ 170.9, 166.5, 150.6 (ddd, J_{CF} = 246.7/9.7/4.2 Hz), 138.4 (dt, J_{CF} = 249.5/15.6 Hz), 136.8, 136.8–136.7 (m), 136.5–136.3 (td, J_{CF} = 8.1/4.4 Hz), 133.5, 131.6, 128.9, 128.2, 127.7, 127.0, 111.6–111.0 (m), 56.4, 52.3; *m/z* MS $C_{22}H_{17}F_3NO_3$ $[MH]^+$ calcd 400.1, found 400.1.

Methyl 2-(3-fluorobenzamido)-2-(3',4',5'-trifluoro-[1,1'-biphenyl]-4-yl)acetate (5h). 3-Fluorobenzoic acid (114 mg, 0.812 mmol) was coupled to compound **4** (200 mg, 0.677 mmol) according to General Procedure B. The crude product was purified by column chromatography (PE:EtOAc 100:0 to 50:50) to afford compound **5h** as a bright yellow foam (243 mg, 86%). ^{1}H NMR (d_6-DMSO) δ 9.35 (d, J = 7.1 Hz, 1H), 7.82–7.66 (m, 6H), 7.60 (d, J = 8.3 Hz, 2H), 7.54 (ddd, J = 8.0/7.9/5.9 Hz, 1H), 7.44–7.38 (m, 1H), 5.77 (d, J = 7.1 Hz, 1H), 3.69 (s, 3H); ^{19}F NMR (d_6-DMSO) δ -112.9, -134.8 (d, J = 21.7

Hz), -163.3 (dd, J = 21.7/21.7 Hz); ^{13}C NMR (d_6-DMSO) δ 170.7, 165.2 (d, J_{CF} = 2.5 Hz), 161.9 (d, J_{CF} = 244.3 Hz), 150.6 (ddd, J_{CF} = 246.7/9.7/4.1 Hz), 138.4 (dt, J_{CF} = 249.5/15.7 Hz), 136.9–136.6 (m), 136.5, 136.4–136.2 (m), 135.7 (d, J_{CF} = 6.9 Hz), 130.4 (d, J_{CF} = 8.0 Hz), 129.0, 127.0, 123.9 (d, J_{CF} = 2.8 Hz), 118.5 (d, J_{CF} = 21.2 Hz), 114.5 (d, J_{CF} = 22.9 Hz), 112.1–110.6 (m), 56.5, 52.4; *m/z* MS $C_{22}H_{16}F_4NO_3$ $[MH]^+$ calcd 418.1, found 418.1.

Methyl 2-(4-fluorobenzamido)-2-(3',4',5'-trifluoro-[1,1'-biphenyl]-4-yl)acetate (5i). 4-Fluorobenzoic acid (114 mg, 0.812 mmol) was coupled to compound **4** (200 mg, 0.677 mmol) according to General Procedure B. The crude product was purified by column chromatography (PE:EtOAc 100:0 to 50:50) to afford compound **5i** as a bright yellow foam (150 mg, 53%). ^{1}H NMR (d_6-DMSO) δ 9.28 (d, J = 7.2 Hz, 1H), 8.08–7.97 (m, 2H), 7.75 (d, J = 8.3 Hz, 2H), 7.72–7.64 (m, 2H), 7.60 (d, J = 8.3 Hz, 2H), 7.34–7.25 (m, 2H), 5.77 (d, J = 7.2 Hz, 1H), 3.69 (s, 3H); ^{19}F NMR (d_6-DMSO) δ -108.8, -134.8 (d, J = 21.6 Hz), -163.4 (dd, J = 21.6/21.6 Hz); ^{13}C NMR (d_6-DMSO) δ 170.8, 165.4, 164.1 (d, J_{CF} = 249.1 Hz), 150.6 (ddd, J_{CF} = 246.8/9.7/4.1 Hz), 138.4 (dt, J_{CF} = 249.6/15.6 Hz), 136.8–136.7 (m), 136.6, 136.4 (td, J_{CF} = 8.1/4.4 Hz), 130.4 (d, J_{CF} = 9.1 Hz), 123.0 (d, J_{CF} = 2.9 Hz), 128.9, 127.0, 115.1 (d, J_{CF} = 21.8 Hz), 111.2 (m), 56.5, 52.3; *m/z* MS $C_{22}H_{16}F_4NO_3$ $[MH]^+$ calcd 418.1, found 417.8.

Methyl 2-(3-methoxybenzamido)-2-(3',4',5'-trifluoro-[1,1'-biphenyl]-4-yl)acetate (5j). 3-Methoxybenzoic acid (247 mg, 1.63 mmol) was coupled to compound **4** (400 mg, 1.36 mmol) according to General Procedure B. The crude product was purified by column chromatography (PE:EtOAc 100:0 to 50:50) to afford compound **5j** as a bright yellow foam (578 mg, 99%). ^{1}H NMR (d_6-DMSO) δ 9.25 (d, J = 7.2 Hz, 1H), 7.75 (d, J = 8.4 Hz, 2H), 7.69 (m, 2H), 7.61 (d, J = 8.3 Hz, 2H), 7.56–7.51 (m, 1H), 7.51–7.48 (m, 1H), 7.39 (t, J = 7.9 Hz, 1H), 7.15–7.09 (m, 1H), 5.78 (d, J = 7.2 Hz, 1H), 3.81 (s, 3H), 3.69 (s, 3H); ^{19}F NMR (d_6-DMSO) δ -134.8 (d, J = 21.7 Hz), -163.3 (dd, J = 21.6/21.6 Hz); ^{13}C NMR (d_6-DMSO) δ 170.9, 166.2, 159.1, 150.6 (ddd, J_{CF} = 246.8/9.8/4.2 Hz), 138.4 (dt, J_{CF} = 249.5/15.6 Hz), 136.9–136.7 (m, 2C), 136.4 (td, J_{CF} = 8.1/4.4 Hz), 134.9, 129.4, 128.9, 127.0, 120.0, 117.5, 112.8, 112.0–110.4 (m), 56.5, 55.3, 52.3; *m/z* MS $C_{23}H_{19}F_3NO_4$ $[MH]^+$ calcd 430.1, found 429.9.

Methyl 2-(4-methoxybenzamido)-2-(3',4',5'-trifluoro-[1,1'-biphenyl]-4-yl)acetate (5k). 4-Methoxybenzoic acid (199 mg, 1.31 mmol) was coupled to compound **4** (322 mg, 1.09 mmol) according to General Procedure B. The crude product was purified by column chromatography (PE:EtOAc 100:0 to 50:50) to afford compound **5k** as a white solid (154 mg, 33%). ^{1}H NMR ($CDCl_3$) δ 7.80 (d, J = 8.9 Hz, 2H), 7.54–7.49 (m, 2H), 7.48–7.42 (m, 2H), 7.29 (d, J = 6.7 Hz, 1H), 7.13 (m, 2H), 6.90 (d, J = 8.9 Hz, 2H), 5.81 (d, J = 6.8 Hz, 1H), 3.82 (s, 3H), 3.78 (s, 3H); ^{19}F NMR ($CDCl_3$) δ -134.0 (d, J = 20.5 Hz), -162.3 (dd, J = 20.5 Hz); ^{13}C NMR ($CDCl_3$) δ 171.5, 166.3, 162.7, 151.5 (ddd, J_{CF} = 249.7/9.9/4.2 Hz), 139.5 (dt, J_{CF} = 252.2/15.5 Hz), 138.6–138.4 (m), 137.2, 136.7 (td, J_{CF} = 7.7/4.6 Hz), 129.2, 128.2, 127.5, 125.7, 113.9, 111.1 (m), 56.6, 55.5, 53.1; *m/z* MS $C_{23}H_{19}F_3NO_4$ $[MH]^+$ calcd 430.1, found 429.9.

Methyl 2-(3-cyanobenzamido)-2-(3',4',5'-trifluoro-[1,1'-biphenyl]-4-yl)acetate (5n). Oxalyl chloride (130 µL, 1.51 mmol) was added dropwise to a mixture of 3-carbamoylbenzoic acid (167 mg, 1.01 mmol) in DCM (10 mL) containing a catalytic amount of DMF (20 µL). After stirring the mixture at rt for 1 h the DCM was concentrated *in vacuo.* A mixture of DIPEA (126 µL, 1.31 mmol) and compound **4** (300 mg, 1.01 mmol) in DCM (10 mL) was added to the acid chloride. The reaction mixture was stirred at rt for 30 min and then diluted with water (15 mL) and extracted with DCM (3 × 10 mL). The combined organic layers were dried over Na_2SO_4, filtered and concentrated *in vacuo*. LC-MS of the crude product indicated dehydration of the carboxamide group occurred to form a cyano analogue. The crude product was purified by column chromatography (PE:EtOAc 100:0 to 0:100) to afford compound **5n** as a clear oil (383 mg, 89%). ^{1}H NMR ($CDCl_3$) δ 8.12 (s, 1H), 8.06 (d, J = 7.9 Hz, 1H), 7.80 (d, J = 7.8 Hz, 1H), 7.58 (t, J = 7.7 Hz, 1H), 7.54–7.48 (m, 4H), 7.44 (d, J = 6.7 Hz, 1H), 7.19–7.10 (m, 2H), 5.79 (d, J = 6.7 Hz, 1H), 3.81 (s, 3H); ^{19}F NMR ($CDCl_3$) δ -133.7 (d, J = 20.6 Hz), -161.9 (dd, J = 20.6/20.6 Hz); ^{13}C NMR ($CDCl_3$) δ 171.1, 164.7, 151.6 (ddd, J_{CF} = 250.0/10.1/4.2 Hz), 139.6 (dt, J_{CF} = 252.4/15.4 Hz), 138.9–138.7 (m), 136.6–136.5 (m), 136.4, 135.3, 134.7, 131.5, 131.2, 129.8, 128.2, 127.7, 117.9, 113.2, 112.0–110.2 (m), 56.8, 53.4; *m/z* MS $C_{23}H_{14}F_3N_2O_3$ $[M-H]^-$ calcd 423.1, found 423.1.

Methyl 2-(4-cyanobenzamido)-2-(3',4',5'-trifluoro-[1,1'-biphenyl]-4-yl)acetate (5o). Oxalyl chloride (130 μL, 1.51 mmol) was added dropwise to a mixture of 4-carbamoylbenzoic acid (167 mg, 1.01 mmol) in DCM (10 mL) containing a catalytic amount of DMF (20 μL). After stirring the mixture at rt for 1 h the DCM was removed *in vacuo.* A mixture of DIPEA (126 μL, 1.31 mmol) and compound **4** (300 mg, 1.01 mmol) in DCM (10 mL) was added to the acid chloride. The reaction mixture was stirred at rt for 30 min, then diluted with water (15 mL) and extracted with DCM (3 × 10 mL). The combined organic layers were dried over anhydrous Na_2SO_4, filtered and concentrated *in vacuo*. LC-MS of the crude product indicated dehydration of the carboxamide group occurred to form a cyano analogue. The crude product was purified by column chromatography (PE:EtOAc 100:0 to 0:100) to afford compound **5o** as a yellow oil (185 mg, 43%). ^{1}H NMR ($CDCl_3$) δ 7.98–7.73 (m, 4H), 7.54–7.45 (m, 4H), 7.34 (app. t, J = 6.6 Hz, 1H), 7.19–7.11 (m, 2H), 5.79 (d, J = 6.6 Hz, 1H), 3.81 (s, 3H); ^{19}F NMR ($CDCl_3$) δ -133.7 (d, J = 20.5 Hz), -161.9 (dd, J = 20.5/20.5 Hz); ^{13}C NMR ($CDCl_3$) δ 171.1, 164.9, 151.6 (ddd, J_{CF} = 250.0/10.1/4.3 Hz), 139.6 (dt, J_{CF} = 252.5/15.3 Hz), 139.0–138.8 (m), 137.4, 136.8–136.3 (m, 2C), 132.7, 128.2, 128.0, 127.7, 118.0, 115.8, 111.9–110.6 (m), 56.7, 53.5; *m/z* MS $C_{23}H_{16}F_3N_2O_3$ $[MH]^+$ calcd 425.1, found 425.1.

Methyl 2-(3-carbamoylbenzamido)-2-(3',4',5'-trifluoro-[1,1'-biphenyl]-4-yl)acetate (5r). 3-Carbamoylbenzoic acid (205 mg, 1.24 mmol) was coupled to compound **4** (332 mg, 1.13 mmol) according to General Procedure A. The crude product was purified by column chromatography (PE:EtOAc 50:50 to 0:100) to afford compound **5r** as a light yellow solid (328 mg, 66%). ^{1}H NMR (d_6-DMSO) δ 9.37 (d, J = 7.1 Hz, 1H), 8.42 (t, J = 1.6 Hz, 1H), 8.07 (br. s, 1H), 8.06–7.99 (m, 2H), 7.78–7.69 (m, 4H), 7.64–7.54 (m, 3H), 7.50 (br. s, 1H), 5.78 (d, J = 7.1 Hz, 1H), 3.69 (s, 3H); ^{19}F NMR (d_6-DMSO) δ -134.8 (d, J = 21.7 Hz), -163.3 (dd, J = 21.7/21.7 Hz); ^{13}C NMR (d_6-DMSO) δ 170.9, 167.5, 166.2, 150.7 (ddd, J_{CF} = 246.6/9.7/4.1 Hz), 138.4 (dt, J_{CF} = 249.5/15.6 Hz), 136.9–136.8 (m), 136.7, 136.4 (td, J_{CF} = 8.1/4.4 Hz), 134.5, 133.6, 130.5, 130.4, 129.0, 128.4, 127.1, 126.9, 112.9–109.9 (m), 56.6, 52.5; *m/z* MS $C_{23}H_{18}F_3N_2O_4$ $[MH]^+$ calcd 443.1, found 443.1.

Methyl 2-(4-carbamoylbenzamido)-2-(3',4',5'-trifluoro-[1,1'-biphenyl]-4-yl)acetate (5s). 4-Carbamoylbenzoic acid (246 mg, 1.49 mmol) was coupled to compound **4** (400 mg, 1.35 mmol) according to General Procedure A. The crude product was purified by column chromatography (PE:EtOAc 50:50 to 0:100) to afford compound **5s** as a light yellow solid (383 mg, 64%). ^{1}H NMR (d_6-DMSO) δ 9.38 (d, J = 7.2 Hz, 1H), 8.10 (br. s, 1H), 8.02–7.91 (m, 4H), 7.84–7.68 (m, 4H), 7.60 (d, J = 8.3 Hz, 2H), 7.52 (br. s, 1H), 5.77 (d, J = 7.1 Hz, 1H), 3.68 (s, 3H); ^{19}F NMR (d_6-DMSO) δ -134.8 (d, J = 21.8 Hz), -163.2 (dd, J = 21.7/21.7 Hz); ^{13}C NMR (d_6-DMSO) δ 170.8, 167.2, 165.9, 150.6 (ddd, J_{CF} = 246.4/9.5/4.1 Hz), 138.4 (dt, J_{CF} = 249.8/15.7 Hz), 136.9, 136.4 (td, J_{CF} = 8.2/5.5 Hz), 135.8–135.7 (m), 133.4, 132.2, 129.0, 127.7, 127.4, 127.1, 111.6–111.1 (m), 56.5, 52.5; *m/z* MS $C_{23}H_{18}F_3N_2O_4$ $[MH]^+$ calcd 443.1, found 443.1.

Methyl 2-(4-(methylcarbamoyl)benzamido)-2-(3',4',5'-trifluoro-[1,1'-biphenyl]-4-yl)acetate (5t). 4-(Methylcarbamoyl)benzoic acid (97.3 mg, 0.504 mmol) was coupled to compound **4** (107 mg, 0.364 mmol) according to the General Procedure B. Upon completion, the mixture was added to a 0.1 M HCl solution (50 mL) and extracted with EtOAc (3 × 50 mL). The combined organic layers were washed with brine (50 mL), dried over anhydrous Na_2SO_4, filtered and concentrated under reduced pressure. The residue was then taken up in minimal DMF and added to an ice-water mixture. The precipitate was filtered and washed with minimal MeOH to afford compound **5t** as a yellow solid (98.4 mg, 59%) ^{1}H NMR (d_6-DMSO) δ 9.38 (d, J = 7.1 Hz, 1H), 8.57 (d, J = 4.5 Hz, 1H), 8.04–7.96 (m, 2H), 7.92 (d, J = 8.4 Hz, 2H), 7.79–7.67 (m, 4H), 7.60 (d, J = 8.3 Hz, 2H), 5.78 (d, J = 7.1 Hz, 1H), 3.69 (s, 3H), 2.80 (d, J = 4.5 Hz, 3H); ^{19}F NMR (d_6-DMSO) δ -134.8 (d, J = 21.7 Hz), -163.3 (dd, J = 21.7/21.7 Hz); ^{13}C NMR (d_6-DMSO) δ 170.8, 166.0 (2C), 150.7 (ddd, J_{CF} = 246.4/9.7/4.2 Hz), 139.9–137.1 (m), 137.2, 136.9 (br, S), 136.6, 136.5–136.4 (m), 129.0, 127.8, 127.1, 127.0, 112.7–108.5 (m), 56.6, 52.5, 26.3; *m/z* MS $C_{24}H_{20}F_3N_2O_4$ $[MH]^+$ calcd 457.1, found 456.8.

Methyl 2-(4-(dimethylcarbamoyl)benzamido)-2-(3',4',5'-trifluoro-[1,1'-biphenyl]-4-yl)acetate (5u). 4-(Dimethylcarbamoyl)benzoic acid (102 mg, 0.491 mmol) was coupled to compound **4** (114 mg,

0.385 mmol) according to General Procedure B. Upon completion, the mixture was added to a 0.1 M HCl solution (50 mL) and extracted with EtOAc (3 × 50 mL). The combined organic layers were washed with brine (50 mL), dried over anhydrous Na_2SO_4, filtered and concentrated under reduced pressure. The residue was then taken up in minimal DMF and added to an ice-water mixture. The precipitate was filtered and washed with minimal MeOH to afford compound **5u** as a white solid (92.0 mg, 51%) ^{1}H NMR (d_6-DMSO) δ 9.36 (d, J = 7.2 Hz, 1H), 8.07–7.86 (m, 2H), 7.79–7.68 (m, 4H), 7.60 (d, J = 8.3 Hz, 2H), 7.53–7.46 (m, 2H), 5.77 (d, J = 7.2 Hz, 1H), 3.68 (s, 3H), 2.99 (s, 3H), 2.88 (s, 3H); ^{19}F NMR (d_6-DMSO) δ -134.8 (d, J = 21.7 Hz), -163.3 (dd, J = 21.8/21.8 Hz); ^{13}C NMR (d_6-DMSO) δ 171.0, 169.7, 166.3, 150.8 (ddd, J_{CF} = 14.1/ 9.4/3.6 Hz), 139.9–137.2 (m), 139.7, 137.0 (d, J_{CF} = 1.5 Hz), 136.8, 136.69–136.36 (m), 134.2, 129.2, 128.0, 127.2, 127.0, 111.4 (dd, J_{CF} = 16.2/5.3 Hz), 56.7, 52.6, 34.9; *m/z* MS $C_{25}H_{22}F_3N_2O_4$ $[MH]^+$ calcd 471.2, found 470.9.

Methyl 2-(4-(ethylcarbamoyl)benzamido)-2-(3',4',5'-trifluoro-[1,1'-biphenyl]-4-yl)acetate (5v). Carboxylic acid **12** (102 mg, 0.491 mmol) was coupled to compound **4** (114 mg, 0.385 mmol) according to General Procedure B. Upon completion, the mixture was added to a 0.1 M HCl solution (50 mL) and extracted with EtOAc (3 × 50 mL). The combined organic layers were washed with brine (50 mL), dried over anhydrous Na_2SO_4, filtered and concentrated under reduced pressure. The residue was then taken up in minimal DMF and added to an ice-water mixture. The precipitate was filtered and washed with minimal MeOH to afford compound **5v** as a yellow solid (92.0 mg, 51%). ^{1}H NMR (d_6-DMSO) δ 9.39 (d, J = 7.1 Hz, 1H), 8.61 (t, J = 5.5 Hz, 1H), 8.03–7.98 (m, 2H), 7.93 (d, J = 8.4 Hz, 2H), 7.76 (d, J = 8.3 Hz, 2H), 7.71 (dd, J = 9.4, 6.8 Hz, 2H), 7.61 (d, J = 8.3 Hz, 2H), 5.78 (d, J = 7.1 Hz, 1H), 3.69 (s, 3H), 3.34–3.26 (m, 2H), 1.14 (t, J = 7.2 Hz, 3H); ^{19}F NMR (d_6-DMSO) δ -134.8 (d, J = 21.7 Hz), -163.3 (dd, J = 21.7/21.7 Hz); ^{13}C NMR (d_6-DMSO) δ 170.8, 165.9, 165.2, 150.6 (ddd, J_{CF} = 246.8/9.6/4.4 Hz), 138.4 (dt, J_{CF} = 33.6/15.7 Hz), 137.3, 136.8, 136.6, 136.4 (td, J_{CF} = 8.1/4.6 Hz), 129.0, 127.7, 127.07, 127.05, 111.3 (dd, J_{CF} = 15.9/5.5 Hz), 56.5, 52.4, 34.2, 14.7; *m/z* MS $C_{25}H_{22}F_3N_2O_4$ $[MH]^+$ calcd 471.2, found 470.9.

Methyl 2-(4-(isopropylcarbamoyl)benzamido)-2-(3',4',5'-trifluoro-[1,1'-biphenyl]-4-yl)acetate (5w). 4-(Isopropylcarbamoyl)benzoic acid (119 mg, 0.573 mmol) was coupled to compound **4** (118 mg, 0.401 mmol) according to General Procedure B. Upon completion, the mixture was added to a 0.1 M HCl solution (50 mL) and extracted with EtOAc (3 × 50 mL). The combined organic layers were washed with brine (50 mL), dried over anhydrous Na_2SO_4, filtered and concentrated under reduced pressure. The residue was then taken up in minimal DMF and added to an ice-water mixture. The precipitate was filtered and washed with minimal MeOH to afford compound **5w** as a white solid (177 mg, 91%). ^{1}H NMR (d_6-DMSO) δ 9.40 (d, J = 7.1 Hz, 1H), 8.37 (d, J = 7.7 Hz, 1H), 8.02 (d, J = 8.5 Hz, 2H), 7.95 (d, J = 8.4 Hz, 2H), 7.76 (d, J = 8.3 Hz, 2H), 7.69 (dd, J = 9.3, 6.8 Hz, 2H), 7.62 (d, J = 8.3 Hz, 2H), 5.80 (d, J = 7.1 Hz, 1H), 4.22 – 4.00 (m, 1H), 3.70 (s, 3H), 1.18 (d, J = 6.6 Hz, 6H); ^{19}F NMR (d_6-DMSO) δ -130.0 (d, J = 21.6 Hz), -158.5 (dd, J = 21.6/21.6 Hz); ^{13}C NMR (d_6-DMSO) δ 170.90, 166.0, 164.7, 153.0–148.6 (m), 138.4 (dt, J_{CF} = 30.9/13.8 Hz), 137.5, 136.9, 136.6, 136.5–136.3 (m), 135.5, 129.0, 127.7, 127.2, 127.1, 111.3 (dd, J_{CF} = 18.9/2.5 Hz), 56.6, 52.4, 41.2, 22.3; *m/z* MS $C_{26}H_{24}F_3N_2O_4$ $[MH]^+$ calcd 485.2, found 484.9.

Methyl 2-(4-((2-hydroxyethyl)carbamoyl)benzamido)-2-(3',4',5'-trifluoro-[1,1'-biphenyl]-4-yl)acetate (5x). A sealed vessel containing COMU (2.23 g, 0.584 mmol), TEA (1.10 mL, 7.89 mmol), carboxylic acid **14** (746 mg, 3.56 mmol) and compound **4** (761 mg, 2.58 mmol) was purged twice with nitrogen and charged with DMF (5 mL). The reaction mixture was allowed to stir at rt overnight. The mixture was then added to a half sat. $NaHCO_3$ solution (80 mL) and extracted with EtOAc (3 × 80 mL). The combined organic layers were washed with brine (50 mL), dried over anhydrous Na_2SO_4, filtered and concentrated under reduced pressure. The residue was then taken up in minimal DMF and added to an ice-water mixture. The precipitate was filtered and washed with minimal MeOH and further purified by column chromatography (DCM:MeOH 98:2 to 94:6) to afford compound **5x** as a cream solid after lyophilization (182 mg, 14%). ^{1}H NMR (d_6-DMSO) δ 9.41 (d, J = 7.2 Hz, 1H), 8.61 (t, J = 5.7 Hz, 1H), 8.06–7.99 (m, 2H), 8.00–7.93 (m, 2H), 7.78–7.72 (m, 2H), 7.67 (dd, J = 9.4, 6.6 Hz, 2H), 7.65–7.58 (m,

2H), 5.80 (d, J = 7.1 Hz, 1H), 4.81 (br, s, 1H), 3.70 (s, 3H), 3.56 (t, J = 6.2 Hz, 2H), 3.38 (q, J = 6.0, 2H); ^{19}F NMR (d_6-DMSO) δ -134.8 (d, J = 21.8 Hz), -163.2 (dd, J = 21.7/21.7 Hz); ^{13}C NMR (d_6-DMSO) δ 170.9, 166.1, 165.8, 150.7 (ddd, J_{CF} = 246.8/9.7/4.2 Hz), 138.5 (dt, J_{CF} = 30.6/12.4 Hz), 137.3, 137.0, 136.7, 136.5 (td, J_{CF} = 8.1/4.4 Hz), 135.7, 129.1, 127.8, 127.3, 127.1, 111.3 (dd, J_{CF} = 16.0/5.5 Hz), 59.8, 56.7, 52.5, 42.4; *m/z* MS $C_{25}H_{22}F_3N_2O_5$ $[MH]^+$ calcd 487.1, found 486.8.

Methyl 2-(4-sulfamoylbenzamido)-2-(3',4',5'-trifluoro-[1,1'-biphenyl]-4-yl)acetate (5y). 4-Carboxybenzenesulfonamide (274 mg, 1.36 mmol) was coupled to compound **4** (290 mg, 0.981 mmol) according to General Procedure B. Upon completion, the mixture was added to a 0.1 M HCl solution (50 mL) and extracted with EtOAc (3 × 50 mL). The combined organic layers were washed with brine (50 mL), dried over anhydrous Na_2SO_4, filtered and concentrated under reduced pressure. The residue was then taken up in minimal DMF and added to an ice-water mixture. The fine precipitate was centrifuged, the supernatant removed and the solid resuspended in EtOAc twice to afford compound **5y** as a light yellow solid after lyophilization (101 mg, 22%). ^{1}H NMR (d_6-DMSO) δ 9.46 (d, J = 7.1 Hz, 1H), 8.07 (d, J = 8.4 Hz, 2H), 7.91 (d, J = 8.3 Hz, 2H), 7.79–7.69 (m, 4H), 7.60 (d, J = 8.2 Hz, 2H), 7.51 (s, 2H), 5.76 (d, J = 7.0 Hz, 1H), 3.68 (s, 3H); ^{19}F NMR (d_6-DMSO) δ -134.8 (d, J = 21.4 Hz), -163.2 (dd, J = 21.5/21.5 Hz); ^{13}C NMR (d_6-DMSO) δ 171.2, 166.1, 151.1 (ddd, J_{CF} = 13.9/ 9.3/3.7 Hz), 147.1, 140.8–137.5 (m), 137.4, 136.9, 136.8, 129.5, 128.9, 127.5, 126.1, 111.8 (dd, J_{CF} = 16.0/5.4 Hz), 57.1, 52.9; *m/z* MS $C_{22}H_{18}F_3N_2O_5S$ $[MH]^+$ calcd 479.1, found 478.8.

Methyl 2-(3-((tert-butoxycarbonyl)amino)benzamido)-2-(3',4',5'-trifluoro-[1,1'-biphenyl]-4-yl)acetate (5z). 3-((*tert*-Butoxycarbonyl)amino)benzoic acid (289 mg, 1.22 mmol) was coupled to compound **4** (300 mg, 1.02 mmol) according to General Procedure B. The crude product was purified by column chromatography (PE:EtOAc 100:0 to 50:50) to afford compound **5z** as a yellow oil (353 mg, 67%). ^{1}H NMR (d_6-DMSO) δ 9.48 (s, 1H), 9.17 (d, J = 7.3 Hz, 1H), 7.99 (m, 1H), 7.78–7.66 (m, 4H), 7.63–7.56 (m, 3H), 7.54–7.48 (m, 1H), 7.34 (t, J = 7.9 Hz, 1H), 5.74 (d, J = 7.1 Hz, 1H), 3.68 (s, 3H), 1.48 (s, 9H); ^{19}F NMR (d_6-DMSO) δ -134.8 (d, J = 21.7 Hz), -163.4 (dd, J = 21.7/21.7 Hz); ^{13}C NMR

(d_6-DMSO) δ 170.8, 166.7, 152.8, 150.6 (ddd, J_{CF} = 246.7/9.7/4.3 Hz), 139.9–136.9 (m) (2C), 136.8, 136.7–136.6 (m), 136.4 (td, J_{CF} = 8.1/4.4 Hz), 134.3, 128.9, 128.4, 127.0, 121.2, 121.2, 117.8, 113.1–110.3 (m), 79.2, 56.4, 52.3, 28.1; *m/z* MS $C_{27}H_{26}F_3N_2O_5$ $[MH]^+$ calcd 515.2, found 515.1.

Methyl 2-(4-((tert-butoxycarbonyl)amino)benzamido)-2-(3',4',5'-trifluoro-[1,1'-biphenyl]-4-yl)acetate (5aa). 4-((*tert*-Butoxycarbonyl)amino)benzoic acid (289 mg, 1.22 mmol) was coupled to compound **4** (300 mg, 1.02 mmol) according to General Procedure B. The crude product was purified by column chromatography (PE:EtOAc 100:0 to 50:50) to afford compound **5aa** as a bright yellow foam (370 mg, 70%). ^{1}H NMR (d_6-DMSO) δ 9.62 (s, 1H), 9.04 (d, J = 7.2 Hz, 1H), 7.86 (d, J = 8.8 Hz, 2H), 7.78–7.67 (m, 4H), 7.58 (d, J = 8.3 Hz, 2H), 7.53 (d, J = 8.8 Hz, 2H), 5.74 (d, J = 8.5 Hz, 1H), 3.67 (s, 3H), 1.48 (s, 9H); ^{19}F NMR (d_6-DMSO) δ -134.8 (d, J = 21.7 Hz), -163.3 (dd, J = 21.7/21.7 Hz); ^{13}C NMR (d_6-DMSO) δ 171.0, 166.0, 152.6, 150.6 (ddd, J_{CF} = 246.5/9.7/4.1 Hz), 142.7, 138.4 (dt, J_{CF} = 249.9/15.7 Hz), 136.9, 136.8–136.6 (m), 136.4 (td, J_{CF} = 8.1/4.3 Hz), 128.9, 128.6, 127.0, 126.7, 117.0, 111.5–111.0 (m), 79.5, 56.4, 52.3, 28.0; *m/z* MS $C_{27}H_{24}F_3N_2O_5$ $[M-H]^-$ calcd 513.2, found 512.9.

Methyl 2-(4-(methylsulfonamido)benzamido)-2-(3',4',5'-trifluoro-[1,1'-biphenyl]-4-yl)acetate (5ad). 4-((Methyl)sulfonylamino)benzoic acid (106 mg, 0.494 mmol) was coupled to compound **4** (118 mg, 0.401 mmol) according to General Procedure B. Upon completion, the mixture was added to a 0.1 M HCl solution (50 mL) and extracted with EtOAc (3 × 50 mL). The combined organic layers were washed with brine (50 mL), dried over anhydrous Na_2SO_4, filtered and concentrated under reduced pressure. The residue was then taken up in minimal DMF and added to an ice-water mixture. The precipitate was filtered and washed with minimal MeOH to afford compound **5ad** as a light yellow solid (142 mg, 72%). ^{1}H NMR (d_6-DMSO) δ 10.14 (s, 1H), 9.14 (d, J = 7.2 Hz, 1H), 7.95–7.88 (m, 2H), 7.78–7.68 (m, 4H), 7.58 (d, J = 8.3 Hz, 2H), 7.30–7.18 (m, 2H), 5.74 (d, J = 7.2 Hz, 1H), 3.67 (s, 3H), 3.07 (s, 3H); ^{19}F NMR (d_6-DMSO) δ -134.8 (d, J = 21.8 Hz), -163.3 (dd, J = 21.7/21.7 Hz); ^{13}C NMR (d_6-DMSO) δ 171.0, 165.9, 150.7 (ddd, J_{CF} = 246.7/9.7/4.2 Hz), 141.6, 136.8-136.7(m), 136.8, 136.4 (td, J_{CF} = 7.8/4.2

Hz), 129.2, 129.0, 128.2, 127.0, 117.9, 111.3 (dd, J_{CF} = 16.0/5.5 Hz), 56.5, 52.4, 40.6; *m/z* MS $C_{23}H_{20}F_3N_2O_5S$ $[MH]^+$ calcd 493.1, found 492.8.

Methyl 2-(4-(sulfamoylamino)benzamido)-2-(3',4',5'-trifluoro-[1,1'-biphenyl]-4-yl)acetate (5ae). Carboxylic acid **15** (160 mg, 0.742 mmol) was coupled to compound **4** (191 mg, 0.645 mmol) according to General Procedure B. Upon completion, the mixture was added to a 0.1 M HCl solution (50 mL) and extracted with EtOAc (3 × 50 mL). The combined organic layers were washed with brine (50 mL), dried over anhydrous Na_2SO_4, filtered and concentrated under reduced pressure. The residue was then taken up in minimal DMF and added to an ice-water mixture. The precipitate was sonicated in Et_2O for 10 mins and then centrifuged. The supernatant was removed and the solid resuspended in Et_2O twice to afford compound **5ae** as a cream solid (170 mg, 53%). ^{1}H NMR (d_6-DMSO) δ 9.94 (s, 1H), 9.05 (d, J = 7.2 Hz, 1H), 7.86 (d, J = 8.8 Hz, 2H), 7.80–7.63 (m, 4H), 7.58 (d, J = 8.3 Hz, 2H), 7.29 (s, 2H), 7.18 (d, J = 8.8 Hz, 2H), 5.73 (d, J = 7.2 Hz, 1H), 3.67 (s, 3H).; ^{19}F NMR (d_6-DMSO) δ -134.8 (d, J = 21.7 Hz), -163.3 (dd, J = 21.7/21.7 Hz); ^{13}C NMR (d_6-DMSO) δ 171.1, 166.1, 150.7 (ddd, J_{CF} = 246.3/9.6/4.0 Hz), 142.8, 138.5 (dt, J_{CF} = 30.9/15.2 Hz), 137.0, 136.8, 136.5 (td, J_{CF} = 8.1/4.4 Hz), 129.0, 128.9, 127.0, 126.3, 116.3, 111.3 (dd, J_{CF} = 16.0/5.4 Hz), 56.5, 52.4; *m/z* MS $C_{22}H_{19}F_3N_3O_5S$ $[MH]^+$ calcd 494.1, found 493.8.

Methyl 2-(3,4-dimethoxybenzamido)-2-(3',4',5'-trifluoro-[1,1'-biphenyl]-4-yl)acetate (5af). 3,4-Dimethoxybenzoic acid (148 mg, 0.813 mmol) was coupled to compound **4** (200 mg, 0.677 mmol) according to General Procedure B. The crude product was purified by column chromatography (PE:EtOAc 100:0 to 50:50) to afford compound **5af** as a bright yellow foam (233 mg, 75%). ^{1}H NMR (d_6-DMSO) δ 9.10 (d, J = 7.1 Hz, 1H), 7.80–7.65 (m, 4H), 7.64–7.56 (m, 3H), 7.53 (d, J = 2.0 Hz, 1H), 7.03 (d, 7.1 Hz, 1H), 5.76 (d, J = 7.2 Hz, 1H), 3.82 (s, 3H), 3.81 (s, 3H), 3.69 (s, 3H); ^{19}F NMR (d_6-DMSO) δ -134.8 (d, J = 21.7 Hz), -163.3 (dd, J = 21.7/21.7 Hz); ^{13}C NMR (d_6-DMSO) δ 171.1, 165.9, 151.7, 150.6 (ddd, J_{CF} = 246.7/9.7/4.2 Hz), 148.2, 138.4 (dt, J_{CF} = 249.7/15.7 Hz), 136.9, 136.8–136.7

(m), 136.4 (td, J_{CF} = 8.1/4.5 Hz), 129.0, 127.0, 125.6, 121.3, 111.4–111.1 (m), 111.0, 110.8, 56.5, 55.60, 55.58, 52.3; *m/z* MS $C_{24}H_{21}F_3NO_5$ $[MH]^+$ calcd 460.1, found 460.1.

Methyl 2-(1*H*-indole-5-carboxamido)-2-(3',4',5'-trifluoro-[1,1'-biphenyl]-4-yl)acetate (5aj). 1*H*-Indole-5-carboxylic acid (98 mg, 0.610 mmol) was coupled to compound **4** (150 mg, 0.508 mmol) according to General Procedure B. Upon completion, the DCM was concentrated *in vacuo*. The solution was quenched with a 1 M HCl solution and extracted with EtOAc (1 × 30 mL). The organic phase was then washed with a saturated $NaHCO_3$ solution (20 mL) and finally brine (20 mL). The organic phase was dried over anhydrous Na_2SO_4, filtered and concentrated *in vacuo.* The crude product was purified by flash column chromatography (PE:EtOAc 100:0 to 60:40) to afford compound **5aj** as a maroon solid (220 mg, 99%). ^{1}H NMR (MeOD) δ 8.19 (dd, *J* = 1.7/0.5 Hz, 1H), 7.69–7.58 (m, 5H), 7.46–7.39 (m, 3H), 7.32 (d, *J* = 3.2 Hz, 1H), 6.56 (dd, *J* = 3.2/0.8 Hz, 1H), 5.81 (s, 1H), 3.77 (s, 3H); ^{19}F NMR (MeOD) δ -136.9 (d, *J* = 19.8 Hz), -166.0 (dd, *J* = 19.8/19.8 Hz); ^{13}C NMR (MeOD) δ 172.8, 171.4, 152.6 (ddd, J_{CF} = 247.8/9.8/4.1 Hz), 141.9–139.2 (m), 139.7, 139.2, 138.5–138.3 (m), 138.3, 129.8 (2C), 129.0, 128.3 (2C), 127.3, 125.6, 121.9, 121.9, 112.3–112.0 (m, 3C), 103.7, 58.4, 53.2; *m/z* MS (system A) $C_{24}H_{16}F_3N_2O_3$ $[M-H]^-$ calcd 437.1, found 437.1.

Methyl 2-(1*H*-indazole-5-carboxamido)-2-(3',4',5'-trifluoro-[1,1'-biphenyl]-4-yl)acetate (5ak). 1*H*-Indazole-5-carboxylic acid (59 mg, 0.366 mmol) was coupled to compound **4** (90 mg, 0.305 mmol) according to General Procedure B. Upon completion, the DCM was concentrated *in vacuo*. The solution was quenched with a 1 M HCl solution and extracted with EtOAc (1 × 30 mL). The organic phase was then washed with a saturated $NaHCO_3$ solution (20 mL) and finally brine (20 mL). The organic phase was dried over anhydrous Na_2SO_4, filtered and concentrated *in vacuo.* The crude product was purified by flash chromatography (PE:EtOAc 100:0 to 40:60) to afford compound **5ak** as a white solid (76 mg, 57%). ^{1}H NMR (d_6-DMSO) δ 9.24 (d, *J* = 7.2 Hz, 1H), 8.46 (s, 1H), 8.22 (s, 1H), 7.91 (dd, *J* = 8.8/1.5 Hz, 1H), 7.80–7.68 (m, 5H), 7.65–7.56 (m, 3H), 5.79 (d, *J* = 7.2 Hz, 1H), 3.69 (s, 3H); ^{19}F NMR (d_6-

DMSO) δ -134.8 (d, J = 21.7 Hz), -163.3 (dd, J = 21.7/21.7 Hz); ^{13}C NMR (d_6-DMSO) δ 171.0, 166.8, 150.6 (ddd, J_{CF} = 246.7/9.7/4.1 Hz), 141.0, 139.8–136.9 (m), 136.9, 136.7, 136.6–136.3 (m), 134.9, 128.9 (2C), 127.0 (2C), 126.0, 125.7, 122.3, 121.4, 111.3 (dd, J_{CF} = 16.1/5.4 Hz), 109.7, 56.5, 52.3; *m/z* MS $C_{23}H_{17}F_3N_3O_3$ $[MH]^+$ calcd 440.1, found 439.8.

Methyl 2-(1*H*-benzo*[d]*[1,2,3]triazole-5-carboxamido)-2-(3',4',5'-trifluoro-[1,1'-biphenyl]-4-yl)acetate (5al). 1*H*-Benzo[*d*][1,2,3]triazole-5-carboxylic acid (60 mg, 0.366 mmol) was coupled to compound **4** (90 mg, 0.305 mmol) according to General Procedure B. Upon completion, the DCM was concentrated *in vacuo*. The solution was quenched with a 1 M HCl solution and extracted with EtOAc (1 × 30 mL). The organic phase was then washed with a saturated $NaHCO_3$ solution (20 mL) and finally brine (20 mL). The organic phase was dried over anhydrous Na_2SO_4, filtered and concentrated *in vacuo.* The crude product was purified by flash chromatography (PE:EtOAc 100:0 to 40:60) to afford compound **5al** as a white solid (100 mg, 75%). ^{1}H NMR (MeOD) δ 8.47 (s, 1H), 7.98 (dd, J = 8.7/1.5 Hz, 1H), 7.88 (d, J = 8.7 Hz, 1H), 7.66–7.56 (m, 4H), 7.43–7.35 (m, 2H), 5.82 (s, 1H), 3.78 (s, 3H); ^{19}F NMR (MeOD) δ -136.8 (d, J = 19.9 Hz), -165.8 (dd, J = 19.8/19.8 Hz); ^{13}C NMR (MeOD) δ 172.5, 169.5, 152.7 (ddd, J_{CF} = 248.0/9.9/4.2 Hz), 141.9–139.0 (m), 139.5, 139.2, 138.5–138.2 (m), 137.8*, 132.5, 129.9 (2C), 129.8, 128.4, 128.4 (2C), 126.8, 112.4 – 112.1 (m, 2C), 58.6, 53.2; *m/z* MS $C_{22}H_{16}F_3N_4O_3$ $[MH]^+$ calcd 441.1, found 440.8. *May account for 2 carbons, as there are many overlapping quaternary carbons in this region.

Methyl 2-(1*H*-benzo*[d]*imidazole-5-carboxamido)-2-(3',4',5'-trifluoro-[1,1'-biphenyl]-4-yl)acetate (5am). 1*H*-Benzo[*d*]imidazole-5-carboxylic acid (99 mg, 0.610 mmol) was coupled to compound **4** (150 mg, 0.508 mmol) according to General Procedure B. Upon completion, the DCM was concentrated *in vacuo*. The solution was quenched with a 1 M HCl solution and extracted with EtOAc (1 × 30 mL). The organic phase was then washed with a saturated $NaHCO_3$ solution (20 mL) and finally brine. The organic phase was dried over anhydrous Na_2SO_4, filtered and concentrated *in vacuo*. The

crude product was purified by flash column chromatography (DCM:MeOH 100:0 to 90:10) to afford compound **5am** as a dull yellow/brown solid (174 mg, 78%). ^{1}H NMR (MeOD) δ 8.30 (s, 1H), 8.21 (d, J = 1.1 Hz, 1H), 7.83 (dd, J = 8.5/1.6 Hz, 1H), 7.69–7.58 (m, 5H), 7.45–7.37 (m, 2H), 5.81 (s, 1H), 3.78 (s, 3H); ^{19}F NMR (MeOD) δ -136.8 (d, J = 19.8 Hz), -165.9 (dd, J = 19.8/19.8 Hz); ^{13}C NMR (MeOD) δ 172.6, 170.3, 152.6 (ddd, J_{CF} = 248.1/10.0/4.1 Hz), 144.8, 141.0–140.8 (m), 141.8–138.8 (m), 139.3, 139.1, 138.6–138.1 (m), 137.9, 129.8 (2C), 129.5, 128.3 (2C), 123.5, 116.9, 115.8, 112.1 (m, 2C), 58.5, 53.3; *m/z* MS (system A) $C_{23}H_{17}F_3N_3O_3$ $[MH]^+$ calcd 440.1, found 439.8.

Methyl 2-(2-oxoindoline-5-carboxamido)-2-(3',4',5'-trifluoro-[1,1'-biphenyl]-4-yl)acetate (5an). 2-Oxoindoline-5-carboxylic acid (72 mg, 0.406 mmol) was coupled to compound **4** (100 mg, 0.339 mmol) in DMF according to General Procedure B. Upon completion, the reaction mixture was poured onto ice-water. The precipitate was filtered, washed through with water and Et_2O to afford compound **5an** as a brown solid (152 mg, 99%). ^{1}H NMR (MeOD) δ 7.83–7.76 (m, 2H), 7.67–7.62 (m, 2H), 7.59–7.55 (m, 2H), 7.42 (dd, J = 9.3/6.6 Hz, 2H), 6.94 (dd, J = 8.1/0.5 Hz, 1H), 5.76 (s, 1H), 3.76 (s, 3H); ^{19}F NMR (MeOD) δ -136.8 (d, J = 19.8/19.8 Hz), -165.9 (dd, J = 19.8/19.8 Hz); ^{13}C NMR (MeOD) δ 179.9, 172.6, 169.7, 152.7 (ddd, J_{CF} = 248.0/10.0/4.1 Hz), 148.3, 141.9–138.9 (m), 139.4–139.1 (m), 138.4–138.2 (m), 138.0, 129.8 (2C), 129.5, 128.6, 128.3 (2C), 127.2, 125.2, 112.2 (m, 2C), 110.3, 58.4, 53.2, 39.6; *m/z* MS (system A) $C_{24}H_{18}F_3N_2O_4$ $[MH]^+$ calcd 455.1, found 455.7.

Methyl 2-(2-phenylacetamido)-2-(3',4',5'-trifluoro-[1,1'-biphenyl]-4-yl)acetate (5ao). Phenylacetic acid (99.6 mg, 0.732 mmol) was coupled to compound **4** (180 mg, 0.610 mmol) according to General Procedure B. The crude product was purified by column chromatography (PE:EtOAc 100:0 to 50:50) to afford compound **5ao** as a yellow solid (100 mg, 40%). ^{1}H NMR ($CDCl_3$) δ 7.43–7.37 (m, 2H), 7.37–7.19 (m, 7H), 7.16–7.04 (m, 2H), 6.60 (d, J = 6.9 Hz, 1H), 5.57 (d, J = 7.0 Hz, 1H), 3.68 (s, 3H), 3.59 (s, 2H); ^{19}F NMR ($CDCl_3$) δ -133.9 (d, J = 20.5 Hz), -162.2 (dd, J = 20.5/20.5 Hz); ^{13}C NMR ($CDCl_3$) δ 171.1, 170.5, 151.5 (ddd, J_{CF} = 249.8/10.0/4.3 Hz), 139.5 (dt, J_{CF} = 252.4/15.4 Hz), 138.5–

138.4 (m), 136.9, 136.6 (td, J_{CF} = 7.7/4.5 Hz), 129.5, 129.2, 127.9, 127.6, 127.5, 111.5–110.9 (m), 56.2, 53.1, 43.6; *m/z* MS $C_{23}H_{19}F_3NO_3$ $[MH]^+$ calcd 414.1, found 413.9.

Methyl 2-(2-(3-fluorophenyl)acetamido)-2-(3',4',5'-trifluoro-[1,1'-biphenyl]-4-yl)acetate (5ap). 2-(3-Fluorophenyl)acetic acid (125 mg, 0.813 mmol) was coupled to compound **4** (200 mg, 0.667 mmol) according to General Procedure B. The crude product was purified by column chromatography (PE:EtOAc 100:0 to 50:50) to afford compound **5ap** as a white solid (248 mg, 85%). ^{1}H NMR (d_6-DMSO) δ 9.08 (d, *J* = 7.1 Hz, 1H), 7.75 (d, *J* = 8.4 Hz, 2H), 7.72–7.63 (m, 2H), 7.51 (d, *J* = 8.3 Hz, 2H), 7.38–7.28 (m, 1H), 7.12 (m, 2H), 7.08–6.98 (m, 1H), 5.51 (d, *J* = 7.1 Hz, 1H), 3.64 (s, 3H), 3.61 (app. d, *J* = 4.3 Hz, 2H); ^{19}F NMR (d_6-DMSO) δ -113.9, -134.8 (d, *J* = 21.6 Hz), -163.3 (dd, *J* = 21.7/21.7 Hz); ^{13}C NMR (d_6-DMSO) δ 170.8, 169.7, 162.0 (d, J_{CF} = 242.9 Hz), 150.6 (ddd, J_{CF} = 246.7/9.7/4.1 Hz), 138.8 (d, J_{CF} = 7.9 Hz), 138.4 (dt, J_{CF} = 249.7/15.7 Hz), 136.9 (d, *J* = 1.2 Hz), 136.5, 136.3 (td, J_{CF} = 8.1/4.4 Hz), 123.0 (d, J_{CF} = 8.4 Hz), 128.4, 127.2, 125.2 (d, J_{CF} = 2.7 Hz), 115.8 (d, J_{CF} = 21.4 Hz), 113.2 (d, J_{CF} = 20.8 Hz), 111.8–110.3 (m), 56.0, 52.3, 41.1; *m/z* MS $C_{23}H_{18}F_4NO_3$ $[MH]^+$ calcd 432.1, found 431.8.

Methyl 2-(2-(4-fluorophenyl)acetamido)-2-(3',4',5'-trifluoro-[1,1'-biphenyl]-4-yl)acetate (5aq). 2-(4-Fluorophenyl)acetic acid (94.0 mg, 0.610 mmol) was coupled to compound **4** (150 mg, 0.508 mmol) according to General Procedure B. The crude product was purified by column chromatography (PE:EtOAc 100:0 to 50:50) to afford compound **5aq** as a white solid (155 mg, 71%). ^{1}H NMR ($CDCl_3$) δ 7.35 (d, *J* = 8.4 Hz, 2H), 7.27 (d, *J* = 8.3 Hz, 2H), 7.19–7.12 (m, 2H), 7.08–7.01 (m, 2H), 6.98–6.91 (m, 2H), 6.61 (d, *J* = 6.9 Hz, 1H), 5.51 (d, *J* = 7.0 Hz, 1H), 3.63 (s, 3H), 3.50 (s, 2H); ^{19}F NMR ($CDCl_3$) δ -115.1, -133.9 (d, *J* = 20.5 Hz), -162.1 (dd, *J* = 20.5/20.5 Hz); ^{13}C NMR ($CDCl_3$) δ 171.1, 170.2, 162.3 (d, J_{CF} = 246.1 Hz), 151.5 (ddd, J_{CF} = 249.8/10.0/4.3 Hz), 140.9–137.8 (dt, J_{CF} = 252.2/15.2 Hz), 138.7–138.5 (m), 136.8, 136.6 (td, J_{CF} = 7.8/4.7 Hz), 131.0 (d, J_{CF} = 8.1 Hz), 130.3 (d, J_{CF} = 3.3 Hz), 128.0, 127.5, 115.9 (d, J_{CF} = 21.5 Hz), 111.1 (m), 56.2, 53.1, 42.5; *m/z* MS $C_{23}H_{18}F_4NO_3$ $[MH]^+$ calcd 432.1, found 431.8.

Methyl 2-(2-(4-methoxyphenyl)acetamido)-2-(3',4',5'-trifluoro-[1,1'-biphenyl]-4-yl)acetate (5ar). 2-(4-Methoxyphenyl)acetic acid (270 mg, 1.63 mmol) was coupled to compound **4** (400 mg, 1.35 mmol) according to General Procedure B. The crude product was purified by column chromatography (PE:EtOAc 100:0 to 50:50) to afford compound **5ar** as a white solid (195 mg, 32%). ^{1}H NMR ($CDCl_3$) δ 7.42 (d, J = 8.3 Hz, 2H), 7.35 (d, J = 8.3 Hz, 2H), 7.19 (d, J = 8.6 Hz, 2H), 7.12 (m, 2H), 6.89 (d, J = 8.6 Hz, 2H), 6.70 (d, J = 7.0 Hz, 1H), 5.61 (d, J = 7.1 Hz, 1H), 3.80 (s, 3H), 3.71 (s, 3H), 3.55 (s, 2H); ^{19}F NMR ($CDCl_3$) δ -133.9 (d, J = 20.5 Hz), -162.2 (dd, J = 20.5/20.5 Hz); ^{13}C NMR ($CDCl_3$) δ 171.1, 170.9, 159.0, 151.5 (ddd, J_{CF} = 249.8/10.0/4.2 Hz), 139.5 (dt, J_{CF} = 32.4/15.4 Hz), 138.4–138.4 (m), 136.9, 136.6 (td, J_{CF} = 7.8/4.6 Hz), 130.5, 127.9, 127.4, 126.4, 114.5, 111.1 (m), 56.1, 55.3, 53.0, 42.6; *m/z* MS $C_{24}H_{21}F_3NO_4$ $[MH]^+$ calcd 444.1, found 443.9.

Methyl 2-(2-(4-carbamoylphenyl)acetamido)-2-(3',4',5'-trifluoro-[1,1'-biphenyl]-4-yl)acetate (5at). 2-(4-Carbamoylphenyl)acetic acid (146 mg, 0.813 mmol) was coupled to compound **4** (200 mg, 0.677 mmol) according to General Procedure B. Upon completion, the reaction mixture was diluted with sat. $NaHCO_3$ (15 mL) and extracted with DCM (3 × 15 mL). The combined organic layers were dried over anhydrous Na_2SO_4, filtered and concentrated *in vacuo* to afford compound **5at** as a white solid (261 mg, 85%). ^{1}H NMR (d_6-DMSO) δ 9.09 (d, J = 7.2 Hz, 1H), 7.91 (br. s, 1H), 7.87–7.65 (m, 6H), 7.51 (d, J = 8.3 Hz, 2H), 7.34 (d, J = 8.3 Hz, 2H), 7.30 (br. s, 1H), 5.50 (d, J = 7.1 Hz, 1H), 3.64 (s, 3H), 3.62 (d, J = 2.3 Hz, 2H); ^{19}F NMR (d_6-DMSO) δ -134.8 (d, J = 21.7 Hz), -163.2 (dd, J = 21.7/21.7 Hz); ^{13}C NMR (d_6-DMSO) δ 170.9, 169.8, 167.8, 150.6 (ddd, J_{CF} = 246.7/9.7/4.2 Hz), 139.4, 138.4 (dt, J_{CF} = 249.5/15.5 Hz), 137.0–136.8 (m), 136.6, 136.2 (td, J_{CF} = 8.1/4.3 Hz), 132.5, 128.9, 128.5, 127.4, 127.2, 111.6–111.0 (m), 56.0, 52.4, 41.4; *m/z* MS $C_{24}H_{20}F_3N_2O_4$ $[MH]^+$ calcd 457.1, found 456.9.

Methyl 2-(2-(3,4-dimethoxyphenyl)acetamido)-2-(3',4',5'-trifluoro-[1,1'-biphenyl]-4-yl)acetate (5au). 2-(3,4-Dimethoxyphenyl)acetic acid (319 mg, 1.63 mmol) was coupled to compound **4** (400 mg, 1.35 mmol) according to General Procedure B. The crude product was purified by column chromatography (PE:EtOAc 100:0 to 50:50) to afford compound **5au** as a white solid (446 mg, 70%).

^{1}H NMR (d_6-DMSO) δ 9.03 (d, J = 7.3 Hz, 1H), 7.87–7.62 (m, 4H), 7.51 (d, J = 8.3 Hz, 2H), 6.94–6.75 (m, 3H), 5.51 (d, J = 7.2 Hz, 1H), 3.72 (s, 3H), 3.71 (s, 3H), 3.64 (s, 3H), 3.48 (s, 2H); ^{19}F NMR (d_6-DMSO) δ -134.8 (d, J = 21.7 Hz), -163.3 (dd, J = 21.7/21.7 Hz); ^{13}C NMR (d_6-DMSO) δ 170.9, 170.4, 150.6 (ddd, J_{CF} = 246.8/9.8/4.3 Hz), 148.5, 147.5, 138.4 (dt, J_{CF} = 30.6/15.6 Hz), 136.9–136.8 (m), 136.7, 136.3 (td, J_{CF} = 8.1/4.4 Hz), 128.5, 128.4, 127.1, 121.0, 112.9, 111.7, 111.3 (dd, J_{CF} = 16.0/5.6 Hz), 55.9, 55.5, 55.3, 52.3, 41.2; *m/z* MS $C_{25}H_{23}F_3NO_5$ $[MH]_+$ calcd 474.1, found 473.9.

Methyl 2-(2-(3-fluoro-4-methoxyphenyl)acetamido)-2-(3',4',5'-trifluoro-[1,1'-biphenyl]-4-yl)acetate (5aw). 2-(3-Fluoro-4-methoxyphenyl)acetic acid (187 mg, 1.02 mmol) was coupled to compound **4** (250 mg, 0.847 mmol) according to General Procedure B. The crude product was purified by column chromatography (PE:EtOAc 100:0 to 50:50) to afford compound **5aw** as a yellow solid (134 mg, 34%). ^{1}H NMR ($CDCl_3$) δ 7.45 (d, J = 8.4 Hz, 2H), 7.36 (d, J = 8.2 Hz, 2H), 7.14 (m, 2H), 7.05–6.90 (m, 3H), 6.60 (d, J = 6.9 Hz, 1H), 5.59 (d, J = 7.0 Hz, 1H), 3.89 (s, 3H), 3.73 (s, 3H), 3.54 (s, 2H); ^{19}F NMR ($CDCl_3$) δ -133.9 (d, J = 20.5 Hz), -134.2, -162.1 (dd, J = 20.5/20.5 Hz); ^{13}C NMR ($CDCl_3$) δ 171.1, 170.2, 152.5 (d, J_{CF} = 246.9 Hz), 151.6 (ddd, J_{CF} = 249.8/10.0/4.2 Hz), 147.2 (d, J_{CF} = 10.6 Hz), 139.6 (dt, J_{CF} = 252.3/15.3 Hz), 138.7–138.5 (m), 136.82, 136.6 (td, J_{CF} = 7.8/4.7 Hz), 128.0, 127.6, 127.2 (d, J_{CF} = 6.4 Hz), 125.3 (d, J_{CF} = 3.6 Hz), 117.2 (d, J_{CF} = 18.6 Hz), 113.9 (d, J_{CF} = 2.2 Hz), 111.2 (m), 56.4, 56.3, 53.2, 42.5 (d, J_{CF} = 1.0 Hz); *m/z* MS $C_{23}H_{20}F_4NO_4$ $[MH]^+$ calcd 462.1, found 461.9.

Methyl 2-(2-(4-fluoro-3-methoxyphenyl)acetamido)-2-(3',4',5'-trifluoro-[1,1'-biphenyl]-4-yl)acetate (5ay). 2-(4-Fluoro-3-methoxyphenyl)acetic acid (225 mg, 1.22 mmol) was coupled to compound **4** (300 mg, 1.02 mmol) according to General Procedure B. The crude product was purified by column chromatography (PE:EtOAc 100:0 to 50:50) to afford compound **5ay** as a white solid (410 mg, 87%). ^{1}H NMR ($CDCl_3$) δ 7.47–7.32 (m, 4H), 7.18–7.10 (m, 2H), 7.08–7.00 (m, 1H), 6.89 (dd, J = 8.1/2.1 Hz, 1H), 6.78 (ddd, J = 8.2/4.2/2.1 Hz, 1H), 6.66 (d, J = 7.0 Hz, 1H), 5.60 (d, J = 7.0 Hz, 1H), 3.85 (s, 3H), 3.72 (s, 3H), 3.57 (s, 2H); ^{19}F NMR ($CDCl_3$) δ -133.8 (d, J = 20.5 Hz), -137.0, -162.1 (dd, J = 20.5/20.5 Hz); ^{13}C NMR ($CDCl_3$) δ 171.1, 170.1, 151.9 (d, J_{CF} = 245.8 Hz), 151.53 (ddd, J_{CF} =

249.9/10.0/4.2 Hz), 147.97 (d, J_{CF} = 10.8 Hz), 139.5 (dt, J_{CF} = 252.4/15.4 Hz), 138.6 (d, J_{CF} = 1.6 Hz), 136.8, 136.5 (td, J_{CF} = 7.8/4.7 Hz), 130.76 (d, J = 4.0 Hz), 128.0, 127.5, 121.6 (d, J_{CF} = 6.9 Hz), 116.4 (d, J_{CF} = 18.4 Hz), 114.5 (d, J_{CF} = 2.0 Hz), 111.1 (dd, J_{CF} = 15.9/6.0 Hz), 56.3, 56.2, 53.1, 43.0; *m/z* MS $C_{24}H_{20}F_4NO_4$ $[MH]^+$ calcd 462.1, found 461.8.

2-Acetamido-N-hydroxy-2-(3',4',5'-trifluoro-[1,1'-biphenyl]-4-yl)acetamide (6a). Compound **5a** (101 mg, 0.300 mmol) was converted to the corresponding hydroxamic acid according to General Procedure C. The crude product was purified by column chromatography (DCM:MeOH:AcOH 99:0:1 to 90:9:1) to afford compound **6a** as a pink solid (64 mg, 65%). ^{1}H NMR (d_6-DMSO) δ 11.02 (s, 1H), 9.01 (s, 1H), 8.71 (d, J = 8.4 Hz, 1H), 7.86–7.64 (m, 4H), 7.49 (d, J = 8.3 Hz, 2H), 5.41 (d, J = 8.4 Hz, 1H), 1.91 (s, 3H); ^{19}F NMR (d_6-DMSO) δ -134.9 (d, J = 21.8 Hz), -163.5 (dd, J = 21.8/21.8 Hz); ^{13}C NMR (d_6-DMSO) δ 169.1, 166.5, 150.7 (ddd, J_{CF} = 13.6/9.8/4.3 Hz), 139.4, 134.0–136.8 (m), 136.7–136.4 (m), 136.3–135.9 (m), 127.7, 126.8, 111.3 (dd, J_{CF} = 16.0/5.4 Hz), 53.5, 22.4; *m/z* HRMS (TOF ES$^+$) $C_{16}H_{14}F_3N_2O_3$ $[MH]^+$ calcd 339.0951, found 339.0953.

3-((2-(Hydroxyamino)-2-oxo-1-(3',4',5'-trifluoro-[1,1'-biphenyl]-4-yl)ethyl)amino)-3-oxopropanoic acid (6c). Compound **5b** (185 mg, 0.485 mmol) was converted to the corresponding hydroxamic acid according to General Procedure C. After 1 d, only partial conversion had occurred and therefore $NH_2OH.HCl$ (135 mg, 1.94 mmol) and KOH (5M in MeOH, 0.486 mL) were added. The reaction mixture was stirred for a further 24 h. LC-MS indicated that **5b** was converted to the desired product and the dihydroxamic acid N^1-hydroxy-N^3-(2-(hydroxyamino)-2-oxo-1-(3',4',5'-trifluoro-[1,1'-biphenyl]-4-yl)ethyl)malonamide (**6d**). These two compounds were isolated by column chromatography (DCM:MeOH:AcOH 99:0:1 to 90:9:1). The desired hydroxamic acid was treated with 20% TFA/DCM (5 mL) and stirred at rt overnight. The reaction mixture was concentrated *in vacuo* and extracted with EtOAc (3 × 5 mL). The combined organic layers were dried over Na_2SO_4, filtered and concentrated *in vacuo*. The crude product was purified by column chromatography (DCM:MeOH:AcOH 99:0:1 to 90:9:1) to afford compound **6c** as a light brown oil (10 mg, 6% over 2 steps). ^{1}H NMR (d_6-DMSO) δ

11.28 (s, 1H), 9.29 (d, J = 8.2 Hz, 1H), 7.86–7.58 (m, 4H), 7.49 (d, J = 8.3 Hz, 2H), 5.41 (d, J = 8.2 Hz, 1H), 3.26–3.06 (m, 2H); ^{19}F NMR (d_6-DMSO) δ -134.9 (d, J = 21.7 Hz), -163.5 (dd, J = 21.8/21.8 Hz); ^{13}C NMR (d_6-DMSO) δ 170.2, 166.9, 166.3, 150.6 (ddd, J_{CF} = 246.5/9.7/4.1 Hz), 139.3, 138.3 (dt, J_{CF} = 251.1/16.7 Hz), 136.6 (td, J_{CF} = 8.1/4.5 Hz), 136.2–136.1 (m), 127.6, 126.8, 113.1–108.6 (m), 53.7, 43.3; *m/z* HRMS (TOF ES$^+$) $C_{17}H_{14}F_3N_2O_5$ $[MH]^+$ calcd 383.0849, found 383.0857.

***N*^{1}-Hydroxy-N^3-(2-(hydroxyamino)-2-oxo-1-(3',4',5'-trifluoro-[1,1'-biphenyl]-4-yl)ethyl)malonamide (6d).** The title compound was synthesised by aminolysis of both methyl and *tert*-butyl esters of compound **5b** as explained above. ^{1}H NMR (d_6-DMSO) δ 10.64 (s, 2H), 9.08 (s, 1H), 8.94 (s, 1H), 8.84 (d, J = 8.2 Hz, 1H), 7.81–7.58 (m, 4H), 7.49 (d, J = 8.3 Hz, 2H), 5.39 (d, J = 8.2 Hz, 1H), 3.07 (s, 2H); ^{19}F NMR (d_6-DMSO) δ -134.9 (d, J = 21.7 Hz), -163.5 (dd, J = 21.7/21.7 Hz); ^{13}C NMR (d_6-DMSO) δ 166.1, 165.9, 163.8, 150.6 (ddd, J = 246.5/9.7/4.4 Hz), 139.4, 138.3 (dt, J = 249.8/19.6 Hz), 136.6 (td, J = 8.2/4.5 Hz), 136.2–136.0 (m), 127.5, 126.8, 111.8–109.8 (m), 53.8, 40.3; *m/z* MS (TOF ES$^-$) $C_{17}H_{13}F_3N_3O_5$ $[M-H]^-$ calcd 396.1, found 396.0; *m/z* HRMS (TOF ES$^+$) $C_{17}H_{15}F_3N_3O_5$ $[MH]^+$ calcd 398.0958, found 398.0954.

4-((2-(Hydroxyamino)-2-oxo-1-(3',4',5'-trifluoro-[1,1'-biphenyl]-4-yl)ethyl)amino)-4-oxobutanoic acid (6e). Compound **5c** (267 mg, 0.675 mmol) was converted to the corresponding hydroxamic acid according to General Procedure C. After 1 d, only partial conversion had occurred, therefore $NH_2OH.HCl$ (188 mg, 2.71 mmol) was added and the reaction mixture was heated at 40 ºC for 2 h. The reaction progressed slowly and therefore the temperature was increased to 50 ºC overnight. LC-MS showed degradation of **5e** to **4**. The reaction was stopped and compounds **4**, **5e**, and **6e** were isolated by column chromatography (DCM:MeOH:AcOH 99:0:1 to 95:4:1). Compound **6e** was obtained as a white solid (15 mg, 6%). ^{1}H NMR (d_6-DMSO) δ 11.95 (s, 1H), 11.01 (s, 1H), 9.04 (s, 1H), 8.72 (d, J = 8.3 Hz, 1H), 8.08–7.61 (m, 4H), 7.49 (d, J = 8.3 Hz, 2H), 5.41 (d, J = 8.3 Hz, 1H), 2.49–2.02 (m, 4H); ^{19}F NMR (d_6-DMSO) δ -134.9 (d, J = 21.8 Hz), -163.5 (dd, J = 21.8/21.8 Hz); ^{13}C NMR (d_6-DMSO) δ 174.1, 171.1, 166.5, 150.7 (ddd, J_{CF} = 246.4/9.7/4.1 Hz), 139.4, 138.4 (dt, J_{CF} = 248.9/15.1 Hz), 136.6

(td, J_{CF} = 8.0/4.3 Hz), 136.3–136.0 (m), 127.7, 126.8, 111.5–111.0 (m), 53.6, 29.9, 29.2; *m/z* HRMS (TOF ES$^+$) $C_{18}H_{16}F_3N_2O_5$ $[MH]^+$ calcd 397.1006, found 397.1018.

***N*^{1}-(2-(Hydroxyamino)-2-oxo-1-(3',4',5'-trifluoro-[1,1'-biphenyl]-4-yl)ethyl)succinamide (6f).** Compound **5f** (84 mg, 0.213 mmol) was converted to the corresponding hydroxamic acid according to General Procedure C. The crude product was purified by column chromatography (DCM:MeOH:AcOH 95:4:1 to 90:9:1) to afford compound **6f** as a white solid (43 mg, 52%). ^{1}H NMR (d_6-DMSO) δ 11.00 (s, 1H), 9.01 (s, 1H), 8.66 (d, J = 8.3 Hz, 1H), 7.79–7.62 (m, 4H), 7.49 (d, J = 8.4 Hz, 2H), 7.27 (br. s, 1H), 6.74 (br. s, 1H), 5.41 (d, J = 8.3 Hz, 1H), 2.43 (t, J = 7.9 Hz, 2H), 2.28 (t, J = 7.2 Hz, 2H); ^{19}F NMR (d_6-DMSO) δ -134.9 (d, J = 21.7 Hz), -163.5 (dd, J = 21.8/21.8 Hz);^{13}C NMR (d_6-DMSO) δ 173.5, 171.4, 166.4, 150.6 (ddd, J_{CF} = 246.4/9.8/4.3 Hz), 139.4, 138.3 (dt, J_{CF} = 258.4/15.8 Hz), 136.6 (td, J_{CF} = 8.1/4.2 Hz), 136.2–135.9 (m), 127.7, 126.8, 111.2 (dd, J_{CF} = 16.0/5.4 Hz), 53.6, 30.4, 30.3; *m/z* HRMS (TOF ES$^+$) $C_{18}H_{17}F_3N_3O_4$ $[MH]^+$ calcd 396.1166, found 396.1173.

***N*-(2-(Hydroxyamino)-2-oxo-1-(3',4',5'-trifluoro-[1,1'-biphenyl]-4-yl)ethyl)benzamide (6g).** Compound **5g** (50 mg) was converted to the corresponding hydroxamic acid according to General Procedure C. The crude product was purified by column chromatography (DCM:MeOH 100:0 to 90:10) followed by preparative HPLC to afford compound **6g** as a white solid (10.7 mg, 21%). ^{1}H NMR (d_6-DMSO) δ 11.08 (s, 1H), 9.06 (s, 1H), 8.94 (d, J = 8.1 Hz, 1H), 7.93 (d, J = 7.3 Hz, 2H), 7.78–7.60 (m, 6H), 7.58–7.39 (m, 3H), 5.68 (d, J = 8.1 Hz, 1H); ^{19}F NMR (d_6-DMSO) δ -134.9 (d, J = 21.6 Hz), -163.5 (dd, J = 21.7/21.7 Hz); ^{13}C NMR (d_6-DMSO) δ 166.5, 166.3, 150.6 (ddd, J_{CF} = 246.6/9.7/4.2 Hz), 138.9, 138.3 (dt, J_{CF} = 249.1/15.4 Hz), 136.6 (td, J_{CF} = 8.0/4.3 Hz), 136.3–136.1 (m), 133.8, 131.5, 128.2, 128.1, 127.8, 126.8, 113.5–109.6 (m), 54.4; *m/z* HRMS (TOF ES$^+$) $C_{21}H_{16}F_3N_2O_3$ $[MH]^+$ calcd 401.1108, found 401.1104.

3-Fluoro-*N*-(2-(hydroxyamino)-2-oxo-1-(3',4',5'-trifluoro-[1,1'-biphenyl]-4-yl)ethyl)benzamide (6h). Compound **5h** (50 mg, 0.120 mmol) was converted to the corresponding hydroxamic acid according to General Procedure C. The crude product was purified by column

chromatography (DCM:MeOH 100:0 to 90:10) followed by preparative HPLC to afford compound **6h** as a white solid (28.6 mg, 57%). ^{1}H NMR (d_6-DMSO) δ 11.08 (s, 1H), 9.11 (d, J = 8.0 Hz, 1H), 9.06 (s, 1H), 7.84–7.59 (m, 8H), 7.52 (dd, J = 13.9/7.9 Hz, 1H), 7.43–7.36 (m, 1H), 5.66 (d, J = 8.0 Hz, 1H); ^{19}F NMR (d_6-DMSO) δ -113.1, -134.9 (d, J = 21.7 Hz), -163.5 (dd, J = 21.6/21.6 Hz); ^{13}C NMR (d_6-DMSO) δ 166.3, 165.0 (d, J_{CF} = 2.4 Hz), 161.8 (d, J_{CF} = 244.0 Hz), 150.6 (ddd, J_{CF} = 246.5/9.7/4.2 Hz), 138.6, 138.3 (dt, J_{CF} = 248.8/15.4 Hz), 136.5 (td, J_{CF} = 8.2/4.7 Hz), 136.4–136.2 (m), 136.1 (d, J_{CF} = 6.9 Hz), 130.3 (d, J_{CF} = 7.9 Hz), 128.2, 126.8, 124.0 (d, J_{CF} = 2.7 Hz), 118.3 (d, J_{CF} = 21.1 Hz), 114.6 (d, J_{CF} = 22.9 Hz), 111.9–110.5 (m), 54.5; *m/z* HRMS (TOF ES$^+$) $C_{21}H_{15}F_4N_2O_3$ [MH]$^+$ calcd 419.1013, found 419.1020.

4-Fluoro-*N*-(2-(hydroxyamino)-2-oxo-1-(3',4',5'-trifluoro-[1,1'-biphenyl]-4-yl)ethyl)benzamide (6i). Compound **5i** (100 mg, 0.240 mmol) was converted to the corresponding hydroxamic acid according to General Procedure C. The crude product was purified by column chromatography (DCM:MeOH 100:0 to 90:10) to afford compound **6i** as a white solid (48 mg, 48%). ^{1}H NMR (d_6-DMSO) δ 11.06 (s, 1H), 9.13–8.97 (m, 2H), 8.08–7.96 (m, 2H), 7.78–7.60 (m, 6H), 7.36–7.22 (m, 2H), 5.67 (d, J = 8.0 Hz, 1H); ^{19}F NMR (d_6-DMSO) δ -109.1, -135.0 (d, J = 21.7 Hz), -163.5 (dd, J = 21.6/21.6 Hz); ^{13}C NMR (d_6-DMSO) δ 166.5, 165.3, 164.0 (d, J_{CF} = 241.0 Hz), 150.6 (ddd, J_{CF} = 246.6/9.7/4.2 Hz), 138.8, 138.3 (dt, J_{CF} = 249.4/15.6 Hz), 136.6 (td, J_{CF} = 8.0/4.3 Hz), 136.3–136.2 (m), 130.5 (d, J_{CF} = 9.0 Hz), 130.3 (d, J_{CF} = 2.9 Hz), 128.1, 126.8, 115.1 (d, J_{CF} = 21.7 Hz), 111.2 (m), 54.5; *m/z* HRMS (TOF ES$^+$) $C_{21}H_{15}F_4N_2O_3$ [MH]$^+$ calcd 419.1013, found 419.1019.

***N*-(2-(Hydroxyamino)-2-oxo-1-(3',4',5'-trifluoro-[1,1'-biphenyl]-4-yl)ethyl)-3-methoxybenzamide (6j).** Compound **5j** (528 mg, 1.23 mmol) was converted to the corresponding hydroxamic acid according to General Procedure C. The crude product was purified by column chromatography (DCM:MeOH 100:0 to 90:10) to afford compound **6j** as a white solid (350 mg, 66%). ^{1}H NMR (d_6-DMSO) δ 8.99 (d, J = 8.1 Hz, 1H), 7.76–7.61 (m, 6H), 7.53 (m, 2H), 7.37 (dd, J = 7.9/7.9 Hz, 1H), 7.10 (dd, J = 8.1/2.3 Hz, 1H), 5.72 (d, J = 8.0 Hz, 1H), 3.81 (s, 3H); ^{19}F NMR (d_6-DMSO) δ -

134.9 (d, J = 21.6 Hz), -163.5 (dd, J = 21.6/21.6 Hz); ^{13}C NMR (d_6-DMSO) δ 166.6, 166.2, 159.2, 150.7 (ddd, J_{CF} = 246.7/9.7/4.1 Hz), 139.0, 138.4 (dt, J_{CF} = 249.5/15.6 Hz), 136.7 (td, J_{CF} = 8.0/4.4 Hz), 136.5–136.0 (m), 135.3, 129.4, 128.2, 126.8, 120.1, 117.6, 112.9, 111.2 (m), 55.3, 54.5; *m/z* HRMS (TOF ES$^+$) $C_{22}H_{18}F_3N_2O_4$ $[MH]^+$ calcd 431.1213, found 431.1207.

***N*-(2-(Hydroxyamino)-2-oxo-1-(3',4',5'-trifluoro-[1,1'-biphenyl]-4-yl)ethyl)-4-methoxybenzamide (6k).** Compound **5k** (154 mg, 0.359 mmol) was converted to the corresponding hydroxamic acid according to General Procedure C. The crude product was purified by column chromatography (DCM:MeOH 100:0 to 90:10) to afford compound **6k** as a white solid (95.3 mg, 62%). ^{1}H NMR (d_6-DMSO) δ 11.06 (s, 1H), 9.05 (s, 1H), 8.76 (d, J = 8.2 Hz, 1H), 7.93 (d, J = 8.9 Hz, 2H), 7.81–7.65 (m, 4H), 7.61 (d, J = 8.4 Hz, 2H), 6.99 (d, J = 8.9 Hz, 2H), 5.66 (d, J = 8.1 Hz, 1H), 3.81 (s, 3H); ^{19}F NMR (d_6-DMSO) δ -134.9 (d, J = 21.7 Hz), -163.5 (dd, J = 21.7/21.7 Hz); ^{13}C NMR (d_6-DMSO) δ 166.6, 165.7, 161.8, 150.6 (ddd, J_{CF} = 246.6/9.7/4.2 Hz), 139.1, 138.3 (dt, J_{CF} = 249.3/15.5 Hz), 136.6 (td, J_{CF} = 8.1/4.5 Hz), 136.2–136.0 (m), 129.7, 128.1, 126.7, 126.0, 113.4, 111.2 (m), 55.4, 54.3; *m/z* HRMS (TOF ES$^+$) $C_{22}H_{18}F_3N_2O_4$ $[MH]^+$ calcd 431.1213, found 431.1216.

3-Hydroxy-*N*-(2-(hydroxyamino)-2-oxo-1-(3',4',5'-trifluoro-[1,1'-biphenyl]-4-yl)ethyl)benzamide (6l). Compound **6j** (230 mg, 0.534 mmol) was treated with BBr_3 (1M in DCM, 2.67 mL, 2.67 mmol) according to General Procedure D. The crude product was purified by preparative HPLC to afford compound **6l** as a white solid (62 mg, 28%). ^{1}H NMR (d_6-DMSO) δ 11.07 (s, 1H), 9.61 (br. s, 1H), 8.79 (d, J = 8.1 Hz, 1H), 7.68 (m, 6H), 7.37 (d, J = 7.8 Hz, 1H), 7.33–7.20 (m, 2H), 6.94 (dd, J = 8.0/1.7 Hz, 1H), 5.65 (d, J = 8.1 Hz, 1H); ^{19}F NMR (d_6-DMSO) δ -134.9 (d, J = 21.7 Hz), -163.5 (dd, J = 21.7/21.7 Hz); ^{13}C NMR (d_6-DMSO) δ 166.6, 166.4, 157.3, 150.7 (ddd, J_{CF} = 246.5/9.7/4.1 Hz), 139.0, 138.4 (dt, J_{CF} = 249.4/15.6 Hz), 136.6 (td, J_{CF} = 8.0/4.3 Hz), 136.4–136.1 (m), 135.3, 129.3, 128.1, 126.8, 118.5, 118.3, 114.7, 111.2 (m), 54.4; *m/z* HRMS (TOF ES$^+$) $C_{21}H_{16}F_3N_2O_4$ $[MH]^+$ calcd 417.1057, found 417.1064.

4-Hydroxy-*N*-(2-(hydroxyamino)-2-oxo-1-(3',4',5'-trifluoro-[1,1'-biphenyl]-4-yl)ethyl)benzamide (6m). Compound **6k** (125 mg, 0.290 mmol) was treated with BBr_3 (1 M in DCM, 2.90 mL, 2.90 mmol) according to General Procedure D. The crude product was purified by column chromatography (DCM:MeOH 100:0 to 90:10) followed by preparative HPLC to afford compound **6m** as a white solid (3.00 mg, 2.5%). ^{1}H NMR (d_6-DMSO) δ 11.03 (s, 1H), 10.0 (s, 1H), 9.03 (s, 1H), 8.60 (d, J = 8.2 Hz, 1H), 7.83–7.78 (m, 2H), 7.76–7.65 (m, 4H), 7.60 (d, J = 8.4 Hz, 2H), 6.83–6.77 (m, 2H), 5.63 (d, J = 8.1 Hz, 1H); ^{19}F NMR (d_6-DMSO) δ -134.9 (d, J = 21.7 Hz), -163.5 (dd, J = 21.7/21.7 Hz); ^{13}C NMR (d_6-DMSO) δ 166.6, 165.8, 160.4, 150.6 (ddd, J_{CF} = 246.5/9.8/4.3 Hz), 139.2, 138.2 (dt, J_{CF} = 247.8/15.7 Hz), 136.8–136.3 (m), 136.2–136.1 (m), 129.7, 128.0, 126.7, 124.4, 114.7, 111.7–110.8 (m), 54.2; *m/z* HRMS (TOF ES$^+$) $C_{21}H_{16}F_3N_2O_4$ $[MH]^+$ calcd 417.1057, found 417.1072.

***N*-(2-(Hydroxyamino)-2-oxo-1-(3',4',5'-trifluoro-[1,1'-biphenyl]-4-yl)ethyl)-3-(N'-hydroxycarbamimidoyl)benzamide (6p).** Compound **5n** (372 mg, 0.883 mmol) was converted to the amidoxime **6j** according to General Procedure C. After stirring at rt for 1 d, the nitrile of **5n** was completely converted to the corresponding amidoxime but none of the ester had converted to the hydroxamic acid. The reaction was left for a further 3 d, but only partial conversion to the desired hydroxamic acid **6p** was observed. $NH_2OH.HCl$ (244mg, 3.51 mmol) and KOH (5M in MeOH, 0.876 mL) were added. After stirring the reaction mixture at rt for 1 d, the reaction was complete and the mixture was purified by column chromatography (DCM:MeOH 100:0 to 90:10) to afford compound **6p** as white flakes (132 mg, 33%). ^{1}H NMR (d_6-DMSO) δ 11.11 (s, 1H), 9.72 (s, 1H), 9.08 (s, 1H), 8.98 (d, J = 8.2 Hz, 1H), 8.20 (s, 1H), 7.86 (dd, J = 20.8/7.9 Hz, 2H), 7.76–7.67 (m, 4H), 7.62 (d, J = 8.4 Hz, 2H), 7.46 (t, J = 7.8 Hz, 1H), 5.93 (s, 2H), 5.68 (d, J = 8.1 Hz, 1H); ^{19}F NMR (d_6-DMSO) δ -134.9 (d, J = 21.7 Hz), -163.5 (dd, J = 21.8/21.8 Hz); ^{13}C NMR (d_6-DMSO) δ 166.4, 166.1, 150.6 (ddd, J_{CF} = 246.5/9.7/4.2 Hz), 150.3, 139.0, 138.3 (dt, J_{CF} = 247.1/14.4 Hz), 136.7–136.4 (m), 136.4–136.2 (m), 133.7, 133.3, 128.3 (2C), 128.2, 128.0, 126.8, 124.7, 112.2–109.2 (m), 54.3; *m/z* HRMS (TOF ES$^+$) $C_{22}H_{18}F_3N_4O_4$ $[MH]^+$ calcd 459.1275, found 459.1276.

***N*-(2-(Hydroxyamino)-2-oxo-1-(3',4',5'-trifluoro-[1,1'-biphenyl]-4-yl)ethyl)-4-(N'-hydroxycarbamimidoyl)benzamide (6q).** Compound **5o** (212 mg, 0.500 mmol) was converted to the corresponding amidoxime **6q** according to General Procedure C. The crude product was purified by column chromatography (DCM:MeOH 100:0 to 95:5) to afford **6q** as a white solid (34 mg, 15%). ^{1}H NMR (d_6-DMSO) δ 11.05 (s, 1H), 9.81 (s, 1H), 9.07 (s, 1H), 9.00 (d, J = 8.1 Hz, 1H), 7.92 (d, J = 8.5 Hz, 2H), 7.79–7.66 (m, 6H), 7.62 (d, J = 8.4 Hz, 2H), 5.91 (s, 2H), 5.66 (d, J = 8.1 Hz, 1H); ^{19}F NMR (d_6-DMSO) δ -134.9 (d, J = 21.8 Hz), -163.5 (dd, J = 21.7/21.7 Hz); ^{13}C NMR (d_6-DMSO) δ 166.5, 165.9, 150.6 (ddd, J_{CF} = 246.2/9.5/4.1 Hz), 150.2, 138.9, 138.3 (m), 136.7–136.4 (m), 136.3–136.2 (m), 136.1, 133.9, 128.1, 127.7, 126.8, 125.0, 111.2 (m), 54.4; *m/z* HRMS (TOF ES$^+$) $C_{22}H_{18}F_3N_4O_4$ $[M+H]^+$ calcd 459.1275, found 459.1281; purity 85%.

***N*-(2-(Hydroxyamino)-2-oxo-1-(3',4',5'-trifluoro-[1,1'-biphenyl]-4-yl)ethyl)isophthalamide (6r).** Compound **5r** (328 mg, 0.741 mmol) was converted to the corresponding hydroxamic acid according to General Procedure C. The crude product was purified by column chromatography (DCM:MeOH 95:5 to 90:10) to afford compound **6r** as a white solid (153 mg, 47%). ^{1}H NMR (d_6-DMSO) δ 11.11 (s, 1H), 9.09 (s, 1H), 9.07 (d, J = 8.2 Hz, 1H), 8.41 (br. s, 1H), 8.07 (br. s, 1H), 8.05–7.95 (m, 2H), 7.77–7.67 (m, 4H), 7.62 (d, J = 8.4 Hz, 2H), 7.55 (dd, J = 7.8/7.8 Hz, 1H), 7.50 (s, 1H), 5.68 (d, J = 8.1 Hz, 1H); ^{19}F NMR (d_6-DMSO) δ -134.9 (d, J = 21.8 Hz), -163.4 (dd, J = 21.7/21.7 Hz); ^{13}C NMR (d_6-DMSO) δ 167.5, 166.4, 165.9, 150.6 (ddd, J_{CF} = 246.5/9.7/4.1 Hz), 140.2–136.8 (m), 138.9, 136.6 (td, J_{CF} = 8.0/4.3 Hz), 136.4–136.3 (m), 134.3, 133.9, 130.6, 130.4, 128.3, 128.1, 126.8, 126.7, 112.6–109.7 (m), 54.4; *m/z* HRMS (TOF ES$^+$) $C_{22}H_{17}F_3N_3O_4$ $[MH]^+$ calcd 444.1166, found 444.1172.

***N*-(2-(Hydroxyamino)-2-oxo-1-(3',4',5'-trifluoro-[1,1'-biphenyl]-4-yl)ethyl)terephthalamide (6s).** Compound **5s** (383 mg, 0.865 mmol) was converted to the corresponding hydroxamic acid according to General Procedure C. The crude product was purified by column chromatography (DCM:MeOH 100:0 to 90:10) to afford compound **6s** as a white solid (38 mg, 10%). ^{1}H NMR (d_6-

DMSO) δ 11.08 (s, 1H), 9.11 (d, J = 8.1 Hz, 1H), 9.07 (br. s, 1H), 8.09 (br. s, 1H), 8.01–7.89 (m, 4H), 7.78–7.58 (m, 6H), 7.50 (br. s, 1H), 5.67 (d, J = 8.1 Hz, 1H); ^{19}F NMR (d_6-DMSO) δ -134.9 (d, J = 21.8 Hz), -163.5 (dd, J = 21.7/21.7 Hz); ^{13}C NMR (d_6-DMSO) δ 167.2, 166.4, 165.8, 150.6 (ddd, J_{CF} = 246.5/9.9/4.3 Hz), 138.7, 138.2 (dt, J_{CF} = 262.9/14.7 Hz), 136.7, 136.5 (dt, J_{CF} = 6.4/5.2 Hz), 136.4–136.2 (m), 136.1, 128.1, 127.8, 127.3, 126.8, 112.3 (dd, J_{CF} = 16.0/5.4 Hz), 54.4; *m/z* HRMS (TOF ES$^+$) $C_{22}H_{17}F_3N_3O_4$ [MH]$^+$ calcd 444.1166, found 444.1172.

***N*^{1}-(2-(Hydroxyamino)-2-oxo-1-(3',4',5'-trifluoro-[1,1'-biphenyl]-4-yl)ethyl)-N^4-methylterephthalamide (6t).** Compound **5t** (52.7 mg, 0.115 mmol) was converted to the corresponding hydroxamic acid according to General Procedure C. Upon completion, the mixture was purified by preparative HPLC to afford compound **6t** as a white fluffy solid after lyophilization (24.5 mg, 47%). ^{1}H NMR (d_6-DMSO) δ 11.09 (s, 1H), 9.11 (d, J = 8.1 Hz, 1H), 9.07 (br, s, 1H), 8.57 (d, J = 4.6 Hz, 1H), 8.00 (d, J = 8.4 Hz, 2H), 7.90 (d, J = 8.4 Hz, 2H), 7.78 – 7.66 (m, 4H), 7.62 (d, J = 8.3 Hz, 2H), 5.67 (d, J = 8.0 Hz, 1H), 2.80 (d, J = 4.5 Hz, 3H); ^{19}F NMR (d_6-DMSO) -134.9 (d, J = 21.8 Hz), -163.5 (dd, J = 21.8/21.8 Hz); ^{13}C NMR (d_6-DMSO) δ 166.4, 165.9, 165.8, 150.6 (ddd, J_{CF} = 246.2/9.3/3.9 Hz), 138.8, 139.8–137.0 (m), 137.0, 136.6 (td, J_{CF} = 7.9/4.8 Hz), 136.3, 135.9, 128.1, 127.8, 126.9, 126.8, 111.2 (dd, J_{CF} = 16.2/5.2 Hz), 54.4, 26.3; *m/z* HRMS (TOF ES$^+$) $C_{23}H_{19}N_3O_4F_3$ [MH]$^+$ calcd, 458.1322; found, 458.1323.

***N*^{1}-(2-(Hydroxyamino)-2-oxo-1-(3',4',5'-trifluoro-[1,1'-biphenyl]-4-yl)ethyl)-*N*^{4},*N*^{4}-dimethylterephthalamide (6u).** Compound **5u** (51.3 mg, 0.109 mmol) was converted to the corresponding hydroxamic acid according to General Procedure C. Upon completion, the mixture was purified by column chromatography (DCM:PE:AcOH 1:1:0.1 to DCM:MeOH:AcOH 95:5:0.1) followed by preparative HPLC to afford compound **6u** as a white fluffy solid after lyophilization (8.0 mg, 16%). ^{1}H NMR (d_6-DMSO) δ 11.07 (s, 1H), 9.08 (d, J = 8.1 Hz, 2H), 7.96 (d, J = 8.4 Hz, 2H), 7.78–7.64 (m, 4H), 7.62 (d, J = 8.4 Hz, 2H), 7.47 (d, J = 8.4 Hz, 2H), 5.66 (d, J = 8.0 Hz, 1H), 2.99 (s, 3H), 2.89 (s,

3H); ^{19}F NMR (d_6-DMSO) δ -134.9 (d, J = 21.7 Hz), -163.5 (dd, J = 21.6/21.6 Hz); *m/z* HRMS (TOF ES$^+$) $C_{24}H_{21}N_3O_4F_3$ $[MH]^+$ calcd, 472.1479; found, 472.1480.

***N*^{1}-Ethyl-*N*^{4}-(2-(hydroxyamino)-2-oxo-1-(3',4',5'-trifluoro-[1,1'-biphenyl]-4-yl)ethyl)terephthalamide (6v).** Compound **5v** (50.7 mg, 0.108 mmol) was converted to the corresponding hydroxamic acid according to General Procedure C. Upon completion, the resulting mixture was purified by column chromatography (DCM:PE:AcOH 1:1:0.1 to DCM:MeOH:AcOH 95:5:0.1) followed by preparative HPLC to afford compound **6v** as a white fluffy solid after lyophilization (10.0 mg, 13%). ^{1}H NMR (d_6-DMSO) δ 11.08 (s, 1H), 9.10 (d, J = 8.1 Hz, 1H), 9.06 (br, s, 1H), 8.59 (t, J = 5.2 Hz, 1H), 7.99 (d, J = 8.4 Hz, 2H), 7.90 (d, J = 8.3 Hz, 2H), 7.75–7.68 (m, 4H), 7.62 (d, J = 8.3 Hz, 2H), 5.66 (d, J = 8.0 Hz, 1H), 3.30 (q, J = 7.1 Hz, 2H), 1.13 (t, J = 7.2 Hz, 3H); ^{19}F NMR (d_6-DMSO) δ -134.9 (d, J = 21.8 Hz), -163.5 (dd, J = 21.6/21.6 Hz); *m/z* HRMS (TOF ES$^+$) $C_{24}H_{21}N_3O_4F_3$ $[MH]^+$ calcd, 472.1479; found, 472.1480.

***N*^{1}-(2-(Hydroxyamino)-2-oxo-1-(3',4',5'-trifluoro-[1,1'-biphenyl]-4-yl)ethyl)-*N*^{4}-isopropylterephthalamide (6w).** Compound **5w** (56.8 mg, 0.117 mmol) was converted to the corresponding hydroxamic acid according to General Procedure C. Upon completion, the mixture was purified by column chromatography (DCM:PE:AcOH 1:1:0.1 to DCM:MeOH:AcOH 95:5:0.1) followed by preparative HPLC to afford compound **6w** as a white fluffy solid after lyophilization (11.6 mg, 20%). ^{1}H NMR (d_6-DMSO) δ 11.09 (s, 1H), 9.10 (d, J = 8.1 Hz, 1H), 9.07 (d, J = 0.8 Hz, 1H), 8.35 (d, J = 7.7 Hz, 1H), 7.99 (d, J = 8.5 Hz, 2H), 7.91 (d, J = 8.5 Hz, 2H), 7.77–7.66 (m, 4H), 7.62 (d, J = 8.4 Hz, 2H), 5.67 (d, J = 8.1 Hz, 1H), 4.19–3.97 (m, 1H), 1.18 (d, J = 6.6 Hz, 6H); ^{19}F NMR (d_6-DMSO) δ -134.9 (d, J = 21.8 Hz), -163.5 (dd, J = 21.8/21.8 Hz); *m/z* HRMS (TOF ES$^+$) $C_{25}H_{23}N_3O_4F_3$ $[MH]^+$ calcd, 486.1635; found, 486.1638.

***N*^{1}-(2-(Hydroxyamino)-2-oxo-1-(3',4',5'-trifluoro-[1,1'-biphenyl]-4-yl)ethyl)-*N*^{4}-(2-hydroxyethyl)terephthalamide (6x).** Compound **5x** (54.1 mg, 0.111 mmol) was converted to the corresponding hydroxamic acid according to General Procedure C. Upon completion, the mixture was

purified by preparative HPLC to afford compound **6x** as a white fluffy solid after lyophilization (18.4 mg, 34%). ^{1}H NMR (d_6-DMSO) δ 11.08 (s, 1H), 9.11 (d, J = 8.1 Hz, 1H), 9.07 (s, 1H), 8.57 (t, J = 5.6 Hz, 1H), 8.00 (d, J = 8.4 Hz, 2H), 7.92 (d, J = 8.4 Hz, 2H), 7.78–7.66 (m, 4H), 7.62 (d, J = 8.3 Hz, 2H), 5.67 (d, J = 8.0 Hz, 1H), 4.74 (s, 1H), 3.52 (q, J = 9.7 Hz, 2H), 3.40–3.30 (m, 2H); ^{19}F NMR (d_6-DMSO) δ -134.9 (d, J = 21.7 Hz), -163.4 (dd, J = 21.7/21.7 Hz); ^{13}C NMR (d_6-DMSO) δ 166.4, 165.8, 165.7, 150.6 (ddd, J_{CF} = 246.8/9.5/4.3 Hz), 138.7, 138.3 (dt, J_{CF} = 31.2/16.1 Hz), 137.0, 136.6 (td, J_{CF} = 8.2/4.7 Hz), 136.3, 135.9, 128.2, 127.8, 127.1, 126.8, 112.4–109.4 (m), 59.7, 54.4, 42.3; *m/z* HRMS (TOF ES$^+$) $C_{24}H_{21}N_3O_5F_3$ $[MH]^+$ calcd, 488.1428; found, 488.1425.

***N*-(2-(Hydroxyamino)-2-oxo-1-(3',4',5'-trifluoro-[1,1'-biphenyl]-4-yl)ethyl)-4-sulfamoylbenzamide (6y).** Compound **5y** (55.2 mg, 0.115 mmol) was converted to the corresponding hydroxamic acid according to General Procedure C. Upon completion, the mixture was then purified by column chromatography (DCM:PE:AcOH 1:1:0.1 to DCM:MeOH:AcOH 95:5:0.1) followed by preparative HPLC to afford compound **6y** as a white fluffy solid after lyophilization (10.0 mg, 18%). ^{1}H NMR (d_6-DMSO) δ 11.09 (d, J = 0.9 Hz, 1H), 9.22 (d, J = 8.0 Hz, 1H), 9.07 (d, J = 1.1 Hz, 1H), 8.15–7.99 (m, 2H), 7.97–7.84 (m, 2H), 7.71 (dt, J = 10.6/6.2 Hz, 4H), 7.62 (d, J = 8.4 Hz, 2H), 7.50 (s, 2H), 5.66 (d, J = 8.0 Hz, 1H); ^{19}F NMR (d_6-DMSO) δ -134.9 (d, J = 21.7 Hz), -163.4 (dd, J = 21.6/21.6 Hz); *m/z* HRMS (TOF ES$^+$) $C_{21}H_{17}F_3N_3O_5S$ $[MH]^+$ calcd, 480.0836; found, 480.0835.

3-Amino-*N*-(2-(hydroxyamino)-2-oxo-1-(3',4',5'-trifluoro-[1,1'-biphenyl]-4-yl)ethyl)benzamide TFA salt (6ab). Compound **5z** (228 mg, 0.443 mmol) was converted to the corresponding hydroxamic acid according to General Procedure C. Upon completion, the mixture was purified by column chromatography (DCM:MeOH 100:0 to 95:5) to afford *tert*-butyl (3-((2-(hydroxyamino)-2-oxo-1-(3',4',5'-trifluoro-[1,1'-biphenyl]-4-yl)ethyl)carbamoyl)phenyl)carbamate (108 mg). This was dissolved in 20% TFA/DCM and stirred at rt for 4 h to remove the boc group. The reaction mixture was concentrated *in vacuo* and purified by preparative HPLC to afford compound **6ab** as a pale brown solid (28.5 mg, 12% over two steps). ^{1}H NMR (d_6-DMSO) δ 11.09 (s, 1H), 8.82 (d, J =

8.0 Hz, 1H), 7.77–7.65 (m, 4H), 7.61 (d, J = 8.3 Hz, 2H), 7.51–7.42 (m, 2H), 7.33 (t, J = 7.8 Hz, 1H), 7.09 (dd, J = 7.9/1.3 Hz, 1H), 6.72 (br. s, 3H), 5.64 (d, J = 8.0 Hz, 1H); ^{19}F NMR (d_6-DMSO) δ -74.5, -134.9 (d, J = 21.7 Hz), -163.5 (dd, J = 21.7/21.7 Hz); ^{13}C NMR (d_6-DMSO, TFA signals are not included) δ 166.4, 166.1, 150.7 (ddd, J_{CF} = 246.6/9.7/4.0 Hz), 141.2–141.0 (m), 138.9, 138.3 (dt, J_{CF} = 31.0/13.9 Hz), 136.6 (td, J_{CF} = 8.3/4.6 Hz), 136.3, 135.0, 129.2, 128.0, 126.8, 121.1, 120.6, 117.5, 111.7–110.6 (m), 54.3; *m/z* HRMS (TOF ES$^+$) $C_{21}H_{17}F_3N_3O_3$ $[MH]^+$ calcd. 416.1217, found 416.1229.

4-Amino-*N*-(2-(hydroxyamino)-2-oxo-1-(3',4',5'-trifluoro-[1,1'-biphenyl]-4-yl)ethyl)benzamide TFA salt (6ac). Compound **5aa** (235 mg, 0.457 mmol) was converted to the corresponding hydroxamic acid according to General Procedure C. Upon completion, the mixture was purified by column chromatography (DCM:MeOH 100:0 to 95:5) to afford *tert*-butyl (4-((2-(hydroxyamino)-2-oxo-1-(3',4',5'-trifluoro-[1,1'-biphenyl]-4-yl)ethyl)carbamoyl)phenyl)carbamate (128 mg). This was dissolved in 20% TFA/DCM and stirred at rt for 4 h to remove the boc group. The reaction mixture was concentrated *in vacuo* and purified by preparative HPLC to afford compound **6ac** as a pale brown solid (69 mg, 28% over two steps). ^{1}H NMR (d_6-DMSO) δ 11.08 (br. s, 1H), 8.53 (d, J = 8.1 Hz, 1H), 7.78 (d, J = 8.6 Hz, 2H), 7.74–7.56 (m, 6H), 7.17 (br. s, 3H), 6.80 (d, J = 8.5 Hz, 2H), 5.66 (d, J = 8.0 Hz, 1H); ^{19}F NMR (d_6-DMSO) δ -74.5, -134.9 (d, J = 21.6 Hz), -163.6 (dd, J = 21.6/21.6 Hz); ^{13}C NMR (d_6-DMSO, TFA signals are not included) δ 166.8, 166.0, 150.7 (ddd, J_{CF} = 246.6/9.7/4.2 Hz), 147.5, 139.4, 138.4 (dt, J_{CF} = 249.4/15.6 Hz), 136.7 (td, J_{CF} = 8.1/4.6 Hz), 136.3 (m), 129.4, 128.1, 127.0, 123.9, 115.4, 111.7–110.6 (m), 54.3; *m/z* HRMS (TOF ES$^+$) $C_{21}H_{17}F_3N_3O_3$ $[MH]^+$ calcd 416.1217, found 416.1234.

***N*-(2-(Hydroxyamino)-2-oxo-1-(3',4',5'-trifluoro-[1,1'-biphenyl]-4-yl)ethyl)-4-(methylsulfonamido)benzamide (6ad).** Compound **5ad** (65.2 mg, 0.132 mmol) was converted to the corresponding hydroxamic acid according to General Procedure C. Upon completion, the mixture was purified by column chromatography (DCM:PE:AcOH 1:1:0.1 to DCM:MeOH:AcOH 95:5:0.1) followed by preparative HPLC to afford compound **6ad** as a white fluffy solid after lyophilization (30.0 mg, 46%).

^{1}H NMR (d_6-DMSO) δ 11.07 (s, 1H), 10.13 (s, 1H), 9.06 (s, 1H), 8.83 (d, J = 8.1 Hz, 1H), 7.92 (d, J = 8.8 Hz, 2H), 7.79–7.65 (m, 4H), 7.60 (d, J = 8.4 Hz, 2H), 7.25 (d, J = 8.8 Hz, 2H), 5.65 (d, J = 8.1 Hz, 1H), 3.07 (s, 3H); ^{19}F NMR (d_6-DMSO) δ -134.9 (d, J = 21.8 Hz), -163.5 (dd, J = 21.8/21.8 Hz); ^{13}C NMR (d_6-DMSO) δ 166.5, 165.6, 150.6 (ddd, J_{CF} = 246.5/9.6/4.3 Hz), 141.4, 139.0, 138.3 (dt, J_{CF} = 31.4/16.1 Hz), 136.6 (td, J_{CF} = 8.2/4.2 Hz), 136.3–136.1 (m), 129.2, 128.5, 128.0, 126.8, 117.8, 111.2 (dd, J_{CF} = 15.8/5.5 Hz), 54.3, 40.6; *m/z* HRMS (TOF ES$^+$) $C_{22}H_{19}F_3N_3O_5S$ [MH]$^+$ calcd, 494.0992; found, 494.0993.

***N*-(2-(Hydroxyamino)-2-oxo-1-(3',4',5'-trifluoro-[1,1'-biphenyl]-4-yl)ethyl)-4-(sulfamoylamino)benzamide (6ae).** Compound **5ae** (54.2 mg, 0.110 mmol) was converted to the corresponding hydroxamic acid according to General Procedure C. Upon completion, the mixture was purified by preparative HPLC to afford compound **6ae** as a beige fluffy solid after lyophilization (39.3 mg, 72%). ^{1}H NMR (d_6-DMSO) δ 11.07 (s, 1H), 9.93 (s, 1H), 8.75 (d, J = 8.2 Hz, 1H), 7.88 (d, J = 8.7 Hz, 2H), 7.81–7.65 (m, 4H), 7.61 (d, J = 8.4 Hz, 2H), 7.29 (s, 2H), 7.19 (d, J = 8.8 Hz, 2H), 5.66 (d, J = 8.1 Hz, 1H); ^{19}F NMR (d_6-DMSO) δ -134.9 (d, J = 21.7 Hz), -163.5 (dd, J = 21.7/21.7 Hz); ^{13}C NMR (d_6-DMSO) δ 166.6, 165.8, 150.7 (ddd, J_{CF} = 246.7/9.8/4.3 Hz), 142.5, 139.1, 138.3 (dt, J_{CF} = 31.1/15.9 Hz), 136.6 (td, J_{CF} = 8.1/4.6 Hz), 136.2 (d, J = 1.5 Hz), 128.8, 128.1, 126.8, 126.6, 116.2, 111.2 (dd, J_{CF} = 16.0/5.4 Hz), 54.2; *m/z* HRMS (TOF ES$^+$) $C_{21}H_{18}F_3N_4O_5S$ [MH]$^+$ calcd, 495.0945; found, 495.0947.

***N*-(2-(Hydroxyamino)-2-oxo-1-(3',4',5'-trifluoro-[1,1'-biphenyl]-4-yl)ethyl)-3,4-dimethoxybenzamide (6af).** Compound **5af** (183 mg, 0.398 mmol) was converted to the corresponding hydroxamic acid according to General Procedure C. The crude product was purified by column chromatography (DCM:MeOH 100:0 to 90:10) to afford compound **6af** as a white solid (93.4 mg, 51%). ^{1}H NMR (d_6-DMSO) δ 11.08 (s, 1H), 9.07 (s, 1H), 8.86 (d, J = 8.2 Hz, 1H), 7.79–7.47 (m, 8H), 7.01 (d, J = 8.6 Hz, 1H), 5.68 (d, J = 8.1 Hz, 1H), 3.82 (s, 3H), 3.81 (s, 3H); ^{19}F NMR (d_6-DMSO) δ -134.9 (d, J = 21.7 Hz), -163.5 (dd, J = 21.7/21.7 Hz); ^{13}C NMR (d_6-DMSO) δ 166.6, 165.8, 151.5, 150.6 (ddd, J_{CF} = 246.6/9.7/4.2 Hz), 148.1, 139.1, 138.3 (dt, J_{CF} = 248.0/15.7 Hz), 136.6 (td, J_{CF} = 8.2/4.5 Hz), 136.3–

135.7 (m), 128.1, 126.8, 126.0, 121.3, 111.4–111.1 (m), 111.1, 110.8, 55.6 (2C), 54.3; *m/z* HRMS (TOF ES$^+$) $C_{23}H_{20}F_3N_2O_5$ $[MH]^+$ calcd 461.1319, found 461.1322.

3,4-Dihydroxy-*N*-(2-(hydroxyamino)-2-oxo-1-(3',4',5'-trifluoro-[1,1'-biphenyl]-4-yl)ethyl)benzamide (6ag). Compound **6af** (200 mg, 0.434mmol) was treated with BBr_3 (1M in DCM, 4.34 mL, 4.34 mmol) according to General Procedure D to form the corresponding catechol. The crude product was purified by preparative HPLC to afford compound **6ag** as a white solid (69.3 mg, 37%). ^{1}H NMR (d_6-DMSO) δ 11.05 (s, 1H), 9.49 (s, 1H), 9.15 (s, 1H), 9.06 (s, 1H), 8.49 (d, J = 8.1 Hz, 1H), 7.80–7.64 (m, 4H), 7.61 (d, J = 8.3 Hz, 2H), 7.39–7.21 (m, 2H), 6.78 (d, J = 8.2 Hz, 1H), 5.63 (d, J = 8.1 Hz, 1H); ^{19}F NMR (d_6-DMSO) δ -134.9 (d, J = 21.6 Hz), -163.5 (dd, J = 21.7/21.7 Hz); ^{13}C NMR (d_6-DMSO) δ 166.8, 166.0, 150.7 (ddd, J_{CF} = 246.6/9.7/4.2 Hz), 148.8, 144.9, 139.3, 138.4 (dt, J_{CF} = 249.5/15.8 Hz), 136.7 (td, J_{CF} = 8.1/4.4 Hz), 136.3–136.2 (m), 128.1, 126.8, 125.0, 119.7, 115.5, 114.9, 112.7–109.9 (m), 54.3; *m/z* HRMS (TOF ES$^+$) $C_{21}H_{16}F_3N_2O_5$ $[MH]^+$ calcd 433.1006, found 433.1003.

3-Fluoro-4-hydroxy-N-(2-(hydroxyamino)-2-oxo-1-(3',4',5'-trifluoro-[1,1'-biphenyl]-4-yl)ethyl)benzamide (6ah). 3-Fluoro-4-hydroxybenzoic acid (194 mg, 1.24 mmol) was coupled to compound **4** (330 mg, 1.12 mmol) according to General Procedure A. Upon completion, the reaction mixture was diluted with a 1 M HCl solution (10 mL) and extracted with DCM (3 × 15 mL). The combined organic layers were washed with water (2 × 20 mL) and brine (20 mL). The organic layer was dried over anhydrous Na_2SO_4, filtered and concentrated under reduced pressure. The crude product was purified by column chromatography (DCM:MeOH 100:0 to 95:5) to afford 430 mg of the desired product (64% of purity). The crude product was converted to the corresponding hydroxamic acid according to General Procedure C. The mixture was purified by column chromatography (DCM:MeOH (100:0 to 90:10) to afford compound **6ah** as a white solid (30 mg, 7%). ^{1}H NMR (d_6-DMSO) δ 11.05 (s, 1H), 10.53 (s, 1H), 9.05 (s, 1H), 8.82 (d, J = 8.1 Hz, 1H), 7.85–7.47 (m, 8H), 6.99 (t, J = 8.7 Hz, 1H), 5.63 (d, J = 8.1 Hz, 1H); ^{19}F NMR (d_6-DMSO) δ -134.9 (d, J = 21.8 Hz), -136.6, -163.5 (dd, J = 21.8/21.8 Hz); ^{13}C NMR (d_6-DMSO) δ 166.5, 164.9 (d, J_{CF} = 2.0 Hz), 150.6 (ddd, J_{CF} = 246.5/9.8/4.2 Hz), 150.3 (d, J_{CF} =

241.0 Hz), 148.1 (d, J_{CF} = 12.1 Hz), 138.9, 138.3 (dt, J_{CF} = 249.1/15.9 Hz), 136.8–136.4 (m), 136.3–136.1 (m), 128.1, 126.7, 125.0 (d, J_{CF} = 2.8 Hz), 124.9 (d, J_{CF} = 5.3 Hz), 117.0 (d, J_{CF} = 2.9 Hz), 115.9 (d, J_{CF} = 19.6 Hz), 111.6–110.6 (m), 54.4; *m/z* HRMS (TOF ES$^+$) $C_{21}H_{15}F_4N_2O_4$ $[MH]^+$ calcd 435.0962, found 435.0968.

4-Fluoro-3-hydroxy-*N*-(2-(hydroxyamino)-2-oxo-1-(3',4',5'-trifluoro-[1,1'-biphenyl]-4-yl)ethyl)benzamide (6ai). 4-Fluoro-3-hydroxybenzoic acid (233 mg, 1.49 mmol) was coupled to compound **4** (400 mg, 1.35 mmol) according to General Procedure A. Upon completion, the reaction mixture was diluted with a 1 M HCl solution (10 mL) and extracted with DCM (3 × 15 mL). The combined organic layers were washed with water (2 × 20 mL) and brine (20 mL). The organic layer was dried over anhydrous Na_2SO_4, filtered and concentrated under reduced pressure. The crude was purified by column chromatography (DCM:MeOH 98:2 to 90:10) to afford 577 mg of a white solid (53% of purity). The product was converted to the corresponding hydroxamic acid according to General Procedure C. After stirring at rt for 1 d, 40% of the starting material had converted to compound **6ai**. The reaction was left for a further 6 d reaching 70% conversion according to LC-MS. The reaction was stopped and starting material and compound **6ai** were isolated by column chromatography (DCM:MeOH 100:0 to 90:10) in which 68 mg (13%) of compound **6ai** was obtained as pale yellow solid and 10 mg of the starting material was recovered. ^{1}H NMR (d_6-DMSO) δ 11.04 (s, 1H), 10.11 (s, 1H), 9.04 (s, 1H), 8.87 (d, *J* = 8.1 Hz, 1H), 7.74–7.66 (m, 4H), 7.60 (d, *J* = 8.4 Hz, 2H), 7.49 (dd, *J* = 8.6/2.2 Hz, 1H), 7.41 (ddd, *J* = 8.4/4.3/2.2 Hz, 1H), 7.21 (dd, *J* = 11.0/8.5 Hz, 1H), 5.60 (d, *J* = 8.1 Hz, 1H); ^{19}F NMR (d_6-DMSO) δ -132.2, -134.9 (d, *J* = 21.7 Hz), -163.5 (dd, *J* = 21.7/21.7 Hz); ^{13}C NMR (d_6-DMSO) δ 166.5, 165.5, 153.1 (d, J_{CF} = 246.2 Hz), 150.6 (ddd, J_{CF} = 246.4/10.2/4.0 Hz), 144.6 (d, J_{CF} = 12.4 Hz), 138.9, 138.3 (dt, J_{CF} = 243.0/12.5 Hz), 136.6 (td, J_{CF} = 7.9/4.6 Hz), 136.3–136.1 (m), 130.6 (d, J_{CF} = 3.1 Hz), 128.1, 126.8, 119.3 (d, J_{CF} = 7.4 Hz), 117.7 (d, J_{CF} = 3.9 Hz), 115.8 (d, J_{CF} = 18.9 Hz), 111.9–110.6 (m), 54.4; *m/z* MS (TOF ES$^-$) $C_{21}H_{13}F_4N_2O_4$ $[M-H]^-$ calcd 433.1, found 433.1; *m/z* HRMS (TOF ES$^+$) $C_{21}H_{15}F_4N_2O_4$ $[MH]^+$ calcd 435.0962, found 435.0973.

***N*-(2-(hydroxyamino)-2-oxo-1-(3',4',5'-trifluoro-[1,1'-biphenyl]-4-yl)ethyl)-1*H*-indole-5-carboxamide (6aj)**. Compound **5aj** (200 mg, 0.456 mmol) was converted to the corresponding hydroxamic acid according to General Procedure C. Upon completion, the solvent was concentrated *in vacuo*. An aqueous 10% citric acid solution was added dropwise to the crude residue. The precipitate was filtered and purified by flash column chromatography (PE:EtOAc 100:0 to 15:85) to afford compound **6aj** as a white solid (129 mg, 64%). ^{1}H NMR (MeOD) δ 8.19 (d, J = 1.3 Hz, 1H), 7.69–7.59 (m, 5H), 7.47–7.36 (m, 3H), 7.32 (d, J = 3.2 Hz, 1H), 6.56 (dd, J = 3.2, 0.8 Hz, 1H), 5.73 (s, 1H); ^{19}F NMR (MeOD) δ -136.9 (d, J = 19.8 Hz), -166.0 (dd, J = 19.9/19.9 Hz); ^{13}C NMR (MeOD) δ 171.0, 169.5, 152.6 (ddd, J_{CF} = 247.9/9.9/4.2 Hz), 141.8–139.2 (m), 139.7, 139.5, 139.0, 138.5 (td, J_{CF} = 7.8/4.5 Hz), 129.2 (2C), 129.0, 128.2 (2C), 127.4, 125.6, 121.8, 121.7, 112.3–111.9 (m, 3C), 103.7, 56.2; *m/z* HRMS (TOF ES$^+$) $C_{23}H_{17}F_3N_3O_3$ [MH]$^+$ calcd 440.1217, found 440.1210.

***N*-(2-(hydroxyamino)-2-oxo-1-(3',4',5'-trifluoro-[1,1'-biphenyl]-4-yl)ethyl)-1*H*-indazole-5-carboxamide (6ak)**. Compound **5ak** (45 mg, 0.102 mmol) was converted to the corresponding hydroxamic acid according to General Procedure C. Upon completion, the solvent was concentrated *in vacuo*. An aqueous 10% citric acid solution was added dropwise to the crude residue. The precipitate was filtered and washed through with water, then triturated with Et_2O to afford compound **6ak** as an off-white solid (40 mg, 89%). ^{1}H NMR (d_6-DMSO) δ 13.32 (s, 1H), 11.11 (s, 1H), 9.09 (s, 1H), 8.93 (d, J = 8.1 Hz, 1H), 8.48 (s, 1H), 8.21 (s, 1H), 7.91 (dd, J = 8.8/1.2 Hz, 1H), 7.80–7.52 (m, 7H), 5.70 (d, J = 8.0 Hz, 1H); ^{19}F NMR (d_6-DMSO) δ -134.9 (d, J = 21.7 Hz), -163.5 (dd, J = 21.7/21.7 Hz); ^{13}C NMR (d_6-DMSO) δ 167.0, 166.9, 150.9 (ddd, J_{CF} = 246.9/9.7/4.2 Hz), 141.4, 139.2, 138.6 (dt, J_{CF} = 31.4/15.9 Hz), 136.8 (td, J_{CF} = 7.9/4.4 Hz), 136.6, 135.3, 128.4 (2C), 127.1 (2C), 126.4, 126.0, 122.6, 121.7, 111.4 (m, 2C), 110.1, 54.8; *m/z* HRMS (TOF ES$^+$) $C_{22}H_{16}F_3N_4O_3$ [MH]$^+$ calcd 441.1169, found 441.1176.

***N*-(2-(hydroxyamino)-2-oxo-1-(3',4',5'-trifluoro-[1,1'-biphenyl]-4-yl)ethyl)-1*H*-benzo*[d]*[1,2,3]triazole-5-carboxamide (6al)**. Compound **5al** (90 mg, 0.204 mmol) was converted to

the corresponding hydroxamic acid according to General Procedure C. Upon completion, the solvent was concentrated *in vacuo*. An aqueous 10% citric acid solution was added dropwise to the crude residue. The precipitate was filtered and washed through with water, then triturated in Et_2O to afford compound **6al** as a yellow solid (75 mg, 83%). ^{1}H NMR (d_6-DMSO) δ 11.09 (s, 1H), 9.22 (d, J = 8.0 Hz, 1H), 9.07 (s, 1H), 8.60 (s, 1H), 8.02–7.91 (m, 2H), 7.79–7.61 (m, 7H), 5.75–5.63 (m, 1H); ^{19}F NMR (d_6-DMSO) δ -134.9 (d, J = 21.7 Hz), -163.5 (dd, J = 21.7/21.7 Hz); ^{13}C NMR (d_6-DMSO, rotamers) δ 171.9, 171.5, 166.6, 166.3, 150.8 (ddd, J_{CF} = 246.8/9.8/4.3 Hz), 138.9 (2C), 138.5 (dt, J_{CF} = 248.9/15.7 Hz), 136.8–136.6 (m)*, 136.5, 129.0, 128.4 (3C), 127.0, 126.9 (3C), 111.6–111.2 (m), 54.8; *m/z* HRMS (TOF ES$^+$) $C_{21}H_{15}F_3N_5O_3$ $[MH]^+$ calcd 442.1122, found 442.1127.

***N*-(2-(hydroxyamino)-2-oxo-1-(3',4',5'-trifluoro-[1,1'-biphenyl]-4-yl)ethyl)-1*H*-benzo[d]imidazole-5-carboxamide (6am)**. Compound **5am** (80 mg, 0.182 mmol) was converted to the corresponding hydroxamic acid according to General Procedure C. Upon completion, the solvent was concentrated *in vacuo*. An aqueous 10% citric acid solution was added dropwise to the crude residue. The resultant solid was filtered and washed through with water, then triturated in Et_2O to afford compound **6am** as an off-white solid (75 mg, 94%). ^{1}H NMR (MeOD) δ 8.33 (s, 1H), 8.22 (d, J = 1.0 Hz, 1H), 7.85 (dd, J = 8.5/1.6 Hz, 1H), 7.71–7.61 (m, 5H), 7.46–7.37 (m, 2H), 5.73 (s, 1H); ^{19}F NMR (MeOD) δ -136.8 (d, J = 19.8 Hz), -165.9 (dd, J = 19.8/19.8 Hz); ^{13}C NMR (MeOD) δ 170.0, 169.4, 152.6 (ddd, J_{CF} = 247.9/9.9/4.1 Hz), 144.8, 141.9–138.3 (m), 140.7, 139.2, 139.1, 138.6, 138.5–138.3 (m), 129.8, 129.3 (2C), 128.2 (2C), 123.6, 116.8, 115.8, 112.1 (m, 2C), 56.5; *m/z* HRMS (TOF ES$^+$) $C_{22}H_{16}F_3N_4O_3$ $[MH]^+$ calcd 441.1169, found 441.1176.

***N*-(2-(hydroxyamino)-2-oxo-1-(3',4',5'-trifluoro-[1,1'-biphenyl]-4-yl)ethyl)-2-oxoindoline-5-carboxamide (6an).** Compound **5an** (70 mg, 0.154 mmol) was converted to the corresponding hydroxamic acid according to General Procedure C. Upon completion, the solvent was concentrated *in vacuo*. An aqueous 10% citric acid solution was added dropwise to the crude residue. The resultant solid

was filtered and washed through with water. The solid was purified by flash column chromatography (DCM:MeOH 100:0 to 90:10) to afford compound **6an** as a dull yellow solid (30 mg, 43%). ^{1}H NMR (d_6-DMSO) δ 11.05 (s, 1H), 10.63 (s, 1H), 9.05 (s, 1H), 8.72 (d, J = 8.1 Hz, 1H), 7.82 (d, J = 7.7 Hz, 2H), 7.76–7.65 (m, 4H), 7.60 (d, J = 8.4 Hz, 2H), 6.86 (d, J = 8.5 Hz, 1H), 5.64 (d, J = 8.1 Hz, 1H), 3.53 (s, 2H); ^{19}F NMR (d_6-DMSO) δ -134.9 (d, J = 21.8 Hz), -163.5 (dd, J = 21.7/21.7 Hz); ^{13}C NMR (d_6-DMSO) δ 177.9, 167.3, 166.9, 151.2 (ddd, J_{CF} = 247.0/9.8/4.2 Hz), 147.18, 139.12, 138.9 (dt, J_{CF} = 32.1/15.4 Hz), 137.1–136.8 (m, 2C), 128.6 (3C), 127.4 (2C), 127.2, 126.3, 124.5, 111.7 (m, 2C), 109.3, 54.9, 36.1; *m/z* HRMS (TOF ES$^+$) $C_{23}H_{17}F_3N_3O_4$ $[MH]^+$ calcd 456.1166, found 456.1172.

***N*-Hydroxy-2-(2-phenylacetamido)-2-(3',4',5'-trifluoro-[1,1'-biphenyl]-4-yl)acetamide (6ao).** Compound **5ao** (54.0 mg, 0.131 mmol) was converted to the corresponding hydroxamic acid according to General Procedure C. The crude product was purified by column chromatography (DCM:MeOH 100:0 to 90:0) to afford compound **6ao** as a white solid (26.7 mg, 49%). ^{1}H NMR (d_6-DMSO) δ 11.0 (s, 1H), 9.04 (s, 1H), 8.92 (d, J = 8.3 Hz, 1H), 7.76–7.64 (m, 4H), 7.50 (d, J = 8.3 Hz, 2H), 7.32–7.17 (m, 5H), 5.42 (d, J = 8.3 Hz, 1H), 3.58 (s, 2H); ^{19}F NMR (d_6-DMSO) δ -134.9 (d, J = 21.7 Hz), -163.5 (dd, J = 21.7/21.7 Hz); ^{13}C NMR (d_6-DMSO) δ 169.9, 166.3, 150.6 (ddd, J_{CF} = 246.4/9.8/4.3 Hz), 139.3, 138.3 (dt, J_{CF} = 31.3/16.9 Hz), 136.5 (td, J_{CF} = 7.8/4.1 Hz), 136.4, 136.2–136.1 (m), 129.1, 128.2, 127.5, 126.8, 126.3, 111.8–110.3 (m), 53.5, 41.7; *m/z* HRMS (TOF ES$^+$) $C_{22}H_{18}F_3N_2O_3$ $[MH]^+$ calcd 415.1264, found 415.1264.

2-(2-(3-Fluorophenyl)acetamido)-N-hydroxy-2-(3',4',5'-trifluoro-[1,1'-biphenyl]-4-yl)acetamide (6ap). Compound **5ap** (198 mg, 0.459 mmol) was converted to the corresponding hydroxamic acid according to General Procedure C. The crude product was purified by column chromatography (DCM:MeOH 100:0 to 90:10) followed by preparative HPLC to afford compound **6ap** as a white solid (101 mg, 51%). ^{1}H NMR (d_6-DMSO) δ 11.07 (s, 1H), 9.07 (s, 1H), 8.99 (d, J = 8.2 Hz, 1H), 7.84–7.61 (m, 4H), 7.51 (d, J = 8.2 Hz, 2H), 7.32 (dd, J = 14.5/7.5 Hz, 1H), 7.18–6.90 (m, 3H),

5.43 (d, J = 8.2 Hz, 1H), 3.63 (s, 2H); ^{19}F NMR (d_6-DMSO) δ -113.8, -134.9 (d, J = 21.7 Hz), -163.5 (dd, J = 21.6/21.6 Hz); ^{13}C NMR (d_6-DMSO) δ 169.4, 166.4, 162.0 (d, J_{CF} = 243.0 Hz), 150.6 (ddd, J_{CF} = 246.7/9.7/4.1 Hz), 139.2 (d, J = 4.3 Hz), 139.1, 138.3 (dt, J_{CF} = 249.5/15.7 Hz), 136.5 (td, J_{CF} = 8.1/4.4 Hz), 136.3 (m), 130.0 (d, J_{CF} = 8.4 Hz), 127.6, 126.8, 125.2 (d, J_{CF} = 2.5 Hz), 115.8 (d, J_{CF} = 21.3 Hz), 113.2 (d, J_{CF} = 20.8 Hz), 111.2 (m), 53.6, 41.3; *m/z* HRMS (TOF ES$^+$) $C_{22}H_{17}F_4N_2O_3$ $[MH]^+$ calcd 433.1170, found 433.1188.

2-(2-(4-Fluorophenyl)acetamido)-N-hydroxy-2-(3',4',5'-trifluoro-[1,1'-biphenyl]-4-yl)acetamide (6aq). Compound **5aq** (47 mg, 0.109 mmol) was converted to the corresponding hydroxamic acid according to General Procedure C. The crude product was purified by column chromatography (DCM:MeOH 100:0 to 90:10) followed by preparative HPLC to afford compound **6aq** as a white solid (40.6 mg, 38%). ^{1}H NMR (d_6-DMSO) δ 11.05 (s, 1H), 9.06 (s, 1H), 8.94 (d, J = 8.3 Hz, 1H), 7.82–7.61 (m, 4H), 7.50 (d, J = 8.2 Hz, 2H), 7.31 (m, 2H), 7.10 (t, J = 8.8 Hz, 2H), 5.42 (d, J = 8.3 Hz, 1H), 3.58 (s, 2H); ^{19}F NMR (d_6-DMSO) δ -116.78 (s), -134.9 (d, J = 21.7 Hz), -163.5 (dd, J = 21.7/21.7 Hz); ^{13}C NMR (d_6-DMSO) δ 169.8, 166.4, 161.0 (d, J_{CF} = 241.9 Hz), 150.6 (ddd, J_{CF} = 246.7/9.8/4.2 Hz), 139.2, 138.3 (dt, J_{CF} = 249.5/15.6 Hz), 136.5 (td, J_{CF} = 8.0/ 4.4 Hz), 136.3–136.1 (m), 132.5 (d, J_{CF} = 3.0 Hz), 130.9 (d, J_{CF} = 8.0 Hz), 127.5, 126.8, 114.9 (d, J = 21.1 Hz), 111.5–110.7 (m), 53.5, 40.8; *m/z* HRMS (TOF ES$^+$) $C_{22}H_{17}F_4N_2O_3$ $[MH]^+$ calcd 433.1170, found 433.1173.

***N*-Hydroxy-2-(2-(4-methoxyphenyl)acetamido)-2-(3',4',5'-trifluoro-[1,1'-biphenyl]-4-yl)acetamide (6ar).** Compound **5ar** (195 mg, 0.440 mmol) was converted to the corresponding hydroxamic acid according to General Procedure C. The crude product was purified by column chromatography (DCM:MeOH 100:0 to 90:10) to afford compound **6ar** as a white solid (124 mg, 64%). ^{1}H NMR (d_6-DMSO) δ 11.03 (s, 1H), 9.04 (s, 1H), 8.83 (d, J = 8.4 Hz, 1H), 7.95–7.61 (m, 4H), 7.49 (d, J = 8.3 Hz, 2H), 7.19 (d, J = 8.7 Hz, 2H), 6.84 (d, J = 8.7 Hz, 2H), 5.41 (d, J = 8.3 Hz, 1H), 3.71 (s, 3H), 3.50 (s, 2H); ^{19}F NMR (d_6-DMSO) δ -134.9 (d, J = 21.7 Hz), -163.5 (dd, J = 21.7/21.7 Hz); ^{13}C NMR (d_6-DMSO) δ 170.2, 166.4, 157.9, 150.6 (ddd, J_{CF} = 246.6/9.7/4.1 Hz), 139.3, 138.3 (dt, J_{CF} = 249.2/15.6

Hz), 136.5 (td, J_{CF} = 8.1/4.4 Hz), 136.2–136.0 (m), 130.0, 128.3, 127.5, 126.8, 113.6, 111.2 (m), 55.0, 53.4, 40.9; *m/z* HRMS (TOF ES$^+$) $C_{23}H_{20}F_3N_2O_4$ $[MH]^+$ calcd 445.1370, found 445.1362.

***N*-Hydroxy-2-(2-(4-hydroxyphenyl)acetamido)-2-(3',4',5'-trifluoro-[1,1'-biphenyl]-4-yl)acetamide (6as).** Compound **6ar** (184 mg, 0.414 mmol) was treated with BBr_3 (1 M in DCM, 2.07 ml, 2.07 mmol) according to General Procedure D. The crude product was purified by preparative HPLC to afford compound **6as** as a white solid (58 mg, 32%). ^{1}H NMR (d_6-DMSO) δ 11.05 (s, 1H), 9.21 (s, 1H), 9.05 (s, 1H), 8.78 (d, *J* = 8.4 Hz, 1H), 7.75–7.63 (m, 4H), 7.50 (d, *J* = 8.3 Hz, 2H), 7.07 (d, *J* = 8.5 Hz, 2H), 6.68 (d, *J* = 8.5 Hz, 2H), 5.42 (d, *J* = 8.3 Hz, 1H), 3.45 (s, 2H); ^{19}F NMR (d_6-DMSO) δ -134.9 (d, *J* = 21.7 Hz), -163.5 (dd, *J* = 21.7/21.7 Hz); ^{13}C NMR (d_6-DMSO) δ 170.5, 166.4, 155.9, 150.6 (ddd, J_{CF} = 246.6/9.7/4.2 Hz), 139.4, 138.3 (dt, J_{CF} = 249.3/15.7 Hz), 136.6 (td, J_{CF} = 8.1/4.4 Hz), 136.3 – 136.0 (m), 130.0, 127.5, 126.8, 126.5, 115.0, 111.6–110.9 (m), 53.5, 41.0; *m/z* HRMS (TOF ES$^+$) $C_{22}H_{18}F_3N_2O_4$ $[MH]^+$ calcd 431.1213, found 431.1214.

4-(2-((2-(Hydroxyamino)-2-oxo-1-(3',4',5'-trifluoro-[1,1'-biphenyl]-4-yl)ethyl)amino)-2-oxoethyl)benzamide (6at). Compound **5at** (198 mg, 0.434 mmol) was converted to the corresponding hydroxamic acid according to General Procedure C. The crude product was purified by column chromatography followed by preparative HPLC to afford compound **6at** as a white solid (33.5 mg, 17%). ^{1}H NMR (d_6-DMSO) δ 11.05 (s, 1H), 9.05 (s, 1H), 8.99 (d, *J* = 8.3 Hz, 1H), 7.90 (br. s, 1H), 7.78 (d, *J* = 8.2 Hz, 2H), 7.74–7.64 (m, 4H), 7.50 (d, *J* = 8.3 Hz, 2H), 7.33 (d, *J* = 8.2 Hz, 2H), 7.29 (br. s, 1H), 5.41 (d, *J* = 8.3 Hz, 1H), 3.64 (s, 2H); ^{19}F NMR (d_6-DMSO) δ -134.9 (d, *J* = 21.7 Hz), -163.5 (dd, *J* = 21.7/21.7 Hz); ^{13}C NMR (d_6-DMSO) δ 169.5, 167.8, 166.3, 150.6 (ddd, J_{CF} = 246.3/9.4/4.6 Hz), 139.7, 139.9–139.0 (m), 139.2, 136.5 (td, J_{CF} = 5.3/2.2 Hz), 136.3–136.1 (m), 132.5, 128.9, 127.5, 127.4, 126.8, 111.4–111.0 (m), 53.5, 41.5; *m/z* HRMS (TOF ES$^+$) $C_{23}H_{19}F_3N_3O_4$ $[MH]^+$ calcd 458.1322, found 458.1320.

2-(2-(3,4-Dimethoxyphenyl)acetamido)-*N*-hydroxy-2-(3',4',5'-trifluoro-[1,1'-biphenyl]-4-yl)acetamide (6au). Compound **5au** (413 mg, 0.872 mmol) was converted to the corresponding

hydroxamic acid according to General Procedure C. The crude product was purified by column chromatography (DCM:MeOH 100:0 to 90:0) to afford compound **6au** as a white solid (100 mg, 24%). ^{1}H NMR (d_6-DMSO) δ 11.04 (s, 1H), 9.04 (s, 1H), 8.84 (d, J = 8.4 Hz, 1H), 7.75–7.63 (m, 4H), 7.50 (d, J = 8.3 Hz, 2H), 6.92 (d, J = 1.9 Hz, 1H), 6.85 (d, J = 8.2 Hz, 1H), 6.78 (dd, J = 8.2/1.9 Hz, 1H), 5.42 (d, J = 8.4 Hz, 1H), 3.72 (s, 3H), 3.71 (s, 3H), 3.49 (s, 2H); ^{19}F NMR (d_6-DMSO) δ -134.9 (d, J = 21.7 Hz), -163.5 (dd, J = 21.7/21.7 Hz); ^{13}C NMR (d_6-DMSO) δ 170.1, 166.4, 150.6 (ddd, J_{CF} = 246.5,/9.7/4.2 Hz), 148.5, 147.5, 139.3, 138.3 (dt, J_{CF} = 31.0/15.7 Hz), 136.5 (td, J_{CF} = 8.0/4.3 Hz), 136.2–136.1 (m), 128.8, 127.5, 126.8, 121.0, 112.9, 111.8, 111.5–110.5 (m), 55.5, 55.4, 53.4, 41.4; *m/z* HRMS (TOF ES$^+$) $C_{24}H_{22}F_3N_2O_5$ $[MH]^+$ calcd 475.1475, found 475.1477.

2-(2-(3,4-Dihydroxyphenyl)acetamido)-*N*-hydroxy-2-(3',4',5'-trifluoro-[1,1'-biphenyl]-4-yl)acetamide (6av). Compound **6au** (213 mg, 0.449 mmol) was treated with BBr_3 (1 M in DCM, 4.49 mL, 4.49 mmol) according to General Procedure D to form the corresponding catechol. The crude product was purified by preparative HPLC to afford compound **6av** as a white solid (97.9 mg, 49%). ^{1}H NMR (d_6-DMSO) δ 11.05 (s, 1H), 9.05 (br. s, 1H), 8.85–8.53 (m, 3H), 7.76–7.62 (m, 4H), 7.49 (d, J = 8.3 Hz, 2H), 6.69 (d, J = 2.0 Hz, 1H), 6.64 (d, J = 8.0 Hz, 1H), 6.53 (dd, J = 8.0/2.0 Hz, 1H), 5.41 (d, J = 8.3 Hz, 1H), 3.39 (s, 2H); ^{19}F NMR (d_6-DMSO) δ -134.9 (d, J = 21.7 Hz), -163.5 (dd, J = 21.7/21.7 Hz); ^{13}C NMR (d_6-DMSO) δ 170.5, 166.4, 150.7 (ddd, J_{CF} = 246.5/9.6/4.1 Hz), 145.0, 143.9, 139.4, 138.3 (dt, J_{CF} = 236.0/15.9 Hz), 136.6 (td, J_{CF} = 8.2/4.4 Hz), 136.3–136.2 (m), 127.5, 127.1, 126.8, 119.9, 116.6, 115.4, 112.6–109.0 (m), 53.4, 41.3; *m/z* HRMS (TOF ES$^+$) $C_{22}H_{18}F_3N_2O_5$ $[MH]^+$ calcd 447.1162, found 444.1162.

2-(2-(3-Fluoro-4-hydroxyphenyl)acetamido)-*N*-hydroxy-2-(3',4',5'-trifluoro-[1,1'-biphenyl]-4-yl)acetamide (6ax). Compound **5aw** (104 mg, 0.225 mmol) was converted to the corresponding hydroxamic acid according to General Procedure C, affording 67.2 mg of 2-(2-(3-fluoro-4-methoxyphenyl)acetamido)-*N*-hydroxy-2-(3',4',5'-trifluoro-[1,1'-biphenyl]-4-yl)acetamide (**6aw**). This was treated with BBr_3 (1 M in DCM, 0.724 μL, 0.724 μmol) according to General Procedure D. The

resulting precipitate was filtered to afford compound **6ax** as an off-white solid (46.5 mg, 72%). ^{1}H NMR (d_6-DMSO) 11.07 (s, 1H), 9.71 (br. s, 1H), 8.84 (d, J = 8.2 Hz, 1H), 7.79–7.60 (m, 4H), 7.49 (d, J = 8.3 Hz, 2H), 7.11–6.98 (m, 1H), 6.93–6.74 (m, 2H), 5.40 (d, J = 8.2 Hz, 1H), 3.47 (s, 2H); ^{19}F NMR (d_6-DMSO) δ -134.8 (d, J = 21.7 Hz), -136.8, -163.5 (dd, J = 21.6/21.6 Hz); ^{13}C NMR (d_6-DMSO) δ 170.2, 166.5, 150.8 (d, J = 240.0 Hz), 150.7 (ddd, J = 12.7/9.6/4.2 Hz), 143.4 (d, J = 12.1 Hz), 139.3, 138.4 (dt, J = 249.1/15.4 Hz), 136.6 (td, J = 8.2/4.5 Hz), 136.4–136.3 (m), 127.7, 127.6, 126.9, 125.2 (d, J = 3.0 Hz), 117.5 (d, J = 3.0 Hz), 116.7 (d, J = 18.4 Hz), 111.3 (m), 53.6, 40.7; *m/z* HRMS (TOF ES$^+$) $C_{22}H_{17}F_4N_2O_4$ $[MH]^+$ calcd 449.1117, found 449.1125.

2-(2-(4-Fluoro-3-methoxyphenyl)acetamido)-*N*-hydroxy-2-(3',4',5'-trifluoro-[1,1'-biphenyl]-4-yl)acetamide (6ay). Compound **5ay** (367 mg, 0.795 mmol) was converted to the corresponding hydroxamic acid according to General Procedure C. The crude product was purified by column chromatography (DCM:MeOH 100:0 to 90:0) to afford the desired hydroxamic acid analogue as a white solid (**6ay**) (226 mg, 61%). ^{1}H NMR (d_6-DMSO) δ 11.05 (s, 1H), 9.05 (s, 1H), 8.95 (d, J = 8.3 Hz, 1H), 7.81 – 7.63 (m, 4H), 7.50 (d, J = 8.3 Hz, 2H), 7.19 – 7.01 (m, 2H), 6.81 (ddd, J = 8.2/4.3/2.0 Hz, 1H), 5.41 (d, J = 8.3 Hz, 1H), 3.80 (s, 3H), 3.55 (s, 2H); ^{19}F NMR (d_6-DMSO) δ -134.9 (d, J = 21.7 Hz), -138.9 (s), -163.5 (dd, J = 21.7/21.7 Hz); ^{13}C NMR (d_6-DMSO) δ 169.7, 166.3, 150.6 (ddd, J_{CF} = 246.7/9.8/4.3 Hz), 150.4 (d, J_{CF} = 242.0 Hz), 146.7 (d, J_{CF} = 10.6 Hz), 139.3, 138.3 (dt, J_{CF} = 31.4/15.9 Hz), 136.5 (td, J_{CF} = 8.1/4.4 Hz), 136.3–136.1 (m), 133.1 (d, J_{CF} = 3.7 Hz), 127.5, 126.8, 121.2 (d, J_{CF} = 6.7 Hz), 115.4 (d, J_{CF} = 17.9 Hz), 114.6 (d, J_{CF} = 1.5 Hz), 111.7–110.4 (m), 55.8, 53.5, 41.3; *m/z* MS $C_{23}H_{19}F_4N_2O_4$ $[MH]^+$ calcd 463.1, found 462.8.

2-(2-(4-Fluoro-3-hydroxyphenyl)acetamido)-*N*-hydroxy-2-(3',4',5'-trifluoro-[1,1'-biphenyl]-4-yl)acetamide (6az). Compound **6ay** (205 mg, 0.443 mmol) was treated with BBr_3 (1 M in DCM, 2.22 mL, 2.22 mmol) according to General Procedure D to form the corresponding phenol. The crude product was purified by preparative HPLC to afford compound **6az** as a white solid (156 mg, 78%). ^{1}H NMR (d_6-DMSO) δ 11.05 (s, 1H), 9.73 (s, 1H), 9.06 (s, 1H), 8.89 (d, J = 8.3 Hz, 1H), 7.76–7.63 (m, 4H), 7.49 (d, J = 8.3 Hz, 2H), 7.07–6.96 (m, 1H), 6.88 (dd, J = 8.7/2.1 Hz, 1H), 6.67 (ddd, J = 8.2/4.3/2.1 Hz, 1H), 5.40 (d, J = 8.3 Hz, 1H), 3.48 (s, 2H); ^{19}F NMR (d_6-DMSO) δ -134.9 (d, J = 21.7 Hz), -139.8, -163.5 (dd, J = 21.7/21.7 Hz); ^{13}C NMR (d_6-DMSO) δ 169.9, 166.4, 150.6 (ddd, J_{CF} = 246.5/9.7/4.1 Hz), 150.0 (d, J_{CF} = 239.0 Hz), 144.4 (d, J_{CF} = 12.2 Hz), 139.3, 138.3 (dt, J_{CF} = 249.1/15.5 Hz), 136.6 (td, J_{CF} = 8.0/4.1 Hz), 136.3–136.0 (m), 132.7 (d, J_{CF} = 3.4 Hz), 127.5, 126.8, 119.9 (d, J_{CF} = 6.4 Hz), 118.5 (d, J_{CF} = 2.7 Hz), 115.6 (d, J_{CF} = 18.0 Hz), 111.8–110.8 (m), 53.5, 41.0; *m/z* HRMS (TOF ES$^+$) $C_{22}H_{17}F_4N_2O_4$ $[MH]^+$ calcd 449.1117, found 449.1113.

Methyl 2-((4-fluoro-3-methoxybenzyl)amino)-2-(3',4',5'-trifluoro-[1,1'-biphenyl]-4-yl)acetate (7). 4-fluoro-3-methoxybenzaldehyde (172 mg, 1.12 mmol) was added to a solution of compound **4** (300 mg, 1.02 mmol) in DCE (10 mL) and stirred for 30 min before adding $Na(OAc)_3BH$ (540 mg, 2.55 mmol). The reaction mixture was stirred at rt overnight. Upon completion, the reaction mixture was diluted with sat. $NaHCO_3$ (20 mL) and extracted with DCM (3 × 20 mL). The combined organic layers were dried over anhydrous Na_2SO_4, filtered and concentrated *in vacuo*. The crude product was purified by column chromatography (PE:EtOAc 100:0 to 50:50) to afford compound **7** as a clear oil (405 mg, 92%). ^{1}H NMR ($CDCl_3$) δ 7.53–7.41 (m, 4H), 7.22–7.13 (m, 2H), 7.01–6.93 (m, 2H), 6.83–6.76 (m, 1H), 4.41 (s, 1H), 3.87 (s, 3H), 3.72 (s, 3H), 3.71 (s, 2H), 2.42 (br. s, 1H); ^{19}F NMR ($CDCl_3$) δ -134.0 (d, J = 20.6 Hz), -137.4, -162.3 (dd, J = 20.5/20.5 Hz); ^{13}C NMR ($CDCl_3$) δ 173.2, 151.7 (d, J_{CF} = 244.9 Hz), 151.5 (ddd, J_{CF} = 249.7/10.1/4.3 Hz), 147.6 (d, J_{CF} = 10.8 Hz), 140.9–137.9 (m), 138.3, 138.1–138.0 (m), 136.7 (td, J_{CF} = 7.8/4.7 Hz), 135.6 (d, J_{CF} = 3.7 Hz), 128.3, 127.3, 120.5 (d, J_{CF} = 6.8 Hz), 115.8 (d,

J_{CF} = 18.3 Hz), 113.4 (d, J_{CF} = 1.9 Hz), 111.4–110.6 (m), 63.9, 56.2, 52.5, 51.1; *m/z* MS $C_{23}H_{20}F_4NO_3$ $[MH]^+$ calcd 434.1, found 433.9.

2-((4-Fluoro-3-methoxybenzyl)amino)-*N*-hydroxy-2-(3',4',5'-trifluoro-[1,1'-biphenyl]-4-yl)acetamide (8). Compound **7** (365 mg, 0.842 mmol) was converted to the corresponding hydroxamic acid according to General Procedure C. The crude product was purified by column chromatography (DCM:MeOH 100:0 to 90:0) to afford compound **8** as a white solid (242 mg, 66%). ^{1}H NMR (d_6-DMSO) δ 10.80 (s, 1H), 8.95 (s, 1H), 7.77–7.61 (m, 4H), 7.51 (d, J = 8.3 Hz, 2H), 7.18–7.06 (m, 2H), 6.85 (ddd, J = 8.1/4.4/1.8 Hz, 1H), 4.09 (s, 1H), 3.82 (s, 3H), 3.61 (s, 2H), 3.10 (br. s, 1H); ^{19}F NMR (d_6-DMSO) δ -135.0 (d, J = 21.7 Hz), -138.4, -163.7 (dd, J = 21.7/21.7 Hz); ^{13}C NMR (d_6-DMSO) δ 168.3, 150.6 (ddd, J_{CF} = 246.5/9.7/4.2 Hz), 150.5 (d, J_{CF} = 242.0 Hz), 146.9 (d, J_{CF} = 10.6 Hz), 140.3, 139.8–136.9 (m), 137.0 (d, J_{CF} = 3.5 Hz), 136.7 (td, J_{CF} = 8.1/4.3 Hz), 136.1–135.9 (m), 128.0, 126.6, 119.9 (d, J_{CF} = 6.7 Hz), 115.3 (d, J_{CF} = 17.8 Hz), 113.3 (d, J_{CF} = 1.4 Hz), 111.9–110.6 (m), 61.8, 55.8, 49.9; *m/z* MS $C_{22}H_{19}F_4N_2O_3$ $[MH]^+$ calcd 435.1, found 434.9

2-((4-Fluoro-3-hydroxybenzyl)amino)-*N*-hydroxy-2-(3',4',5'-trifluoro-[1,1'-biphenyl]-4-yl)acetamide HCl salt (9). Compound **8** (200 mg, 0.460 mmol) was treated with BBr_3 (1M in DCM, 2.30 mL, 2.30 mmol) according to General Procedure D. Upon completion, the reaction was quenched with a 1 M HCl solution (3 mL) and stirred vigorously for 10 min. The mixture was neutralised to pH 7 with sat. $NaHCO_3$ and extracted with EtOAc (3 × 10 mL). The combined organic layers were dried over anhydrous Na_2SO_3, filtered and concentrated *in vacuo*. To convert the neutralised product to the corresponding HCl salt, the crude product (126 mg, 0.300 mmol) was dissolved in MeOH (8 mL) before addition of 1 M HCl (600 µL, 0.600 mmol) and stirred overnight at rt. The reaction mixture was concentrated *in vacuo* and lyophilised to remove excess HCl to afford compound **9** as a white solid (125 mg, 27%). ^{1}H NMR (d_6-DMSO) δ 11.55 (s, 1H), 10.21 (s, 1H), 10.13 (br. s, 2H), 9.40 (br. s, 1H), 7.84 (d, J = 8.4 Hz, 2H), 7.81–7.73 (m, 2H), 7.70 (d, J = 8.4 Hz, 2H), 7.23–7.09 (m, 2H), 6.90 (ddd, J = 8.1/4.0/ 2.1 Hz, 1H), 4.84 (s, 1H), 3.93 (q, J = 12.6 Hz, 2H); ^{19}F NMR (d_6-DMSO) δ -134.7 (d, J = 21.7

Hz), -135.7, -162.8 (dd, J = 21.7/21.7 Hz); ^{13}C NMR (d_6-DMSO) δ 162.8, 151.5 (d, J_{CF} = 242.8 Hz), 150.7 (ddd, J_{CF} = 246.7/9.7/4.2 Hz), 144.9 (d, J = 12.3 Hz), 138.6 (dt, J_{CF} = 249.0/15.5 Hz), 137.89–137.7 (m), 135.9 (dt, J_{CF} = 8.4/4.0 Hz), 132.4, 129.1, 127.2, 121.7 (d, J_{CF} = 6.6 Hz), 120.2 (d, J_{CF} = 2.9 Hz), 116.1 (d, J_{CF} = 18.5 Hz), 111.8–110.9 (m), 59.3, 48.5; *m/z* HRMS (TOF ES$^+$) $C_{21}H_{17}F_4N_2O_3$ $[MH]^+$ calcd 421.1170, found 421.1175.

Biology. *Protein Expression and Purification.* A soluble form of human APN ectodomain was expressed and purified as reported previously.[4] In brief, human APN was expressed in a stably transfected HEK293S GnT1$^-$ cell line, which was a kind gift from Professor James Rini from the University of Toronto, Canada. The cell growth and passaging of the cells, as well as collection of the culture supernatant, were conducted by Monash Protein Production Unit. Cells were grown in DMEM/F-12 supplemented with 3% FBS Invitrogen, 1 × penicillin-streptomycin (Invitrogen), 1 mg/liter of doxycycline (Sigma), and 1 mg/liter of aprotinin (Bioshop Canada). The APN–protein A fusion protein was purified by IgG-Sepharose (GE Healthcare) affinity chromatography. The protein A tag was removed by on-column tobacco etch virus protease digestion and the liberated APN was further purified by size exclusion chromatography on a Superdex S200 10/300 column in 50 mM HEPES pH 8.0, 300 mM NaCl, 5% glycerol buffer. Biochemical parameters K_m (31 ± 5 μM) and k_{cat} (456 ± 14 FU/sec^{-1}) were determined in the presence of L-Leucine-7-amido-4-methylcoumarin hydrochloride (H-Leu-NHMec) (Sigma L2145).

APN Enzymatic Analysis. Aminopeptidase assays were based on the modified version of previously published Drinkwater *et al*.[64] The activity of APN was determined by measuring the release of the fluorogenic leaving group, NH_2Mec, from the fluorogenic peptide H-Leu-NHMec (Sigma L2145). The reactions were carried out in 384-well microtitre plates, 50 μL total volume at 37 ºC using a spectrofluorimeter (BMG FLUOstar) with excitation at 355 nm and emission at 460 nm. APN was pre-incubated in 100 mM Tris pH 8.0 at 37 ºC with the inhibitors for 10 min prior to the addition of substrate (25 μM). Inhibitor concentrations were assayed with highest working concentrations of 2 – 320 μM,

diluted 1:4 to assess an overall 1000-fold concentration series. Initially, assays were performed in experimental triplicate, and if a $K_i^{(app)}$ value of ≤ 100 nM was calculated, the inhibitor was considered high priority, and assessed further in biological triplicate. The fluorescence signal was monitored for 1 hour at 37 ºC. Only linear range of velocity was considered in data analysis. $K_i^{(app)}$ values were then calculated by using Morrison equation for competitive and tight-binding inhibitors.[65, 66] Analysis and graphical output was performed in GraphPad Prism® 7.

Ad293 Cellular Viability Assay. Compounds were prepared as a 0.1 M stock solution in DMSO. 5000 Cells/well were plated out in a 96-well sterile clear TC plates in 100 uL of DMEM + 10% FBS + 1 % Penstrep (Invitrogen). The plates were incubated at 37 °C and 5% CO_2 overnight. Media was aspirated off followed by washing with 100 uL of PBS pH 7.4 (Invitrogen). In a separate plate, 240 uL of each compound was prepared at the working concentration by diluting the stock solutions with the media. This was serially diluted in 1:2 ratios across well plate. From the dilution plate, 100 uL of each compound dose was dispensed into the cell-seeded plate. Final concentration ranges of 0 – 800 μM (bestatin) and 0 – 400 μM (compound **6ad** and **6ae**) were achieved. After addition of the compound, the plate was incubated for an additional 72 hours. At the 72 hours mark, 10 uL of CellTiter-Blue® (Promega) was added to the cells followed by an additional 4 hours of incubation. Fluorescence readings were obtained on EnVision (PerkinElmer) at 565/595 nm. The results were expressed as % proliferation relative to a negative DMSO control. CC_{50} values were calculated from dose-response curves (log[compound concentration] verses % proliferation) using GraphPad Prism® 7.

Estimation of Kinetic Solubility using Nephelometry. Compounds in DMSO was spiked into either pH 6.5 phosphate buffer or 0.01 M HCl (approximately pH 2.0) with the final DMSO concentration being 1%. After 30 minutes had elapsed, samples were then analysed via Nephelometry to determine a solubility range.[67]

Estimation of Distribution Coefficient using Chromatography. Partition coefficient values (LogD) of the test compounds were estimated at pH 7.4 by correlation of their chromatographic retention

properties against the characteristics of a series of standard compounds with known partition coefficient values. The method employed is a gradient HPLC based derivation of the method developed by Lombardo *et al*.[68]

In Vitro Metabolic Stability. The metabolic stability assay was performed by incubating each compound in human or mouse liver microsomes at 37 °C and a protein concentration of 0.4 mg/mL. The metabolic reaction was initiated by the addition of an NADPH-regenerating system and quenched at various time points over a 60 min incubation period by the addition of acetonitrile containing diazepam as internal standard. Control samples (containing no NADPH) were included (and quenched at 2, 30 and 60 min) to monitor for potential degradation in the absence of cofactor. The human liver microsomes used in this experiment were supplied by XenoTech, lot # 1410230. The mouse liver microsomes used in this experiment were supplied by XenoTech, lot # 1510256. Microsomal incubations were performed at a substrate concentration of 1 μM.

In Vitro Plasma Stability. Human plasma (pooled; n=3 donors) was separated from whole blood procured from the Victorian Blood Donor Registry. Mouse plasma (pooled; multiple mice) from male Swiss outbred mice was collected in-house. Aliquots of plasma were spiked with DMSO/MeCN/H_2O solutions of test compound to a nominal compound concentration of 1000 ng/mL. The maximum final DMSO and acetonitrile concentrations were 0.2% (v/v) and 0.4% (v/v) respectively. Immediately after compound spiking, plasma was vortex mixed and aliquots of spiked plasma (50 μL) were transferred into fresh micro centrifuge tubes and were maintained at 37 °C under 10% CO_2 conditions. At various time points over the 240 min incubation period, triplicate plasma samples were taken and immediately snap-frozen in dry ice. All samples were stored frozen at -80 °C until analysis by LC-MS. Plasma samples were quantified

relative to calibration standards for prepared using blank plasma of the same species. Calibration standards were spiked with test compound over the range of 0.5 to 10,000 ng/mL. Internal standard (diazepam) was added to calibration standards and incubation samples, and then immediately quenched using two volumes of MeCN to precipitate plasma proteins. Samples were vortex mixed and centrifuged (10,000 rpm for 3 minutes) in a microcentrifuge and the supernatant analysed by LC-MS (Water Micromass Quattro Premier coupled to a Waters Acquity UPLC). The bioanalytical method was validated with respect to calibration range, linearity, accuracy and precision. The mean and standard deviation of measured plasma concentrations were calculated for each time point and expressed as a percentage remaining relative to the initial time point (5 min).

Computational Chemistry. *Molecular Modelling.* Molecular docking of compounds **1**, **6ad**, **6ae**, and **6ag** were carried out using Surflex docking interfaced with SYBYL2.1.1 in SFXC mode. The domain II of reference *Pf*A-M1 structure (PDB ID 4ZX4, residues 392-649) and APN structure (PDB ID 4FYQ, residues 287-546) were chosen for alignment due to the fact this domain incorporates the active site of interest and also shares the highest structural and sequence similarity across M1 aminopeptidase superfamily. A superimposed structural alignment was then performed using Pymol 1.8.23[69] with domain II of both *Pf*A-M1 and APN. The coordinates of compound **1** in the superimposed APN was subsequently extracted for the later use of fragment constraints. The bond constants and charge distribution for **1** were derived using the GAFF[70] and AM1-

BCC model[71, 72] respectively. To prepare the crystal structures, water molecules were removed and any missing regions were modelled using the program Modeller v9.10.[73] The flexible loop ^{891}YGGGSFSF^{898} was not resolved in the unbound structure of APN (PDB ID 4FYQ), however, it was resolved in electron density when APN was bound to either small molecule inhibitors such as bestatin (PDB ID 4FYR) and amastatin (PDB ID 4FYT), or a peptide substrate angiotensin IV (PDB ID 4FYS).[4] We rebuilt the missing loop in 4FYQ using Modeller and the structure was overlaid with the bound APN structures to examine if the flexible loop was modelled into a sensible position. Sidechain amides were protonated and fixed alongside charge addition using Gasteiger-Marsli method.[74] The charge for zinc metal was 2.0. The 2D ligand structures were prepared with default settings from SYBYL2.1.1. In grid generation, the core biphenyl system and hydroxamic acid were set as fragment constraints with a constraint penalty of 10. A total of 20 poses were produced for each ligand that were similar in their conformations and interactions. The differences in the total docking score between the most preferred pose and the second best pose of **1**, **6ad**, **6ae**, and **6ag** were 0.02, 0.003, 0.127, and 0.046, respectively. The best pose according to the total docking scores was selected to perform MD simulations.

MD simulations. The APN-ligand complex models were solvated in a rectangular simulation box leaving at least 12 Å of water shell thickness at all sides of the protein with a periodic box of 117 Å × 125 Å × 120 Å. System charges were neutralized with sodium counter ions.[75] Proteins and ions were modelled using the AMBER force field FF14SB and waters represented using the 3-particle TIP3P model.[75, 76] M1 aminopeptidase zinc and zinc binding residues (His^{388}, His^{392} and Glu^{411})

were prepared as described previously.[48] MD simulations were performed using NAMD 2.9 on an IBM Blue Gene/Q.[77] Equilibration was performed in three stages. First, potential steric clashes in the initial configuration were relieved with 2000 steps of energy minimization. Initial velocities for each system were then assigned randomly according to a Maxwell–Boltzmann distribution at 100 K. Each system was then heated to 300 K over 0.1 ns, under the isothermal-isometric ensemble (NVT) conditions, with the protein atoms (excluding hydrogens) harmonically restrained (with a force constant of 10 kcal mol^{-1} A^{-2}). Following this, each system was simulated for another 0.1 ns under the isothermal-isobaric ensemble (NPT) with applied harmonic restraints. For each system, we repeated the above process three times in order to initiate the production simulations with different initial velocities in NPT. Simulation time step was set to 2 fs and the SHAKE algorithm was used to constrain all bonds involving hydrogen atoms.[78] All simulations were run at constant temperature (300 K) and pressure (1 atm), using a Langevin damping coefficient of 0.5 fs^{-1}, and a Berendsen thermostat relaxation time of τ_P = 1.0 ps.[79, 80] For each simulated system, periodic boundary conditions (PBC) were used together with the Particle-Mesh Ewald (PME) method for long range electrostatic interactions and a real space cut-off of 10 Å was used.[81] To increase the efficiency of sampling, production MD simulations for APN were run in triplicate for 50 ns. The conformation was sampled every 5000 steps (1 snapshot per 10 ps). We then used 1 snapshot per 100 ps to analyse the MD trajectories.

■ ASSOCIATED CONTENT

The atomic coordinates for the X-ray crystal structures used as templates for molecular docking are available from the Protein Data Bank (PDB). *Pf*A-M1-**1** PDB ID 4ZX4 and human APN PDB ID 4FYQ.

Supporting Information

The Supporting Information is available free of charge on the ACS Publications website:

Synthetic procedures (compounds **10** – **16**)

MMP Enzymatic analysis

RMSD of the Cα and ligands of **1**, **6ad**, **6ae**, and **6ag** along the molecular modeling trajectory

Hydrogen bond occupancy analysis of **1**, **6ad**, **6ae**, and **6ag** with APN

Binding scores for the docked poses of **1**, **6ad**, **6ae**, and **6ag** into APN

HPLC traces of biologically evaluated compounds (**6a** – **6az** and **9**)

Molecular formula strings

■ AUTHOR INFORMATION

Corresponding Authors

*Phone: +61 (0)3 9903 9542. Email: Peter.Scammells@monash.edu

*Phone: +61 (0)3 9902 9309. Email: Sheena.McGowan@monash.edu

ORCID

Peter J. Scammells: 0000-0003-2930-895X

Jisook Lee: 0000-0003-3281-2508

Peter M. Grin: 0000-0001-9504-9664

Luke Schembri: 0000-0001-5588-1077

Michelle Gazdik: 0000-0003-1872-2346

Nyssa Drinkwater: 0000-0001-9165-7806

Sheena McGowan: 0000-0001-6863-1106

Author Contributions

The manuscript was written through contributions of all authors. All authors have given approval to the final version of the manuscript.

■ ACKNOWLEDGMENTS

This work was supported by the National Health and Medical Research Council (Project Grant 1063786 to SM and PJS). We thank Professor James Rini at the University of Toronto, Canada for the generous donation of the cell line that expresses the recombinant human APN ectodomain. We thank Miss Cassandra Yong for the kind donation of the Ad293 cell line and for training to perform the cell toxicity assay. We thank the Monash Platforms (Protein Production and Crystallization) for technical assistance. JL is supported by Monash University, Sir James McNeil Foundation and the Cancer Therapeutics CRC for CTx. WY was supported by a postgraduate scholarship from Monash University.

■ ABBREVIATIONS

DIPEA, *N*,*N*-diisopropylethylamine; HCTU, *O*-(1*H*-6-chlorobenzotriazol-l-yl)-1,1,3,3-tetramethyluronium hexafluorophosphate; DMAP, 4-dimethylamonipyridine; EDCI, 1-Ethyl-3-(3-dimethylaminopropyl)carbodiimide; PyBOP, (Benzotriazol-1-. yloxy)tripyrrolidinophosphonium hexafluorophosphate; CSI, chlorosulfonyl isocynate

■ REFERENCES

(1) Maroux, S.; Louvard, D.; Baratti, J. The aminopeptidase from hog intestinal brush border. *Biochim. Biophys. Acta.* **1973,** *321*, 282-295.

(2) Dixon, J.; Kaklamanis, L.; Turley, H.; Hickson, I. D.; Leek, R. D.; Harris, A. L.; Gatter, K. C. Expression of aminopeptidase-n (CD 13) in normal tissues and malignant neoplasms of epithelial and lymphoid origin. *J. Clin. Pathol.* **1994,** *47*, 43-47.

(3) Mina-Osorio, P. The moonlighting enzyme CD13: old and new functions to target. *Trends. Mol. Med.* **2008,** *14*, 361-371.

(4) Wong, A. H.; Zhou, D.; Rini, J. M. The X-ray crystal structure of human aminopeptidase N reveals a novel dimer and the basis for peptide processing. *J. Biol. Chem.* **2012,** *287*, 36804-36813.

(5) Zini, S.; Fournie-Zaluski, M. C.; Chauvel, E.; Roques, B. P.; Corvol, P.; Llorens-Cortes, C. Identification of metabolic pathways of brain angiotensin II and III using specific aminopeptidase inhibitors: predominant role of angiotensin III in the control of vasopressin release. *Proc. Natl. Acad. Sci. U.S.A.* **1996,** *93*, 11968-11973.

(6) Giros, B.; Gros, C.; Solhonne, B.; Schwartz, J. C. Characterization of aminopeptidases responsible for inactivating endogenous (Met5)enkephalin in brain slices using peptidase inhibitors and anti-aminopeptidase M antibodies. *Mol. Pharmacol.* **1986,** *29*, 281-287.

(7) Xu, Y.; Wellner, D.; Scheinberg, D. A. Substance P and bradykinin are natural inhibitors of CD13/aminopeptidase N. *Biochem. Biophys. Res. Commun.* **1995,** *208*, 664-674.

(8) Bosch, B. J.; Smits, S. L.; Haagmans, B. L. Membrane ectopeptidases targeted by human coronaviruses. *Curr. Opin. Virol.* **2014,** *6*, 55-60.

(9) Kolb, A. F.; Hegyi, A.; Maile, J.; Heister, A.; Hagemann, M.; Siddell, S. G. Molecular analysis of the coronavirus-receptor function of aminopeptidase N. *Adv. Exp. Med. Biol.* **1998,** *440*, 61-67.

(10) Yeager, C. L.; Ashmun, R. A.; Williams, R. K.; Cardellichio, C. B.; Shapiro, L. H.; Look, A. T.; Holmes, K. V. Human aminopeptidase N is a receptor for human coronavirus 229E. *Nature.* **1992,** *357*, 420-422.

(11) Mina-Osorio, P.; Ortega, E. Aminopeptidase N (CD13) functionally interacts with FcgammaRs in human monocytes. *J. Leukoc. Biol.* **2005,** *77*, 1008-1017.

(12) Pasqualini, R.; Koivunen, E.; Kain, R.; Lahdenranta, J.; Sakamoto, M.; Stryhn, A.; Ashmun, R. A.; Shapiro, L. H.; Arap, W.; Ruoslahti, E. Aminopeptidase N is a receptor for tumor-homing peptides and a target for inhibiting angiogenesis. *Cancer. Res.* **2000,** *60*, 722-727.

(13) Mina-Osorio, P.; Shapiro, L. H.; Ortega, E. CD13 in cell adhesion: aminopeptidase N (CD13) mediates homotypic aggregation of monocytic cells. *J. Leukoc. Biol.* **2006,** *79*, 719-730.

(14) Chen, L.; Lin, Y. L.; Peng, G.; Li, F. Structural basis for multifunctional roles of mammalian aminopeptidase N. *Proc. Natl. Acad. Sci. U.S.A.* **2012,** *109*, 17966-17971.

(15) Drag, M.; Bogyo, M.; Ellman, J. A.; Salvesen, G. S. Aminopeptidase fingerprints, an integrated approach for identification of good substrates and optimal inhibitors. *J. Biol. Chem.* **2010,** *285*, 3310-3318.

(16) McGowan, S.; Porter, C. J.; Lowther, J.; Stack, C. M.; Golding, S. J.; Skinner-Adams, T. S.; Trenholme, K. R.; Teuscher, F.; Donnelly, S. M.; Grembecka, J.; Mucha, A.; Kafarski, P.; Degori, R.; Buckle, A. M.; Gardiner, D. L.; Whisstock, J. C.; Dalton, J. P. Structural basis for the inhibition of the essential Plasmodium falciparum M1 neutral aminopeptidase. *Proc. Natl. Acad. Sci. U.S.A.* **2009,** *106*, 2537-2542.

(17) Hitzerd, S. M.; Verbrugge, S. E.; Ossenkoppele, G.; Jansen, G.; Peters, G. J. Positioning of aminopeptidase inhibitors in next generation cancer therapy. *Amino Acids.* **2014,** *46*, 793-808.

(18) Bauvois, B.; Dauzonne, D. Aminopeptidase-N/CD13 (EC 3.4.11.2) inhibitors: chemistry, biological evaluations, and therapeutic prospects. *Med. Res. Rev.* **2006,** *26*, 88-130.

(19) Wickstrom, M.; Larsson, R.; Nygren, P.; Gullbo, J. Aminopeptidase N (CD13) as a target for cancer chemotherapy. *Cancer Sci.* **2011,** *102*, 501-508.

(20) Amin, S. A.; Adhikari, N.; Jha, T. Design of aminopeptidase N inhibitors as anti-cancer agents. *J. Med. Chem.* **2018,** *61*, 6468-6490.

(21) Ashmun, R. A.; Look, A. T. Metalloprotease activity of CD13/aminopeptidase N on the surface of human myeloid cells. *Blood.* **1990,** *75*, 462-469.

(22) Hashida, H.; Takabayashi, A.; Kanai, M.; Adachi, M.; Kondo, K.; Kohno, N.; Yamaoka, Y.; Miyake, M. Aminopeptidase N is involved in cell motility and angiogenesis: its clinical significance in human colon cancer. *Gastroenterology.* **2002,** *122*, 376-386.

(23) Kawamura, J.; Shimada, Y.; Kitaichi, H.; Komoto, I.; Hashimoto, Y.; Kaganoi, J.; Miyake, M.; Yamasaki, S.; Kondo, K.; Imamura, M. Clinicopathological significance of aminopeptidase N/CD13 expression in human gastric carcinoma. *Hepato-gastroenterology.* **2007,** *54*, 36-40.

(24) Liang, W.; Gao, B.; Xu, G.; Weng, D.; Xie, M.; Qian, Y. Possible contribution of aminopeptidase N (APN/CD13) to migration and invasion of human osteosarcoma cell lines. *Int. J. Oncol.* **2014,** *45*, 2475-2485.

(25) Nohara, S.; Kato, K.; Fujiwara, D.; Sakuragi, N.; Yanagihara, K.; Iwanuma, Y.; Kajiyama, Y. Aminopeptidase N (APN/CD13) as a target molecule for scirrhous gastric cancer. *Clin. Res. Hepatol. Gastroenterol.* **2016,** *40*, 494-503.

(26) Schmidt, L. H.; Brand, C.; Stucke-Ring, J.; Schliemann, C.; Kessler, T.; Harrach, S.; Mohr, M.; Gorlich, D.; Marra, A.; Hillejan, L.; Muller-Tidow, C.; Lenz, G.; Wardelmann, E.; Wiewrodt, R.; Berdel, W. E.; Schwoppe, C.; Hartmann, W. Potential therapeutic impact of CD13 expression in non-small cell lung cancer. *PloS one.* **2017,** *12*, e0177146.

(27) Tokuhara, T.; Hattori, N.; Ishida, H.; Hirai, T.; Higashiyama, M.; Kodama, K.; Miyake, M. Clinical significance of aminopeptidase N in non-small cell lung cancer. *Clin. Cancer Res.* **2006,** *12*, 3971-3978.

(28) Valastyan, S.; Weinberg, R. A. Tumor metastasis: molecular insights and evolving paradigms. *Cell.* **2011,** *147*, 275-292.

(29) Su, L.; Cao, J.; Jia, Y.; Zhang, X.; Fang, H.; Xu, W. Development of synthetic aminopeptidase N/CD13 inhibitors to overcome cancer metastasis and angiogenesis. *ACS. Med. Chem. Lett.* **2012,** *3*, 959-964.

(30) Wirtz, D.; Konstantopoulos, K.; Searson, P. C. The physics of cancer: the role of physical interactions and mechanical forces in metastasis. *Nat. Rev. Cancer.* **2011,** *11*, 512-522.

(31) Chaffer, C. L.; Weinberg, R. A. A perspective on cancer cell metastasis. *Science.* **2011,** *331*, 1559-1564.

(32) Saiki, I.; Fujii, H.; Yoneda, J.; Abe, F.; Nakajima, M.; Tsuruo, T.; Azuma, I. Role of aminopeptidase N (CD13) in tumor-cell invasion and extracellular matrix degradation. *Int. J. Cancer.* **1993,** *54*, 137-143.

(33) Yoneda, J.; Saiki, I.; Fujii, H.; Abe, F.; Kojima, Y.; Azuma, I. Inhibition of tumor invasion and extracellular matrix degradation by ubenimex (bestatin). *Clin. Exp. Metastasis.* **1992,** *10*, 49-59.

(34) Mucha, A.; Drag, M.; Dalton, J. P.; Kafarski, P. Metallo-aminopeptidase inhibitors. *Biochimie.* **2010,** *92*, 1509-1529.

(35) Zhang, X.; Fang, H.; Zhang, J.; Yuan, Y.; Xu, W. Recent advance in aminopeptidase N (APN/CD13) inhibitor research. *Curr. Med. Chem.* **2011,** *18*, 5011-5021.

(36) Scornik, O. A.; Botbol, V. Bestatin as an experimental tool in mammals. *Curr. Drug. Metab.* **2001,** *2*, 67-85.

(37) Umezawa, H.; Aoyagi, T.; Suda, H.; Hamada, M.; Takeuchi, T. Bestatin, an inhibitor of aminopeptidase B, produced by actinomycetes. *J. Antibiot (Tokyo).* **1976,** *29*, 97-99.

(38) Ichinose, Y.; Genka, K.; Koike, T.; Kato, H.; Watanabe, Y.; Mori, T.; Iioka, S.; Sakuma, A.; Ohta, M.; Group, N. K. L. C. S. Randomized double-blind placebo-controlled trial of bestatin in patients with resected stage I squamous-cell lung carcinoma. *J. Natl. Cancer. Inst.* **2003,** *95*, 605-610.

(39) Ota, K. Review of ubenimex (Bestatin): clinical research. *Biomed. Pharmacother.* **1991,** *45*, 55-60.

(40) Ota, K.; Kurita, S.; Yamada, K.; Masaoka, T.; Uzuka, Y.; Ogawa, N. Immunotherapy with bestatin for acute nonlymphocytic leukemia in adults. *Cancer. Immunol. Immunother.* **1986,** *23*, 5-10.

(41) Urabe, A.; Mutoh, Y.; Mizoguchi, H.; Takaku, F.; Ogawa, N. Ubenimex in the treatment of acute nonlymphocytic leukemia in adults. *Ann. Hematol.* **1993,** *67*, 63-66.

(42) Krige, D.; Needham, L. A.; Bawden, L. J.; Flores, N.; Farmer, H.; Miles, L. E.; Stone, E.; Callaghan, J.; Chandler, S.; Clark, V. L.; Kirwin-Jones, P.; Legris, V.; Owen, J.; Patel, T.; Wood, S.; Box, G.; Laber, D.; Odedra, R.; Wright, A.; Wood, L. M.; Eccles, S. A.; Bone, E. A.; Ayscough, A.; Drummond, A. H. CHR-2797: an antiproliferative aminopeptidase inhibitor that leads to amino acid deprivation in human leukemic cells. *Cancer. Res.* **2008,** *68*, 6669-6679.

(43) Lowenberg, B.; Morgan, G.; Ossenkoppele, G. J.; Burnett, A. K.; Zachee, P.; Duhrsen, U.; Dierickx, D.; Muller-Tidow, C.; Sonneveld, P.; Krug, U.; Bone, E.; Flores, N.; Richardson, A. F.; Hooftman, L.; Jenkins, C.; Zweegman, S.; Davies, F. Phase I/II clinical study of Tosedostat, an inhibitor of aminopeptidases, in patients with acute myeloid leukemia and myelodysplasia. *J. Clin. Oncol.* **2010,** *28*, 4333-4338.

(44) Drinkwater, N.; Vinh, N. B.; Mistry, S. N.; Bamert, R. S.; Ruggeri, C.; Holleran, J. P.; Loganathan, S.; Paiardini, A.; Charman, S. A.; Powell, A. K.; Avery, V. M.; McGowan, S.; Scammells, P. J. Potent dual inhibitors of Plasmodium falciparum M1 and M17 aminopeptidases through optimization of S1 pocket interactions. *Eur. J. Med. Chem.* **2016,** *110*, 43-64.

(45) Kannan Sivaraman, K.; Paiardini, A.; Sienczyk, M.; Ruggeri, C.; Oellig, C. A.; Dalton, J. P.; Scammells, P. J.; Drag, M.; McGowan, S. Synthesis and structure-activity relationships of phosphonic arginine mimetics as inhibitors of the M1 and M17 aminopeptidases from Plasmodium falciparum. *J. Med. Chem.* **2013,** *56*, 5213-5217.

(46) Mistry, S. N.; Drinkwater, N.; Ruggeri, C.; Sivaraman, K. K.; Loganathan, S.; Fletcher, S.; Drag, M.; Paiardini, A.; Avery, V. M.; Scammells, P. J.; McGowan, S. Two-pronged attack: dual

inhibition of Plasmodium falciparum M1 and M17 metalloaminopeptidases by a novel series of hydroxamic acid-based inhibitors. *J. Med. Chem.* **2014,** *57*, 9168-9183.

(47) Li, P.; Merz, K. M., Jr. Metal ion modeling using classical mechanics. *Chem. Rev.* **2017,** *117*, 1564-1686.

(48) Yang, W.; Riley, B. T.; Lei, X.; Porebski, B. T.; Kass, I.; Buckle, A. M.; McGowan, S. Generation of AMBER force field parameters for zinc centres of M1 and M17 family aminopeptidases. *J. Biomol. Struct. Dyn.* **2017**, 1-10.

(49) Yang, W.; Riley, B.; Lei, X.; Porebski, B. T.; Kass, I.; Buckle, A. M.; McGowan, S. Mapping the pathway and dynamics of bestatin inhibition of the Plasmodium falciparum M1 aminopeptidase, PfA-M1. *ChemMedChem.* **2018,** *13*, 2504-2513.

(50) Beebe, X.; Nilius, A. M.; Merta, P. J.; Soni, N. B.; Bui, M. H.; Wagner, R.; Beutel, B. A. Synthesis and SAR evaluation of oxadiazolopyrazines as selective Haemophilus influenzae antibacterial agents. *Bioorg. Med. Chem. Lett.* **2003,** *13*, 3133-3136.

(51) Adediran, S. A.; Cabaret, D.; Lohier, J. F.; Wakselman, M.; Pratt, R. F. Substituted aryl malonamates as new serine beta-lactamase substrates: structure-activity studies. *Bioorg. Med. Chem.* **2010,** *18*, 282-291.

(52) Im, I.; Lee, E. S.; Choi, S. J.; Lee, J. Y.; Kim, Y. C. Structure-activity relationships of heteroaromatic esters as human rhinovirus 3C protease inhibitors. *Bioorg. Med. Chem. Lett.* **2009,** *19*, 3632-3636.

(53) Kam, Y. L.; Rhee, H. K.; Kim, H. J.; Back, S. K.; Na, H. S.; Choo, H. Y. Synthesis and bradykinin inhibitory activity of novel non-peptide compounds, and evaluation of in vivo analgesic activity. *Bioorg. Med. Chem.* **2010,** *18*, 2327-2336.

(54) Williams, S. J.; Zammit, S. C.; Cox, A. J.; Shackleford, D. M.; Morizzi, J.; Zhang, Y.; Powell, A. K.; Gilbert, R. E.; Krum, H.; Kelly, D. J. 3',4'-Bis-difluoromethoxycinnamoylanthranilate (FT061):

an orally-active antifibrotic agent that reduces albuminuria in a rat model of progressive diabetic nephropathy. *Bioorg. Med. Chem. Lett.* **2013,** *23*, 6868-6873.

(55) Butters, M.; Davies, C. D.; Elliott, M. C.; Hill-Cousins, J.; Kariuki, B. M.; Ooi, L. L.; Wood, J. L.; Wordingham, S. V. Synthesis and stereochemical determination of batzelladine C methyl ester. *Org. Biomol. Chem.* **2009,** *7*, 5001-5009.

(56) Sun, W. S.; Park, Y. S.; Yoo, J.; Park, K. D.; Kim, S. H.; Kim, J. H.; Park, H. J. Rational design of an indolebutanoic acid derivative as a novel aldose reductase inhibitor based on docking and 3D QSAR studies of phenethylamine derivatives. *J. Med. Chem.* **2003,** *46*, 5619-5627.

(57) Sadovoy, A. K., A. ; Golubeva, G. ; Sviridova, L. Regioselective synthesis of 1-alkyl-5-(indol-3-yl- and -2-yl)pyrrolidin-2-ones from available reagents. *Chem. Heterocycl. Compd.* **2011,** *46*, 1215-1223.

(58) Romeo, G.; Salerno, L.; Pittala, V.; Modica, M. N.; Siracusa, M. A.; Materia, L.; Buccioni, M.; Marucci, G.; Minneman, K. P. High affinity ligands and potent antagonists for the alpha1D-adrenergic receptor. Novel 3,8-disubstituted [1]benzothieno[3,2-d]pyrimidine derivatives. *Eur. J. Med. Chem.* **2014,** *83*, 419-432.

(59) Valla, A.; Cartier, D.; Zentz, F.; Labia, R. Atypical oxidation reaction by thionyl chloride: easy two-step synthesis of N-Alkyl-1,4-dithiines. *Synth. Commun.* **2006,** *36*, 3591-3597.

(60) Arulsamy, N.; Bohle, D. S. Nucleophilic addition of hydroxylamine, methoxylamine, and hydrazine to malononitrileoxime. *J. Org. Chem.* **2000,** *65*, 1139-1143.

(61) Voros, A.; Mucsi, Z.; Baan, Z.; Timari, G.; Hermecz, I.; Mizsey, P.; Finta, Z. An experimental and theoretical study of reaction mechanisms between nitriles and hydroxylamine. *Org. Biomol. Chem.* **2014,** *12*, 8036-8047.

(62) Luciani, N.; Marie-Claire, C.; Ruffet, E.; Beaumont, A.; Roques, B. P.; Fournie-Zaluski, M. C. Characterization of Glu350 as a critical residue involved in the N-terminal amine binding site of

aminopeptidase N (EC 3.4.11.2): insights into its mechanism of action. *Biochemistry.* **1998,** *37*, 686-692.

(63) Graham, F. L.; Smiley, J.; Russell, W. C.; Nairn, R. Characteristics of a human cell line transformed by DNA from human adenovirus type 5. *J. Gen. Virol.* **1977,** *36*, 59-74.

(64) Stack, C. M.; Lowther, J.; Cunningham, E.; Donnelly, S.; Gardiner, D. L.; Trenholme, K. R.; Skinner-Adams, T. S.; Teuscher, F.; Grembecka, J.; Mucha, A.; Kafarski, P.; Lua, L.; Bell, A.; Dalton, J. P. Characterization of the Plasmodium falciparum M17 leucyl aminopeptidase. A protease involved in amino acid regulation with potential for antimalarial drug development. *J. Biol. Chem.* **2007,** *282*, 2069-2080.

(65) Morrison, J. F. Kinetics of the reversible inhibition of enzyme-catalysed reactions by tight-binding inhibitors. *Biochim. Biophys. Acta.* **1969,** *185*, 269-286.

(66) Williams, J. W.; Morrison, J. F. The kinetics of reversible tight-binding inhibition. *Methods. Enzymol.* **1979,** *63*, 437-467.

(67) Bevan, C. D.; Lloyd, R. S. A high-throughput screening method for the determination of aqueous drug solubility using laser nephelometry in microtiter plates. *Anal. Chem.* **2000,** *72*, 1781-1787.

(68) Lombardo, F.; Shalaeva, M. Y.; Tupper, K. A.; Gao, F. ElogD(oct): a tool for lipophilicity determination in drug discovery. 2. Basic and neutral compounds. *J. Med. Chem.* **2001,** *44*, 2490-2497.

(69) Schrödinger. *The PyMOL Molecular Graphics System, Version 1.8. Schrödinger, LLC.* , 2017.

(70) Wang, J.; Wolf, R. M.; Caldwell, J. W.; Kollman, P. A.; Case, D. A. Development and testing of a general amber force field. *J. Comput. Chem.* **2004,** *25*, 1157-1174.

(71) Jakalian, A. B. L. B. D. B. J. C. I. B. Fast, efficient generation of high-quality atomic charges. AM1-BCC model: I. Method. *J. Comput. Chem.* **2000,** *21*, 132-146.

(72) Jakalian, A. D. B. J. C. I. B. Fast, efficient generation of high-quality atomic charges. AM1-BCC model: II. Parameterization and validation. *J. Comput. Chem.* **2002,** *23*, 1623-1641.

(73) Fiser, A.; Sali, A. Modeller: generation and refinement of homology-based protein structure models. *Methods. Enzymol.* **2003,** *374*, 461-491.

(74) Gasteiger, J.; Marsili, M. Iterative partial equalization of orbital electronegativity—a rapid access to atomic charges. *Tetrahedron.* **1980,** *36*, 3219-3228.

(75) Jorgensen, W. L.; Chandrasekhar, J.; Madura, J. D.; Impey, R. W.; Klein, M. L. Comparison of simple potential functions for simulating liquid water. *J. Chem. Phys.* **1983,** *79*, 926-935.

(76) Case, D. A.; Cheatham, T. E., 3rd; Darden, T.; Gohlke, H.; Luo, R.; Merz, K. M., Jr.; Onufriev, A.; Simmerling, C.; Wang, B.; Woods, R. J. The Amber biomolecular simulation programs. *J. Comput. Chem.* **2005,** *26*, 1668-1688.

(77) Phillips, J. C.; Braun, R.; Wang, W.; Gumbart, J.; Tajkhorshid, E.; Villa, E.; Chipot, C.; Skeel, R. D.; Kale, L.; Schulten, K. Scalable molecular dynamics with NAMD. *J. Comput. Chem.* **2005,** *26*, 1781-1802.

(78) Ryckaert, J.-P.; Ciccotti, G.; Berendsen, H. J. C. Numerical integration of the cartesian equations of motion of a system with constraints: molecular dynamics of n-alkanes. *J. Compu. Phys.* **1977,** *23*, 327-341.

(79) Kawasaki, K. Simple derivations of generalized linear and nonlinear Langevin equations. *J. Phys. A: Math. Nucl. Gen.* **1973,** *6*, 1289.

(80) Berendsen, H. J. C.; Postma, J. P. M.; van Gunsteren, W. F.; DiNola, A.; Haak, J. R. Molecular dynamics with coupling to an external bath. *J. Chem. Phys.* **1984,** *81*, 3684-3690.

(81) Essmann, U.; Perera, L.; Berkowitz, M. L.; Darden, T.; Lee, H.; Pedersen, L. G. A smooth particle mesh Ewald method. *J. Chem. Phys.* **1995,** *103*, 8577-8593.

TOC Graphic

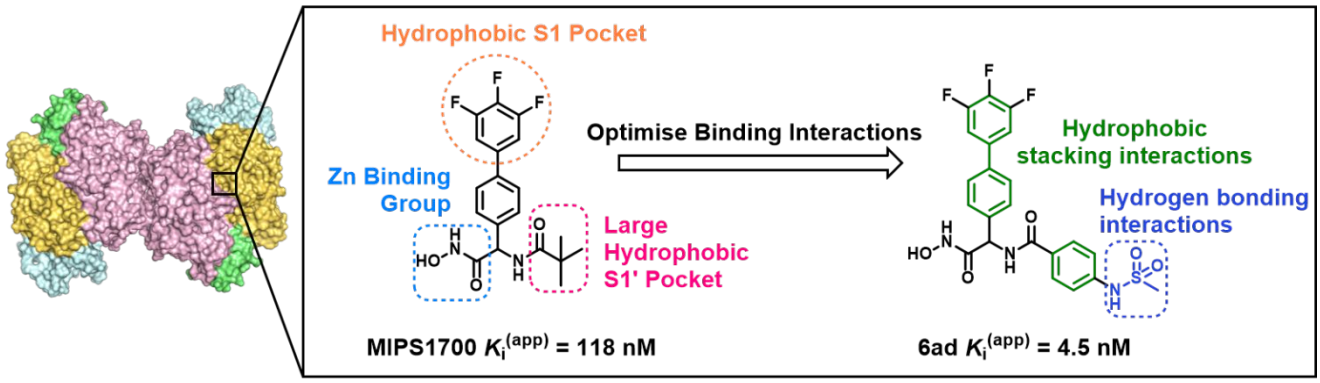
Hydrophobic S1 Pocket
Zn Binding Group
Large Hydrophobic S1' Pocket
Optimise Binding Interactions
Hydrophobic stacking interactions
Hydrogen bonding interactions
MIPS1700 $K_i^{(app)}$ = 118 nM
6ad $K_i^{(app)}$ = 4.5 nM